SHORT TERM CONTRACT FOR THE BIOLOGICAL STUDIES (ICCAT GBYP 08/2022) OF THE ATLANTIC-WIDE RESEARCH PROGRAMME FOR BLUEFIN TUNA (GBYP Phase 12)

Final report

for:

ICCAT

Scientific coordinator:

Dra. Igaratza Fraile (AZTI-Member of Basque Research & Technology Alliance)

Pasaia, June 2nd, 2023

This project is co-funded by the European Union

PARTNERS:

Fundación AZTI – AZTI Fundazioa, (AZTI)

Instituto Español de Oceanografía, (IEO-CSIC)

Galway-Mayo Institute of Technology, (GMIT)

Fisheries Resources Institute, Japan Fisheries Research and Education Agency (FRI)

Universidad de Cádiz, (UCA)

Institut Français de Recherches pour l'Exploitation de la Mer (IFREMER)

Texas A&M University (TAMU)

National Oceanic and Atmospheric Administration (NOAA)

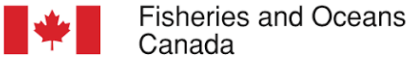

Fisheries and Oceans of Canada (DFO)

SUBCONTRACTORS and COLLABORATORS:

Institute of Marine Research
(IMR)

Instituto Português do Mar e da Atmosfera
(IPMA)

Institut National de la Recherche en Halieutique
(INRH)

Centre d'Estudis Avançats de Blanes
(CEAB-CSIC)

Istambul University

University of Arizona

ThermoFisher

INDEX:

EXECUTIVE SUMMARY:

The main objective of this project is to enhance our knowledge about Atlantic bluefin tuna (ABFT) population structure, mixing, and growth, as well as to develop methodologies that integrate the current knowledge for an effective stock management.

During Phase 12, the Consortium sampled a total of 490 Atlantic bluefin tuna (224 YOY, 3 medium sized fish and 263 large fish) from different regions (52 from the Strait of Gibraltar, 42 from Portugal, 35 from the Canary Islands, 79 from Norway, 100 from the Central North Atlantic, 19 from the South of Spain and 103 from the Balearic Sea and 60 from the Levantine Sea). In total, 980 biological samples (310 otolith samples, 181 fin spines and 489 genetic samples) were collected by the Consortium and incorporated into the tissue bank. The Consortium also received samples apart from those agreed in the contract. In total, the Consortium handled 4555 biological samples (1514 otolith samples, 1221 fin spines and 1820 genetic samples) from 1867 individuals. All these samples have been catalogued and stored together with the biological tissue bank. The information from this and previous phases is being reviewed and uploaded to a new application developed in AZTI.

On genetic analyses, interbreeding dynamics in the Slope Sea confirms a gene-flow from the Mediterranean into the Slope Sea, which is probably a relatively recent event (less than approximately 80 generations). The genetic mixing of Mediterranean and western origin individuals in the Slope Sea could have happened repeatedly in different years during the last decades. An increase in gene flow from 2008 to 2018 could not be confirmed. Also, genomic regions of albacore origin were found in the genome of Slope Sea and Mediterranean individuals for which whole genome sequencing data was available. Our data suggest that variants of albacore origin are associated to adaptive traits. In this phase complete assignments of Atlantic bluefin tuna individuals from feeding aggregates captured at the different ICCAT areas genotyped with the 96 SNP traceability panel from GBYP phase 6 to phase 11 have been updated based on the knowledge on the population structure acquired during the GBYP program. Overall, > 3,200 individuals captured at feeding aggregates showed

varying mixing proportions of Mediterranean, Gulf of Mexico, and unassigned individuals across catch years, supporting the migratory patterns of Atlantic bluefin tuna are dynamic. Additionally, cost-effective tools for kin pair identification for future CKMR studies are presented.

Regarding the task of direct ageing, three subtasks have been addressed: 1) a review and update of bluefin tuna growth studies using calcified structures and methods combined with these structures has been carried out. The status of validation and standardization of the reading of each structure is detailed. 2) two reference collections of 200 samples have been prepared for otoliths and for spines (first spiny ray of the first caudal fin) to serve as quality control of these structures. And 3) a selection of otolith samples has been made to carry out the epigenetic study for the ABFT of the East Atlantic and Mediterranean Sea. This selection has considered all possible factors that may influence the analyses.

Regarding otolith microchemistry, new carbon ($\delta^{13}C$) and oxygen ($\delta^{18}O$) stable isotope analyses were carried out in 125 otoliths of Atlantic bluefin tuna captured in the Central North Atlantic, Canary Island and Norwegian Sea, to determine their nursery area. These results combined with previous analyses suggest that important mixing of the two populations occurs in the central North Atlantic, west of the 45ºW management boundary. Mixing rates were found to be moderate east of this boundary, with the Mediterranean population being the principal contributor to the fishery and western contribution estimated at around 10%. Instead, catches in the Norwegian Sea and Canary Island are exclusively comprised by the Mediterranean bluefin tuna. These new analyses, together with all $\delta^{13}C$ and oxygen $\delta^{18}O$ have been used to re-assign the putative origin of all ABFT individuals analyses in the GBYP framework for stable isotope data to date (~3000 individuals). The baseline used as a reference set, was developed within this phase based on results from previous phases that suggested that spawning adults captured in spawning seasons inside the Mediterranean Sea and the Gulf of Mexico, shoed less overlap in their chemical signature than did YOY baseline. Additionally, in this phase, only adults with genetically confirmed eastern or western origin were used as baseline. Results show that ABFT individuals from both origins can be found in foraging grounds of the Atlantic Ocean, and that mixing proportions vary among years in all regions. Besides,

trace element transects analyzed in Phase-11 in combination with $\delta^{18}O$ profiles showed cyclical patterns in $\delta^{18}O$ values often coinciding with fluctuations in Sr concentrations. This synchronicity was attributed to the direct and indirect influence of temperature on the uptake of Sr into the otolith. We found no evidence of a common migration route between distinct water masses. Instead, our results reflect high levels of individual variability in horizontal and vertical movements. A combined fractionation equation for young of the year and adult Atlantic bluefin tuna was built, which demonstrates that $\delta^{18}O$ closely reflects the temperature and isotopic composition of the water throughout life. This new equation will provide new insights into the reconstruction of environmental histories and detection of movement between water masses.

During this phase, further efforts have been made to combine genetic and chemical markers to develop a combined method of population assignment. Over the last 10 Phases of the GBYP programme ABFT individuals have been routinely analyzed to assign stock of origin based on otolith chemistry and genetic markers separately to investigate the degree of eastern and western population contribution to different mixing areas in the Atlantic Ocean. However, the use of both methods together can provide further insights into the complexity of the stock structure of the species and enhance the understanding of ecological and evolutionary processes that may help to identify stock units with a high degree of confidence. Here, two different approaches were followed: (1) Individual origin was re-assigned using an integrated classification model that includes both genetic and stable isotope data (i.e., Integrated approach) and (2) genetic and stable isotope data was used complementarily (i.e., Combined approach). The integrated method proved to increase the resolving power of stock discrimination in comparison to single approaches and resulted in lower numbers of unassigned individuals than otolith stable isotope only and genetic markers only models. The combined approach showed that can provide insights into ABFT population structure that can be masked when a single technique is used, or when both techniques are integrated, as it considers processes occurring at different temporal scales (i.e., individual life span vs evolutionary).

Finally, ABFT larvae from surveys conducted in the Balearic Sea spawning ground were sorted and identified for potential close-kin analyses. In total, 7638 individuals

from 40 samples collected during 2022 were identified. Bluefin tuna larvae were found in 34 out of the 40 samples analyzed. In addition, stages of larval development were identified (i.e., yolk sac, preflexion, flexion, or postflexion). The sorted individuals were preserved in 100% ethanol in different 4 ml jars and kept in the freezer for a perfect conservation.

Overall, most of the objectives of the project were met. These analyses continue to provide relevant information for a better understanding of the biology of Atlantic bluefin tuna, which in turn improves the stock assessment and management advice of this valuable species.

1. CONTEXT

On August 30th 2022, the consortium coordinated by Fundación AZTI-AZTI Fundazioa, formed by partners Fundación AZTI-AZTI Fundazioa (AZTI), Instituto Español de Oceanografía (IEO-CSIC), Galway-Mayo Institute of Technology (GMIT), Japan Fisheries Research and Education Agency (FRI), University of Cádiz (UCA), Texas A&M University (TAMU), National Oceanic and Atmospheric Administration (NOAA) and Fisheries and Ocean of Canada (DFO), with the subcontracted parties IPMA, IMR, INRH, CEAB-CSIC and Istanbul University for sampling, presented a proposal to the call for tenders on biological and genetic sampling and analysis (ICCAT-GBYP 08/2022).

This proposal was awarded and the final contract between ICCAT and the consortium represented by Fundación AZTI-AZTI Fundazioa was signed on September 23rd 2022.

According to the terms of the contract, a Final Report (Deliverable nº 4) needed to be submitted to ICCAT by the 2nd of June 2023. The present report was prepared in response to such requirement.

2. SAMPLING

Task Leader: Iraide Artetxe-Arrate (AZTI) & Igaratza Fraile (AZTI)

Participants:

AZTI: Naiara Serrano, Ainhoa Arevalo, Goretti Garcia, Maite Cuesta, Naiara Rodriguez-Ezpeleta, Natalia Diaz, Iñaki Mendibil, Iker Zudaire, Martin Cabello de los Cobos, Iñigo Onandia

UCA: Jose Luis Varela, Antonio Medina, Esther Asensio

FRI: Yohei Tsukahara

IEO-CSIC: Enrique Rodriguez Marín, Rosa Delgado de Molina, Pablo Quelle, Patricia Reglero, Aurelio Ortega, David Macías

IMR: Ørjan Sørensen, Leif Nøttestad

IPMA: Pedro Lino, Daniela Rosa

CEAB-CSIC: Ana Gordoa

ISTA: Isik Oray

IFREMER: Tristan Rouyer, Oliver Derridj

2.1 Introduction

The sampling conducted under this project follows a specific design, aimed primarily at contributing to knowledge on population structure and mixing. As such, the sampling conducted under this project is independent from other routine sampling activities for fisheries and fishery resources monitoring (e.g., the Data Collection Framework). The 2022 updated sampling protocols, together with instructions, have been distributed within the Consortium as well as to ICCAT, so that they are distributed to other institutions conducting biological sampling (e.g., as part of tagging activities, Regional Observer Programs, farms, etc.).

2.2 Sampling accomplished

The agreed sampling for Phase 12 has been accomplished (Table 2.1). In total 1100 samples from 510 ABFT individuals have been achieved by the Consortium, consisting of 330 otoliths, 261 dorsal fin spines and 509 muscle tissue for genetics (Table 2.2).

Table 2.1: Individuals sampled within the Consortium, in each area and per each age stratum.

Grand Area	Area	Age 0 <3kg	Juveniles 3-25 kg	Medium 25-100 kg	Large >100 kg	*Total*	Responsible
Strait of Gibraltar	Gibraltar Strait	7			45	52	UCA
	Portugal (Algarve)			3	39	42	AZTI (IPMA)
Western Mediterranean	South Spain	19				19	UCA
	Balearic Sea	12				12	UCA
		91				91	AZTI (CEAB-CSIC)
Eastern Mediterranean	Levantine Sea	80				80	AZTI (ISTA)
East Atlantic-West African Coast	Canary Islands	35				35	IEO
North east Atlantic	Norwegian Sea				79	79	AZTI (IMR)
Central North Atlantic	Central and North Atlantic				100	100	FRI
Total		**224**	**0**	**3**	**263**	**510**	

Table 2.2: Detailed number of otoliths, dorsal fin spines and muscle/fin tissue samples achieved in the framework of the Consortium, in each area.

Grand Area	Area	Otoliths	Spines	Muscle/Fin	*Total*	Responsible
Strait of Gibraltar	Gibraltar Strait	7	7	52	66	UCA
	Portugal (Algarve)			42	42	AZTI (IPMA)
Western Mediterranean	South Spain	19	19	19	57	UCA
	Balearic Sea			12	12	UCA
		91	91	91	273	AZTI (CEAB-CSIC)
Eastern Mediterranean	Levantine Sea	80	80	80	240	AZTI (ISTA)
East Atlantic-West African Coast	Canary Islands	35		35	70	IEO
North east Atlantic	Norwegian Sea	65	64	78	207	AZTI (IMR)
Central North Atlantic	Central and North Atlantic	33		100	133	FRI
Total		**330**	**261**	**509**	**1100**	

The anomalous high temperatures recorded in the Mediterranean Sea in the last years, motivated to resume the sampling of YOYs in the eastern and western Mediterranean basins for Phase 12. In the western Mediterranean, 91 YOY samples have been collected by CEAB-CSIC in collaboration of the recreational fishermen association *©Scientificangler.es*, with otoliths, spines and muscle tissues sampled for all individuals. Besides, 31 YOYs were also sampled from the Western Mediterranean Sea by the UCA, 19 caught in coastal waters of Southern Spain by trolling fisheries operating in the Alboran Sea for which otoliths, spines and muscle tissue were collected, and 12 caught by longline fisheries south of Tarragona for which only muscle tissue was collected. In the eastern Mediterranean 80 YOYs have been collected from the Levantine Sea, for which otolith, spines and muscle tissue will be sampled.

Outside the Gibraltar Strait, UCA also sampled of 7 YOYs and 45 large individuals caught in Ceuta tuna traps and trolling fisheries operating in the Strait, respectively. Muscle tissue was sampled from all of them, while otoliths and spines were collected only for the 7 YOYs. In the Portuguese coast off Algarve 3 medium-sized and 39 large individuals were sampled for muscle tissue by IPMA onboard a freezing vessel during the tuna harvest season (second/third week of October).

In the East Atlantic-West African Coast, the IEO sampled 35 large individuals caught by bait boats fishing around Canary Islands. No spines were taken from these individuals; therefore, the obtained tissue samples consist of 35 otoliths and 35 muscle tissue for genetics. Biological info has not been retrieved yet, but it will be incorporated into the database as soon as it received. Unfortunately, INRH communicated that Moroccan samples were not available for this phase. Thus, although agreed in the initial plan, this subcontracted activity was agreed to be removed from the original sampling plan in the Proposal to amend the "Short-Term contract for Biological Studies (ICCAT GBYP 08/2022) of the Atlantic-Wide Research Programme for Bluefin Tuna (GBYP Phase 12)".

In the North-east Atlantic, 79 large ABFT were sampled by IMR on Norwegian Sea, from which 65 otoliths, 64 spines and 78 muscle tissue for genetics were collected. These individuals were caught mainly from purse seine landings from M/S Spjæringen, while 12 individuals were collected from the IMR Recfish tagging program by rod and reel.

In the Central North Atlantic, 100 large individuals have been sampled by FRI, all for muscle tissue and 33 with otoliths. Since the pandemic outbreak in 2021 observer

activities on board Japanese longliners have been limited, therefore sampling has been conducted at the market, which makes head sampling more difficult.

In addition to the committed samples, 1036 ABFT individuals (32 juveniles, 77 medium size and 927 large individuals) have been sampled by other partners/contracts. Altogether (considering the samples collected by the consortium and those arrived from other contracts/programs) the total number of individuals sampled in this Phase-12 has been 1867, consisting of 224 YOY, 32 juvenile, 81 medium and 1530 large sized ABFT (Table 2.3).

In the western Mediterranean Sea, 330 large individuals caught by purse seiners operating in the Balearic Sea have been sampled by TAXO, which provided spines and muscle tissue samples from all individuals, 328 gonads and 323 otoliths. In the central Mediterranean Sea, ABTL provided samples from 697 individuals (12 medium and 685 large) captured by purse seiners in waters around Malta and the Tyrrhenian Sea, and sampled 684 otoliths, 694 spines and 695 muscle tissues for genetics. The regional observer program (ROP) also provided samples from individuals caught by purse fisheries of the western and central Mediterranean Sea: 11 individuals from the Balearic Sea (1 medium and 10 large), 2 large individuals from South Spain, 41 large individuals from Maltese waters and 3 large individuals from the Tyrrhenian Sea.

In the Bay of Biscay, IFREMER provided samples from 31 juveniles, 48 medium and 157 large ABFT individuals collected in summer 2020, 2021, and 2022. Only muscle tissue was collected. The increased presence of bluefin tuna in the waters of the Bay of Biscay in winter has also made it possible to sample individuals from these waters. AZTI collected samples of 53 (1 juvenile, 17 medium and 35 large) ABFT that arrived to Pasaia fish market in March 2023. All individuals were sampled for genetics, while 4 otoliths, 3 spines and 3 gonads were collected. AZTI also provided muscle tissue and spine from one large individual recaptured at the Gulf of Saint Lawrence and 3 large individuals from the Canary Islands.

Overall, the Consortium handled 4675 biological samples, 1534 otoliths, 1301 spines and 1840 muscle or fin tissue for genetics (Table 2.4). All these samples have been catalogued and stored in the biological tissue bank at AZTI facilities, biological information and sampling availability is detailed in Appendix 3.

Table 2.3: Total number of individuals sampled in each area and per age stratum, including those of the Consortium plus the ones sampled under other contracts and stored by the Consortium.

Grand Area	Area	Age 0 <3kg	Juveniles 3-25 kg	Medium 25-100 kg	Large >100 kg	*Total*	Responsible
Strait of Gibraltar	Gibraltar Strait	7			45	52	UCA
	Portugal (Algarve)			3	39	42	AZTI (IPMA)
Western Mediterranean	South Spain	19				19	UCA
					2	2	ROP
	Balearic Sea	12				12	UCA
		91				91	AZTI (CEAB-CSIC)
					330	330	TAXO
				1	10	11	ROP
Central Mediterranean	Strait of Sicily/Malta				41	41	ROP
					346	346	ABTL
	Thyrrenian Sea			12	339	351	ABTL
					3	3	ROP
Eastern Mediterranean	Levantine Sea	80				80	AZTI (ISTA)
East Atlantic-West African Coast	Canary Islands	35				35	IEO
					3	3	AZTI
Northeast Atlantic	Bay of Biscay		1	17	35	53	AZTI
			31	48	157	236	IFREMER
North east Atlantic	Norwegian Sea				79	79	AZTI (IMR)
Central North Atlantic	Central and North Atlantic				100	100	FRI
Gulf Saint Lawrence	Gulf Saint Lawrence				1	1	AZTI
Total		**244**	**32**	**81**	**1530**	**1887**	

Table 2.4: Detailed number of otoliths, dorsal fin spines and muscle/fin tissue samples achieved in Phase 12 (including those of the Consortium plus the ones taken under other contracts and stored by the Consortium)

Grand Area	Area	Otoliths	Spines	Muscle/Fin	*Total*	Responsible
Strait of Gibraltar	Gibraltar Strait	7	7	52	66	UCA
	Portugal (Algarve)			42	42	AZTI (IPMA)
Western Mediterranean	South Spain	198	19	19	236	UCA
				2	2	ROP
	Balearic Sea			12	12	UCA
		91	91	91	273	AZTI (CEAB-CSIC)
		323	330	330	983	TAXO

		1	1	11	13	ROP
Central Mediterranean	Strait of Sicily/Malta		33	33	66	ROP
		346	346	346	1038	ABTL
	Thyrrenian Sea	351	321	349	1021	ABTL
			3	3	6	ROP
Eastern Mediterranean	Levantine Sea	80	80	80	240	AZTI (ISTA)
East Atlantic-West African Coast	Canary Islands	35			35	IEO
			2	2	4	AZTI
Northeast Atlantic	Bay of Biscay	4	3	53	60	AZTI
				236	236	IFREMER
North east Atlantic	Norwegian Sea	65	64	78	207	AZTI (IMR)
Central North Atlantic	Central and North Atlantic	33		100	133	FRI
Gulf Saint Lawrence	Gulf Saint Lawrence		1	1	2	AZTI
Total		**1534**	**1301**	**1840**	**4675**	

3. MAINTENANCE AND MANAGEMENT OF THE ICCAT GBYP TISSUE BANK AND RELATED INFORMATION SYSTEM

Task Leader: Iraide Artetxe-Arrate (AZTI)

Participants:

AZTI: Igaratza Fraile, Ainhoa Orbe and David Alvarez

The consortium has provided appropriate storage for all the biological samples and hard parts already collected and shipped to AZTI withing this phase (N=4555). When necessary, samples have been relabelled accordingly, and in the case of muscle for genetics, a replicate has been made and storage at two different facilities. The new sampling protocol and datasheet has been circulated among the different partners involved in the sampling. All the information received has been properly recorded in the tissue bank related information system. Data has been standardized according to the criteria agreed in the protocol to follow a common pattern. Metadata is provided following the accorded format of modules: (1) Fish identification data, (2) Sample availability, (3) Sampling information, (4) Biological data, (5) Analytical tasks and (6) Results. In addition, otolith chemistry and genetic stock origin results have been updated with results from Phase 12 Task 4.2 and Task 6.1. All the information from this and previous phases is procured in Appendix 3. Since 2022 AZTI is undergoing a restructuring process in the management of warehouse information, which is why the "Storage at AZTI" section is now managed in a different way than in previous phases. The objective of the restructuring process is the improvement of the practices for sample storage and management as well as the traceability of samples.

The 30th of November, an online meeting with ICCAT´s database specialist Alfonso Pagá was celebrated, to determine the steps needed to be taken with a view to transferring the biological data to ICCAT soon. The database that has been in use to date was created at the beginning of the project, an Excel table of > 30.5 MB which has been transformed and expanded as GBPY evolved, but that is becoming difficult to manage due to the magnitude the project has achieved. AZTI has already developed an application with controlled permissions that perform specific searches and queries on the available samples storage at AZTI. The information from this and previous phases is being reviewed and uploaded to this new application.

4. GENETIC ANALYSES

Task Leader: Natalia Díaz-Arce (AZTI)

Participants:

AZTI: Naiara Rodriguez-Ezpeleta, Iñaki Mendibil, Natalia Gutierrez, Iker Zudaire

4.1 Subtask 1 - Further understand interbreeding dynamics of the Atlantic bluefin tuna spawning components.

4.1.1 Introduction

Previous population genetic analyses have shown that current Atlantic Bluefin tuna (ABFT) descend from two ancestral populations, which are represented by the Mediterranean Sea and Gulf of Mexico (hereafter MED-like and GOM-like) spawning components respectively. Likewise, individuals born in the recently discovered spawning ground in the Slope Sea are genetically heterogeneous, intermediate and admixed, meaning that this area receives immigrants from the Mediterranean and most probably from the Gulf of Mexico at unknown rates. Given that the Slope Sea has been proposed as a major spawning ground for the species (Hernández et al. 2022), and that previous results have confirmed the presence of Mediterranean genetic origin individuals in the Gulf of Mexico (see Phase 9), it is necessary to explore the genetic admixture in the West Atlantic, and in particular in the Slope Sea, to further understand the potential consequences for the conservation of the species.

The objectives of this task are:

1. To **understand interbreeding dynamics** of the two genetic ancestral populations in the Slope Sea and in the Gulf of Mexico.
2. To assess **current and past connectivity patterns** between Atlantic bluefin tuna spawning components.

4.1.2 Materials and Methods

a) Generation of a combined RAD-seq and SNP Array derived genotypes dataset

The datasets containing genotypes obtained through RAD-sequencing (generated in phases 5 and 8) and the SNP array (phases 10 and 11) were merged into one genotype table using the PLINK software (Purcell et al. 2007), keeping only the 7,767 neutral markers that had passed genotype quality filters in both datasets. To avoid technical bias in genetic diversity among samples, low replicability SNPs between both techniques were identified as those with inconsistent genotypes (excluding missing data) in more than 1 of the 50 replicate samples genotyped using both techniques.

b) Admixture tests

The convert function from ADMIXTOOLS software (Patterson et al. 2012) was used to convert the combined dataset generated in section 4.1.3 from PLINK to eigenstrat format and the qp3Pop function was used to calculate F3 statistic and Z-score associated values (Patterson et al. 2012), testing for admixture among the 157 larvae captured in the Gulf of Mexico during 2018 and between 2007 and 2010 separately, and considering adults captured at the spawning season in the Gulf of Mexico and Mediterranean spawning adults, young of the year and larvae as source groups.

c) Genetic variant filtering and local ancestry estimations from whole genome sequencing data

Whole genome sequencing data of 9 spawning adults from the Gulf of Mexico (from which 3 were genetically Mediterranean), 7 larvae, young of the year and spawning adults from the Mediterranean sea, 9 larvae and young of the year from the Slope Sea and 2 albacore (*Thunnus alalunga*) individuals available in AZTI research team were filtered using TRIMMOMATIC (Bolger et al. 2014) to trim low quality reads (reads were screened using sliding window of 3 nucleotide size and quality threshold of 28), discard reads of less than 50 nucleotides length and those containing adapter sequences. Filtered reads were mapped against the most updated version available of the reference genome of the Pacific bluefin tuna (*Thunnus orientalis*, GCA_021601225.1) using BWA-MEM algorithm (Li 2013) and only correctly mapped read pairs and primary alignments were kept. Duplicated read pairs, likely deriving from PCR DNA fragment duplication performed

during library preparation, were marked using the MarkDuplicates module from picard tools (https://github.com/broadinstitute/picard) and removed using SAMtools (Li et al. 2009). Base quality scores of kept reads were recalibrated using the BASERECALIBRATOR module included in GATK (van der Auwera and O'Connor 2020). Genomic variants were called using freebayes (Garrison and Marth 2012) and exported to vcf format. Only SNP variants with minimum quality of 20 and minimum read coverage of 15 were kept using VCFtools (Danecek et al. 2011). Two datasets were generated, including and excluding the two individuals of albacore tuna, and biallelic variants with a minimum allele count of higher than 3 were kept. The following analyses were applied to both datasets: genotype tables were exported to PLINK and structure formats, PCA was performed using the R package adegenet (Jombart and Ahmed 2011) and individuals ancestry proportions were estimated using ADMIXTURE (Alexander et al. 2009) using default parameters and assuming 2 and 3 ancestral populations (K value). Separate vcf files were generated with SNPs from each of the 41 contigs from the reference genome of sizes >5 Mb which constitute >73% of the total reference genome, and for each of the different groups of individuals: ABFT from the Gulf of Mexico, Slope Sea and Mediterranean Sea, and albacore tuna. We estimated local ancestry only across the longest 41 reference contigs in order to avoid bias introduced by highly fragmented tracts, which would result in an underestimation of the number of generations since admixture in the Slope Sea.

Local ancestry levels across the genome of the six young of the year and three larvae from the Slope Sea was inferred using ELAI software (Guan 2014) using the dataset which includes only ABFT individuals and setting as reference groups the adults from the Gulf of Mexico (excluding those that showed Mediterranean ancestry confirmed with ADMIXTURE and PCA results) and all samples from the Mediterranean Sea. Loci with estimated local ancestry for the Mediterranean component ranging from 1.95 to 2 were assumed to have Mediterranean origin.

Same procedure was followed to estimate local ancestry across Slope Sea and Mediterranean individuals using the dataset which includes ABFT and albacore tuna samples setting as reference groups adults from the Gulf of Mexico (excluding those that showed Mediterranean ancestry confirmed with ADMIXTURE and PCA results) and albacore individuals. Loci with estimated local ancestry for the albacore-like component ranging from 0.95 to 1.05 and from 1.95 to 2 were considered to have one and two haplotypes of albacore origin respectively.

d) Dating admixture with Mediterranean individuals in the Slope Sea

The genomic tracts hosting variants of Mediterranean origin were measured as the difference in position between the last and the first variant. Length of genomic tracts of Mediterranean origin at the peaks of the length distribution was used to estimate the time in generations since the strongest admixing events using the following formula described in Racimo et al. (2015):

$$T = 1+[l(1- m)r]^{-1}$$

Where "T" is time in generations since admixture, "m" is the proportion of ancestry within the recipient population (average Mediterranean ancestry in Slope Sea samples estimated using ADMXITURE), "l" is the estimated tract length of genomic tracts of Mediterranean origin and "r" is average recombination rate (in Morgan per base pair per generation). In the absence of recombination rate estimates specifically for Atlantic bluefin tuna, we used an intermediate recombination rate for fish species of 2.82 cM/Mb (Stapley et al. 2017).

4.1.2.5. Estimation of effective population size at the three spawning areas

We estimated current effective popualtion size applying the molecular coancestry method implemented in the software NeEstimator (Do et al. 2014) using a thinned dataset containing 20,000 SNPs discovered through the whole genome sequencing data of 25 ABFT individuals generated as described in section 4.1.2.3 and leaving default parameters. We excluded the previously identified MED-like individuals from the Gulf of Mexico population. We also estimated current popualtion size using the RAD-seq dataset based on 12,936 SNPs from 242 larvae and young of the year from the three spawning areas. Due to the work hours re-allocation needed after the doubled effort invested in subtask 3.1 after the forst round of prepared samples was lost and initial difficulties applying the approach implemented in PSMC (Li, Durbin 2011) we did not reconstruct historical effective population size (Ne). Results and Discussion

4.1.3 Results and Discussion

a) Tracts of Mediterranean genomic regions reveal recent admixture of Mediterranean individuals in the Slope Sea

The genotype dataset obtained from whole genome sequencing of 25 ABFT individuals contained 175,191 SNPs. Individual ancestry estimations (Figure 4.1.1) and PCA (Figure

4.1.2) resulted in similar results to those obtained with SNPs obtained through RAD-seq (generated in phases 5 and 8), showing differences in the ancestry levels between Mediterranean and Gulf of Mexico individuals. Separation of both components in the PCA is clearer based on whole genome sequencing data than based on RAD-seq derived dataset, probably because of the higher number of SNPs used here. Surprisingly, three Mediterranean and one Gulf of Mexico individuals (not one of the Mediterranean-like ones) showed not pure ancestral composition. As expected, Slope Sea individuals were heterogeneous and intermediate and MED-like Gulf of Mexico individuals were pure Mediterranean. Average Mediterranean ancestry composition proportion among Slope Sea samples was 0.23.

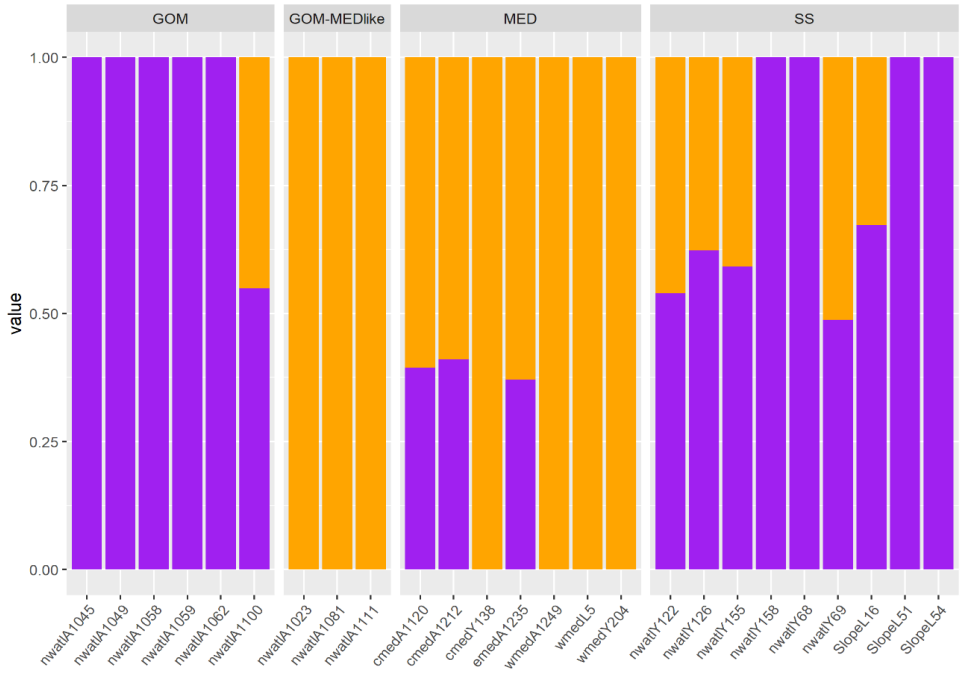

Figure 4.1.1. Individual ancestry composition assuming two ancestral populations. The orange and purple components correspond to the Mediterranean and Gulf of Mexico ancestral populations respectively. Individuals are grouped as captured in the Slope Sea (SS), in the Mediterranean Sea (MED), in the Gulf of Mexico (GOM) and those captured in the Gulf of Mexico but known to show Mediterranean origin (GOM-MEDlike).

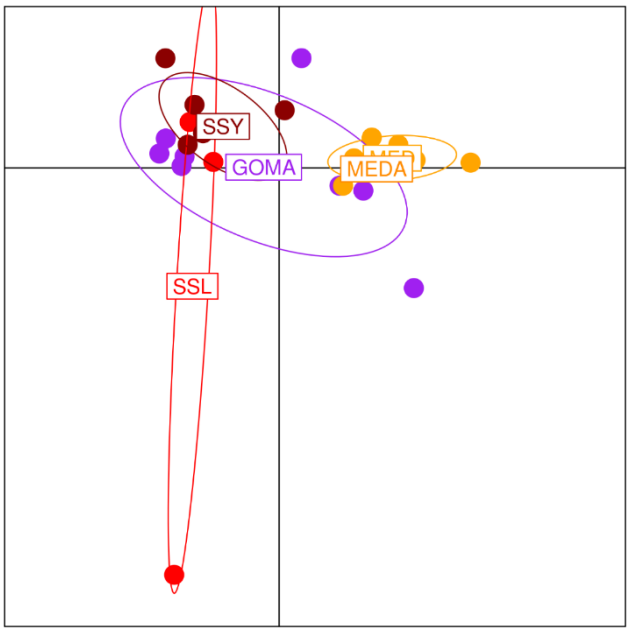

*Figure 4.1.2. PCA showing genetic differentiation between Atlantic bluefin tuna individuals analyzed using whole genome sequencing data. Individuals are grouped according to capture location (MED: Mediterranean Sea in orange, GOM: Gulf of Mexico in purple and SS: Slope Sea in red and dark red) and age class (L: larvae, Y: Young of the Year and A: adult). *Note that in order to distinguish Slope Sea larvae and Young of the year these are shown in red and dark red respectively.*

Dosages of Mediterranean and Gulf of Mexico like variants were estimated at each variant position across the genome of each Slope Sea sequenced individual, and in total 95 tracts of Mediterranean origin were identified across all individuals. An example of the distribution of these dossages in one reference contig is shown in Figure 4.1.3.

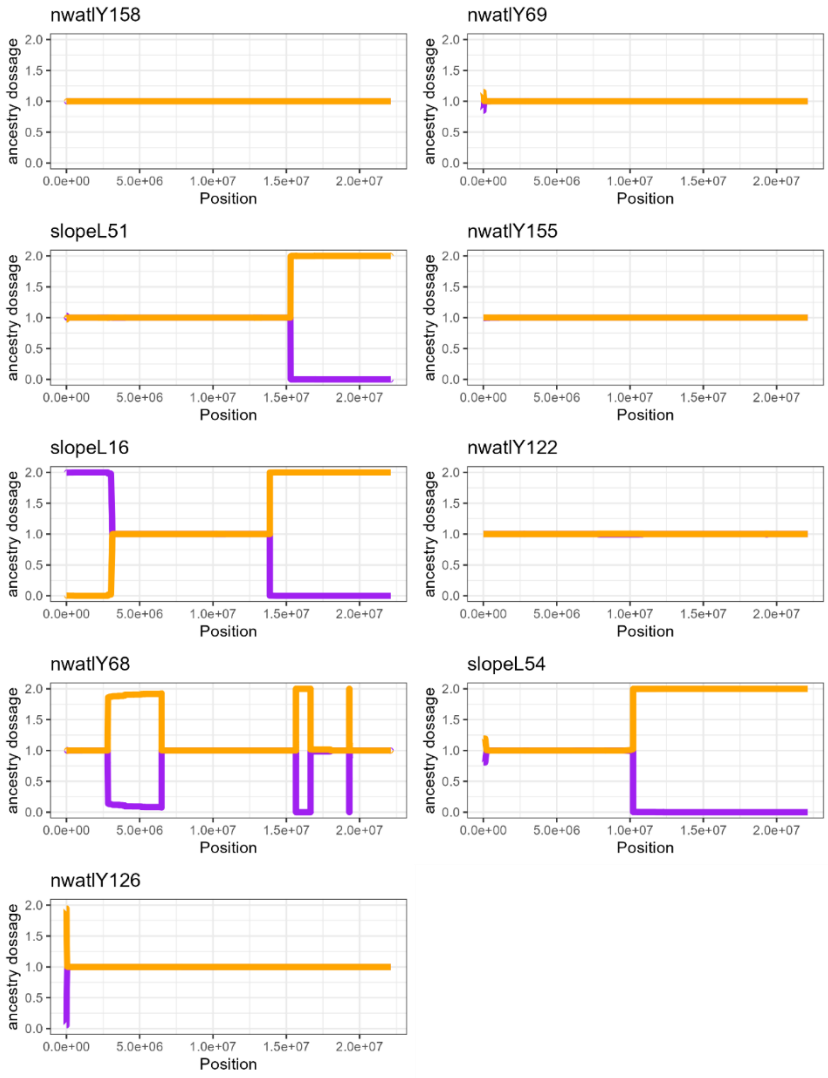

Figure 4.1.3. Proportions of Mediterranean (orange line) and Gulf of Mexico (purple line) ancestral origin estimated at each variant across the contig BOUD01000011 of the reference genome of the Pacific bluefin tuna. The sum of both values is two, corresponding with the two possible haplotypes found in diploid individuals.

The length distribution of genomic tracts of Mediterranean origin across Slope Sea individuals peaked at 588,919.3 bp (Figure 4.1.4). Admixing events may have happened at different moments across generations, therefore instead of using length average to estimate time since admixture we used the values corresponding with the peak of the distribution in order to date the strongest admixing event. Time since admixture between Mediterranean and Slope Sea individuals inferred the length at this peak was 79.2 generations. The presence of secondary peaks in the distribution (Figure 4.1.4) suggests also occurrence of more recent gene-flow events of lower intensities.

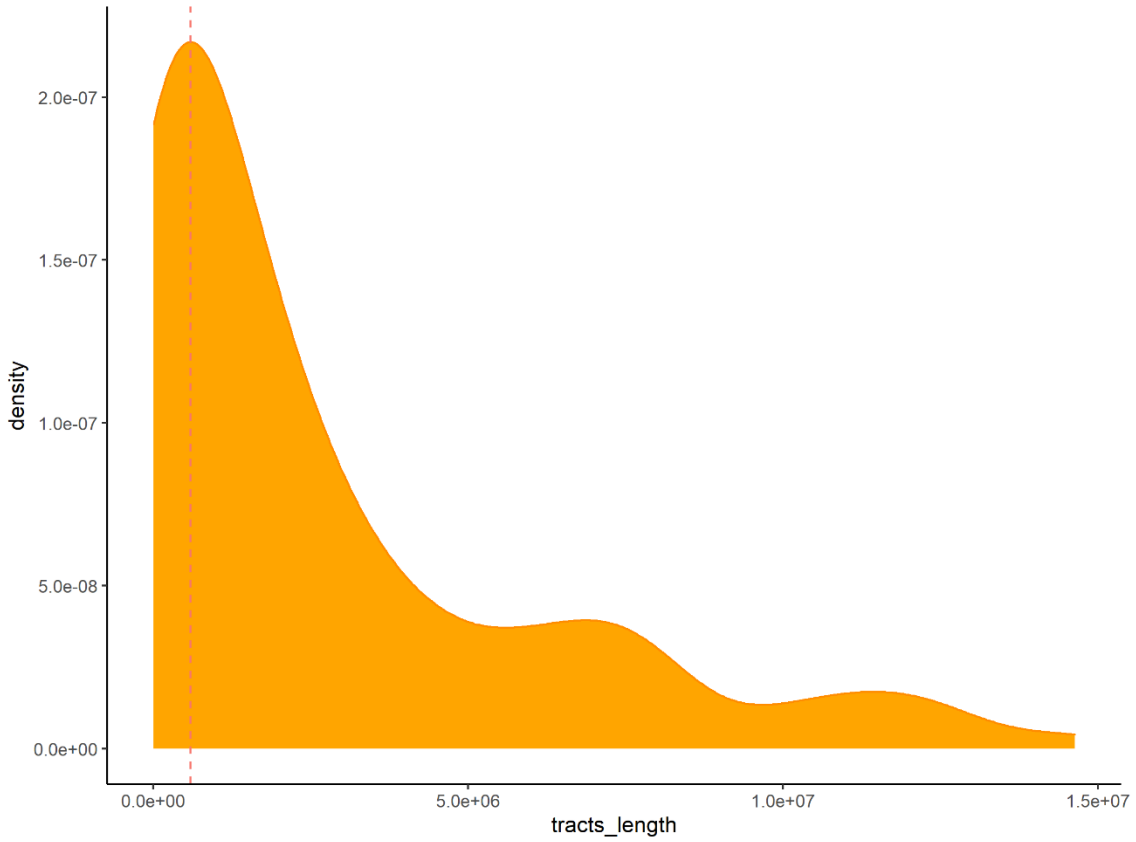

Figure 4.1.4. Density distribution of the length of identified tracts of Mediterranean origin across Slope Sea samples. The vertical dotted line shows the peak of the distribution at 0.59Mb length.

Previous genetic analysis revealed that the Slope Sea was originated from the Gulf of Mexico (see phase 9). Therefore, we have estimated time since hybridization with Mediterranean individuals. Given that both ancestral components are genetically very similar, local ancestry levels are probably biased towards the detection on intermediate ancestry levels. Indeed, most genomic regions show local ancestry loads close to 1, which would in theory correspond with genomic regions at which one haplotype would have Mediterranean origin and the other would have Guld of Mexico origin. By considering only regions where Mediterranean origin was assessed for both haplotypes, we reduced the risk of detecting false positives, potentially underestimating Mediterranean origin tract lengths and consequently overestimating time since admixture.

These estimations are based on the average recombination rate value for ABFT. We used an average value for fish species, but this number can be highly variable among fish species. Therefore, recombination rate calculated specifically or ABFT could result in more accurate estimates of time since admixture in the Slope Sea.

b) Admixture of Mediterranean individuals in the Gulf of Mexico

Tests for admixture among larvae captured in the Gulf of Mexico were not statistically significant, neither among those captured between 2007 and 2010, nor among those captured in 2018 (Table 2). Previous analysis (see Phase 9) supported the presence of genetically Mediterranean spawning individuals in the Gulf of Mexico, while no presence of Mediterranean alleles was detected among larvae. One possible hypothesis to explain this observation, is a recent increase in the migration from the Mediterranean Sea towards the Gulf of Mexico that would not be reflected yet among larvae. However, while negative results for the F3 test support admixture in the target population, positive scores do not involve absence of admixture, meaning that the hypothesis of increasing migration cannot be rejected.

Table 4.1.2. F3 statistic for the different admixture scenarios tested. For each scenario, the target is tested for being admixed from two other sources. Negative F3 values indicate admixture, and Z value informs about significance. The different source groups included are adults captured in the Gulf of Mexico at the spawning season (GOMA), adults captured Sea at the spawning season (MEDA), and larvae (MEDL) and young of the year (MEDY) captured in the Mediterranean Sea.

Source groups		Target	f_3	std. Err	Z
GOMA	MEDL	GOML (2018)	0.00054	0.00009	5.92
GOMA	MEDY	GOML (2018)	0.00048	0.00009	5.55
GOMA	MEDA	GOML (2018)	0.00077	0.00009	8.44
GOMA	MEDL	GOML (2007-2010)	0.00030	0.00024	1.24
GOMA	MEDY	GOML (2007-2010)	0.00014	0.00024	0.60
GOMA	MEDA	GOML (2007-2010)	0.00021	0.00025	0.85

c) Current effective population size

Our estimates for effective population sizes (Ne) based on whole genome sequencing and RAD-seqeuncing data were incredibly small. The values obtained using the whole genome sequencing data had bigger confidence intervals, probably due to the small sample size used for the estimations. For large marine populations, such as that of Atlantic bluefin tuna, it has been shown that large samples sizes are needed (Marandel et al. 2019), meaning that our estimates are probably biased and inaccurate due to small sample sizes and that trustable estimations would require specific sample design.

Table 4.1.3. Effective population size of Mediterranean (MED), Gulf of Mexico (GOM) and Slope Sea (SS) spawning components estimated using the whole genome sequencing (WGS) and the Restriction site Associated DNA sequencing (RAD-seq) datasets. Confidence intervals 95% are shown in brackets.

	Dataset	
	WGS	RAD-seq
MED	6.7 (6.4 - 7.1)	3.7 (3.5 - 3.9)
GOM	6.0 (5.7 - 6.3)	2.0 (1.9 - 2.1)
SS	4.9 (4.6 - 5.1)	5.4 (5.1 - 5.8)

d) Albacore-like genomic tracts in Mediterranean individuals (Subtask 1.4)

Previous analyses have shown traces of introgressed genomic regions of albacore origin in the ABFT genome. To explore the distribution of genomic loci of albacore origin across the genome, we estimated local ancestry at each of the 7 and 9 Mediterranean Sea and Slope Sea individuals for which whole genome sequencing data was available using Gulf of Mexico GOM-like ABFT and albacore tuna individuals as references. We found no individual with both haplotypes being of albacore origin at the same locus. There were 56 heterozygotic regions showing one haplotype of albacore origin across the 15 individuals which were located within 14 reference contigs among the 41 analyzed (Figure 4.1.5).

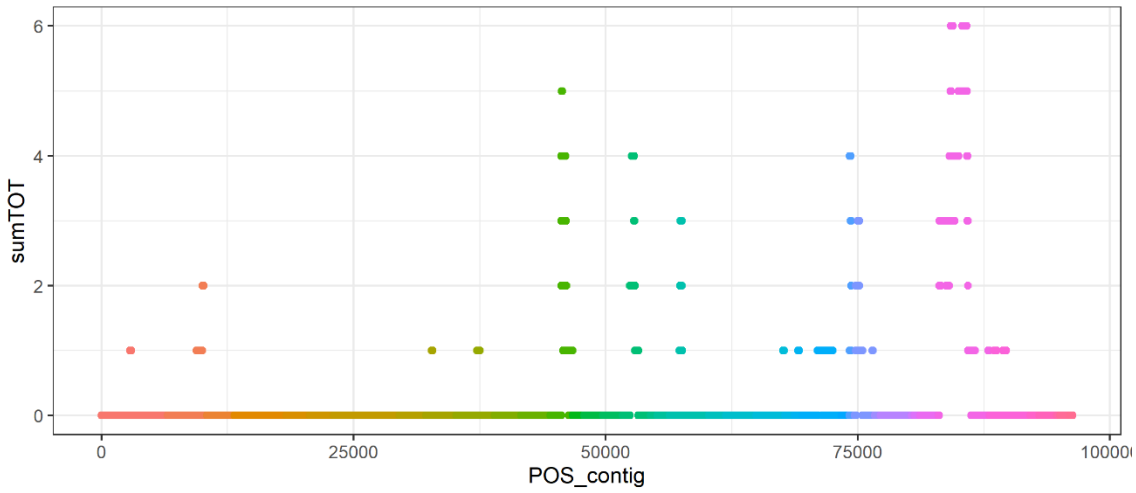

Figure 4.1.5. Number of haplotype variants of albacore origin (y axis) estimated at each variant locus across the 41 reference contigs and among the 15 individuals analyzed (assuming 30 total haplotypes at each position). Variant positions of the different reference contigs are concatenated. Different colors represent each of the 41 different reference contigs.

The higher frequency of albacore origin haplotypes within certain particular regions, suggests that these regions could potentially host adaptive variation. Further analysis of the genes hosted in these regions would be needed to understand their adaptive potential.

Among the 56 haplotypes of albacore origin, only 16 of them were found among the 9 Slope Sea individuals analyzed, and 2 of them were found within contigs in which no Mediterranean individual showed albacore origin haplotypes. This suggest that introgression is much stronger in the Mediterranean Sea, where albacore and Atlantic bluefin tuna share spawning areas, and that introgressed tracts were introduced in the Slope Sea spawned individuals through gene-flow from the Mediterranean Sea.

4.1.4 Conclusions

Interbreeding dynamics in the Slope Sea:

- Genomic regions of Mediterranean origin were found among Slope Sea larvae and young of the year for which whole genome sequencing data was available. This confirms existing gene-flow from the Mediterranean into the Slope Sea. Calculations based on the length of these regions support that the strongest gene-flow event from the Mediterranean Sea into this spawning area happened less than ~80 Atlantic bluefin tuna generation ago. This estimate could be more accurate if average recombination rate of Atlantic bluefin tuna was calculated, for which further analysis would be needed.
- The length frequency distribution of the genomic regions of Mediterranean origin found in the Slope Sea shows several peaks, suggesting that genetic mixing of Mediterranean and western origin individuals in the Slope Sea could have happened repeatedly in different years during the last decades.

Connectivity between Atlantic bluefin tuna spawning areas:

- Combination of RAD-seq and SNP array generated datasets allowed to build a new genotype dataset. Approximately the 25% of the markers showed low reproducibility between both techniques and had to be removed. Merging of RAD-seq (sequencing based) and SNP array (genotyping based) generated datasets would require analyzing high numbers of replicated samples to identify low reproducibility markers.
- The separated test of gene-flow from the Mediterranean Sea into Gulf of Mexico larvae from different years did not confirm increase in gene-flow during the time

period between larvae samples from 2008 to 2018, although this hypothesis could not be rejected.

- Genomic regions of albacore origin were found in the genome of Slope Sea and Mediterranean individuals for which whole genome sequencing data was available. Although found at low frequencies, these regions were hosted within few contigs of the reference genome, highly suggesting that variants of albacore origin are associated to adaptive traits. The identification of these regions will allow searching for specific genes and derived functions to understand how these affects adaptive capability of the Atlantic bluefin tuna to the environment.
- Whole genome sequencing data, generated for 25 Atlantic bluefin and 2 albacore tuna individuals allowed to better understand the mixing dynamics of the different spawning areas by the study of genetic diversity across their genomes.

4.2 Subtask 2 - Further understand ABFT mixing patterns across the North Atlantic

4.2.1 Introduction

Previous analyses have shown that MED-like, GOM-like and genetically intermediate individuals co-occur in the North Atlantic feeding areas, with a larger proportion of MED-like individuals in the West than GOM-like individuals in the East. These findings challenge the assumption of two ABFT stocks separated by the 45ºW meridian line and highlights the importance of characterizing the migratory patterns and distribution of individuals born in the three known spawning areas to provide a complete set of plausible hypotheses about stock structure considering the data needed for the Management Strategy Evaluation (MSE) operational model.

The objective of this task is:

3. To **further understand the Bluefin tuna mixing patterns** by analyzing the distribution of the species genetic profiles.

4.2.2 Materials and Methods

a) Genetic origin assignment of Atlantic bluefin tuna individuals using the 96 SNP traceability tool.

The 96 SNP traceability panel designed during phase 6 to genetically assign Mediterranean or Gulf of Mexico origin was improved during phase 11 to substitute the worst performing 10 markers by newly generated markers including 3 sex markers. In total, 86 SNPs are common between both versions of the panel. We extracted genotype information of these 86 SNPs for all the samples that had been genotyped with both versions of the panel across all phases of the GBYP program (phases from 6 to 11). We also extracted this information from those individuals that had been sequenced using RAD-seq and genotyped with the SNP array. We used the individual ancestry estimations obtained as described in section 4.1.3 to identify the genetic profile of each genotyped sample. The baseline included as reference individuals captured at the Mediterranean Sea and the Gulf of Mexico and showing ancestral values fitting in the distribution of the larvae and young of the year ancestral values of their corresponding spawning area. Adult individuals were only included in the baseline if meeting size (fork length of >185 cm and > 135 cm for Gulf of Mexico and Mediterranean Sea individuals respectively) and catch season (from April to June in the Gulf of Mexico, from June to July for the western or central Mediterranean Sea, and from May to June for the eastern Mediterranean Sea) criteria for being considered spawners from their catch area. We assigned all the available genotyped individuals from different feeding aggregates along the North Atlantic using the Rannala and Mountain (1997) criterion (0.05 threshold) implemented in GENECLASS2 (Piry et al. 2004). For each individual assignment scores (*i.e.*, probability of belonging to each of the baseline populations) were calculated using a leave-one-out approach and using the different baselines excluding the sample being assigned for each calculation. Assignment rates were calculated considering only assignment scores >80%. A total of 3,242 adult samples captured at different feeding grounds in the North Atlantic were assigned as Gulf of Mexico, Mediterranean Sea, or unassigned origin. Proportion of assigned individuals segregated by area, year, age class and sex (when data available) were calculated.

b) Estimation of individual ancestral composition and distribution on inverted chromosomic region of albacore origin

Individual proportions of ancestral populations (assuming two ancestral populations, K=2) were estimated using ADMIXTURE (Alexander et al. 2009) based on the RAD-seq and SNP array combined dataset and the distribution of the values from each location were plotted.

We explored the distribution of the different variants on the potentially introgressed chromosomal inversion using the SNP array dataset generated during Phase 11. Three groups were identified based on individual ancestry proportions which would correspond with homozygous individuals for both versions and with heterozygous individuals carrying both versions.

4.2.3 Results and Discussion

a) Mixing patterns of genetically Mediterranean and Gulf of Mexico origin bluefin tuna across the Atlantic (subtask 2.1)

Proportion of origin assignment of feeding aggregates based on the newly filtered baseline revealed mixing at all the different ICCAT areas as expected, especially in the Western Atlantic (Figure 4.2.1), while mixing proportion slightly varied by catch year (Figure 4.2.2), age class (Figure 4.2.3) and sex (Figure 4.2.4).

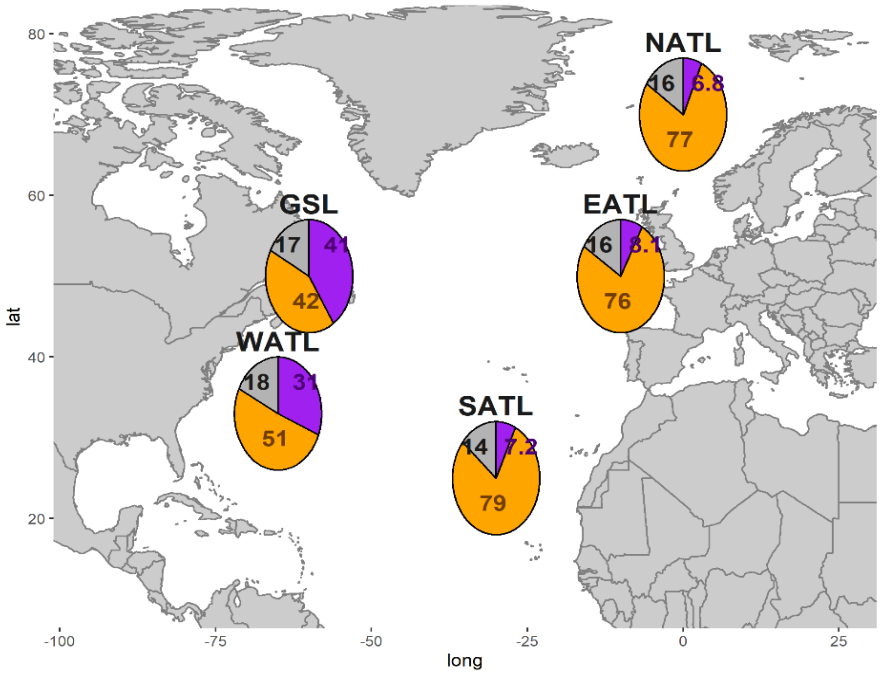

Figure 4.2.1. Proportion of samples assigned to Mediterranean (orange) or Gulf of Mexico (purple origin and unassigned (grey) from the different ICCAT areas (GSL= Gulf Saint Lawrence, WATL=West Atlantic, SATL=South Atlantic, EATL=East Atlantic and NATL=North Atlantic).

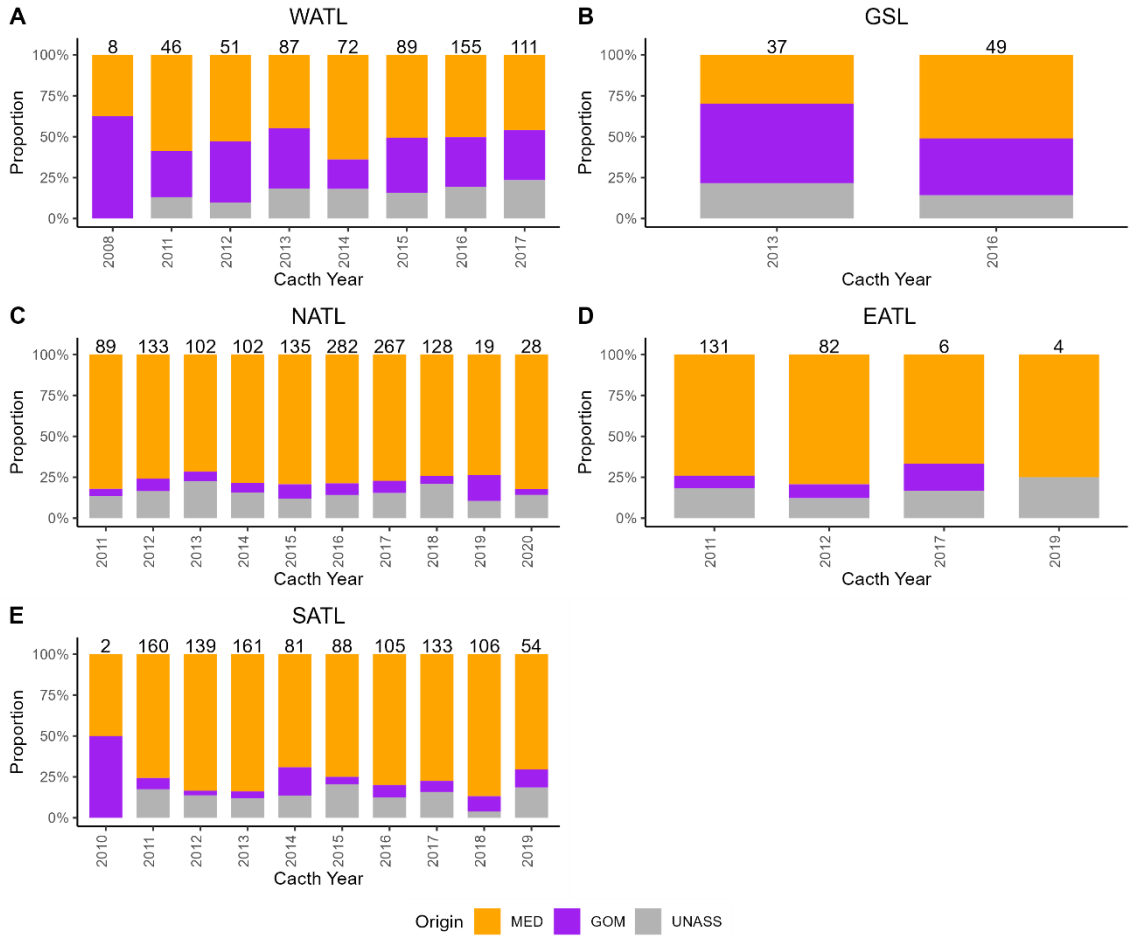

Figure 4.2.2. Proportion of samples assigned to Mediterranean (orange) or Gulf of Mexico (purple origin and unassigned (grey) from the different ICCAT areas (GSL= Gulf Saint Lawrence, WATL=West Atlantic, SATL=South Atlantic, EATL=East Atlantic and NATL=North Atlantic) and catch year.

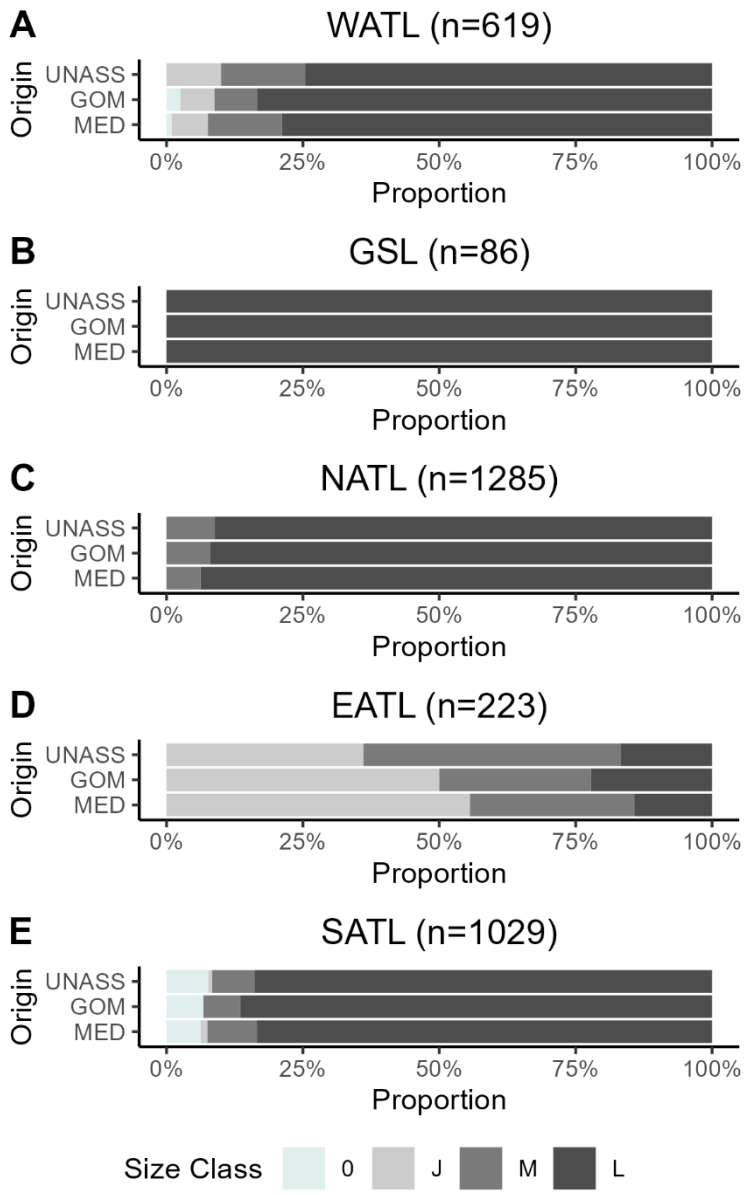

Figure 4.2.3. Proportion of samples assigned to Mediterranean (MED) or Gulf of Mexico (GOM) origin and unassigned (UNASS) from the different ICCAT areas (GSL= Gulf Saint Lawrence, WATL=West Atlantic, SATL=South Atlantic, EATL=East Atlantic and NATL=North Atlantic) and age class (0=Age 0 or <= 3kgs ; J=Juvenile or >3 & <= 25 kg; M=Medium or >25 & <=100kg and L=Large or >100kg).

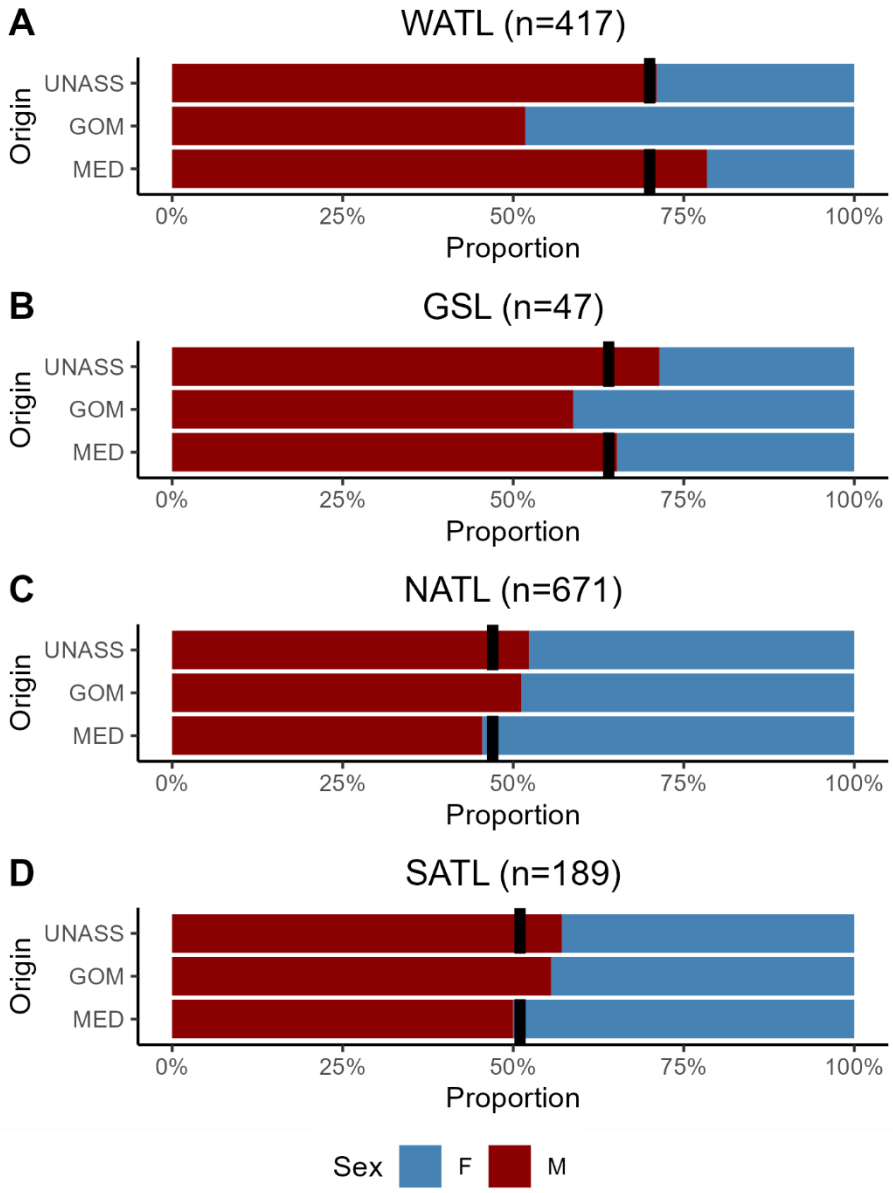

Figure 4.2.4. Proportion of samples assigned to Mediterranean (MED) or Gulf of Mexico (GOM) origin and unassigned (UNASS) from the different ICCAT areas (GSL= Gulf Saint Lawrence, WATL=West Atlantic, SATL=South Atlantic, EATL=East Atlantic and NATL=North Atlantic) and sex when the data was available (F=Female and M=Male). Vertical dotted line indicates sex ratio among included samples.

As shown by previous analysis there is a relatively high proportion of unassigned individuals. These unassignments could be due to a failure of the method or due to the presence of intermediate individuals whose genetic profile overlaps with the two reference genetic groups. Genetic profiles of the 1,132 individuals genotyped at 5,805 highly reproducible common SNPs were available from a combined dataset (obtained through RAD-seq and genotyping with the SNP Array) confirmed the presence of

intermediate individuals at most sampled regions (Figure 4.2.5), supporting that those individuals that were unassigned using the 96 SNP traceability panel could represent genetically intermediate individuals.

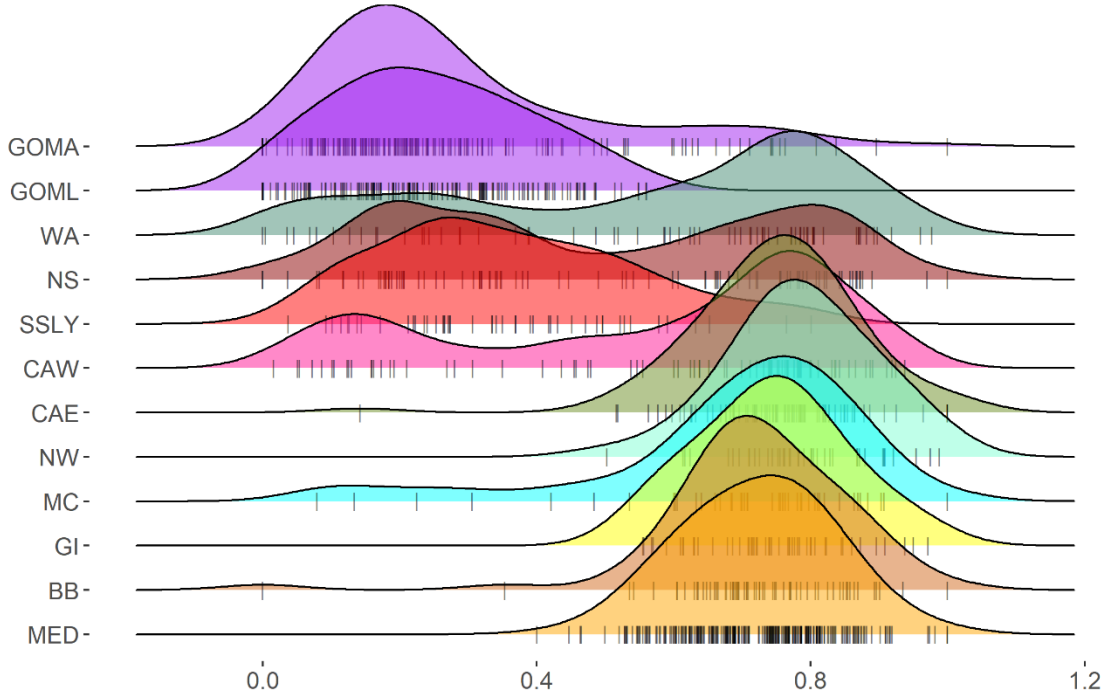

Figure 4.2.5. Distribution of the individual Mediterranean ancestry proportions obtained through a combined dataset of RAD-sequencing and SNP array derived genotype information. The different distributions correspond with individuals captured at different locations (MED = Mediterranean Sea, BB = Bay of Biscay, GI = Gibraltar, MC = Madeira, Canary Islands, NW = Norway, CAE = Central Atlantic - East, CWA = Central Atlantic -West, SSLY = Larvae and Young of the Year from the Slope Sea , NS = Nova Scotia, WA = Western Atlantic, GOML = Larvae from the Gulf of Mexico, GOMA = Adults from the Gulf of Mexico).

b) Frequency distribution of a presumably inverted genomic region or albacore origin across the Atlantic (subtask 2.2)

We explored the geographic distribution of the colinear and inverted versions of the potential inversion introgressed from albacore tuna. The most common version was always the presumably colinear (the not albacore-like) version, while the proportion of the inverted region varied geographically (Figure 4.2.6), the albacore origin haplotype being more frequent in the eastern Atlantic than in the western or southern Atlantic.

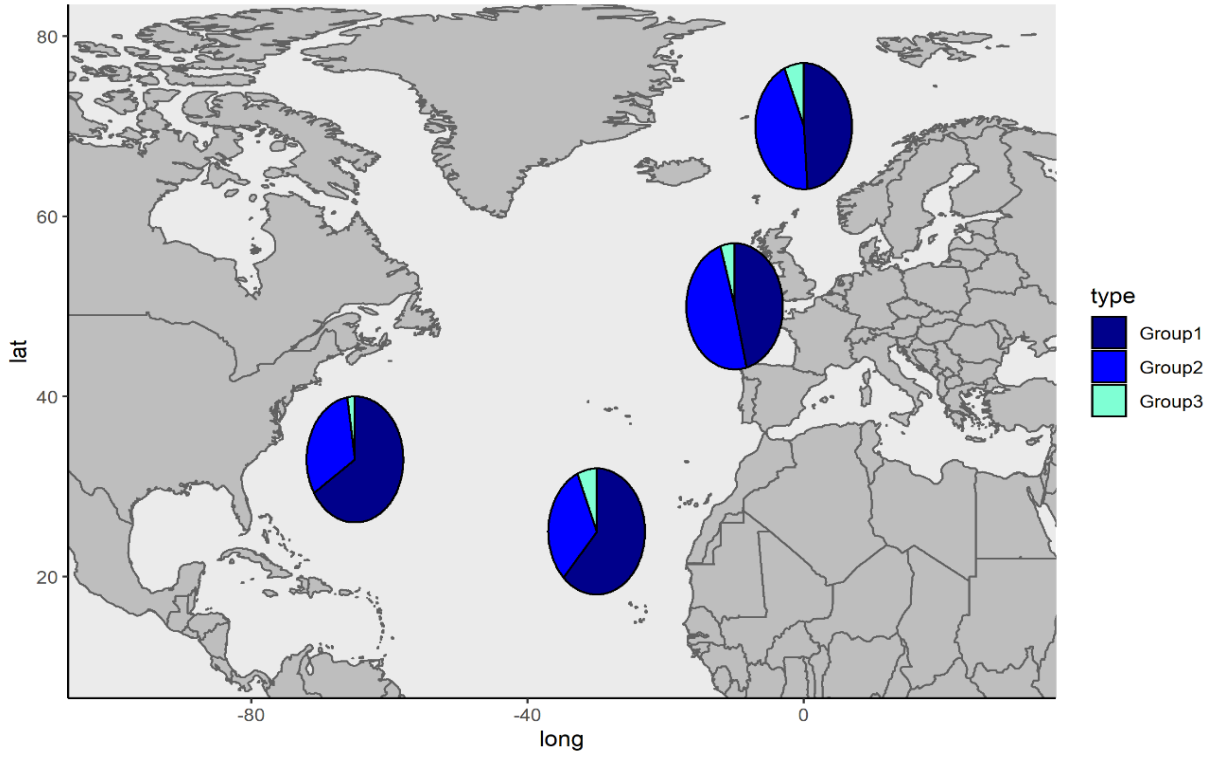

Figure 4.2.6. Proportion of homozygous for the collinear (the not albacore-like) haplotype version (dark blue), homozygous for the inverted (of albacore origin) haplotype (blue) version, and heterozygous (light blue) individuals across the different ICCAT areas.

Frequency distribution of the different combinations also varied across catch (Figure 4.2.7) and born (Figure 4.2.8) years in the different ICCAT areas. However, some sample sizes were too small as to find trends or make conclusions.

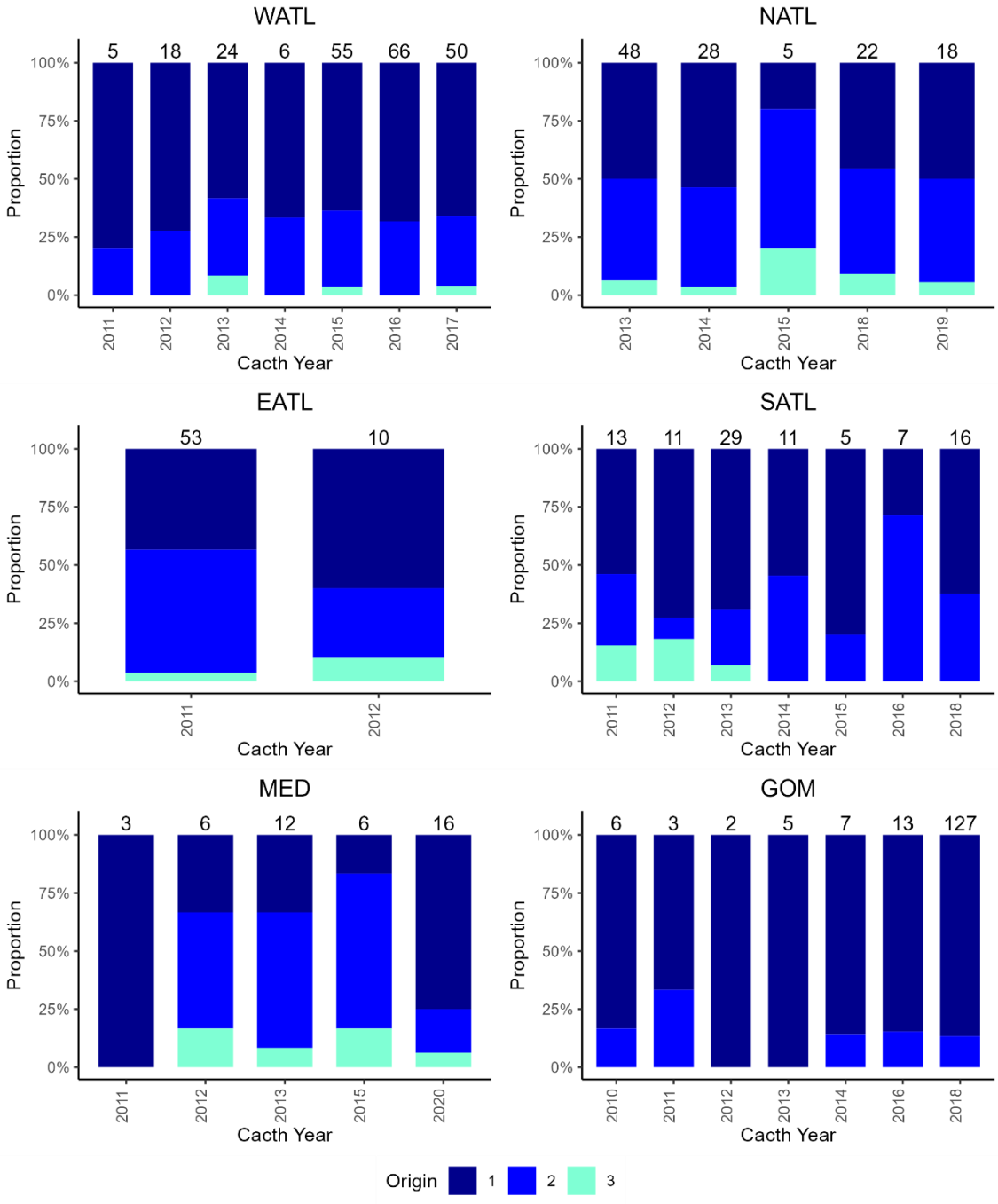

Figure 4.2.7. Histograms show the proportion of homozygous for the collinear (the not albacore-like) haplotype version (dark blue), homozygous for the inverted (of albacore origin) haplotype (blue) version, and heterozygous (light blue) individuals across the different ICCAT areas grouped per catch year.

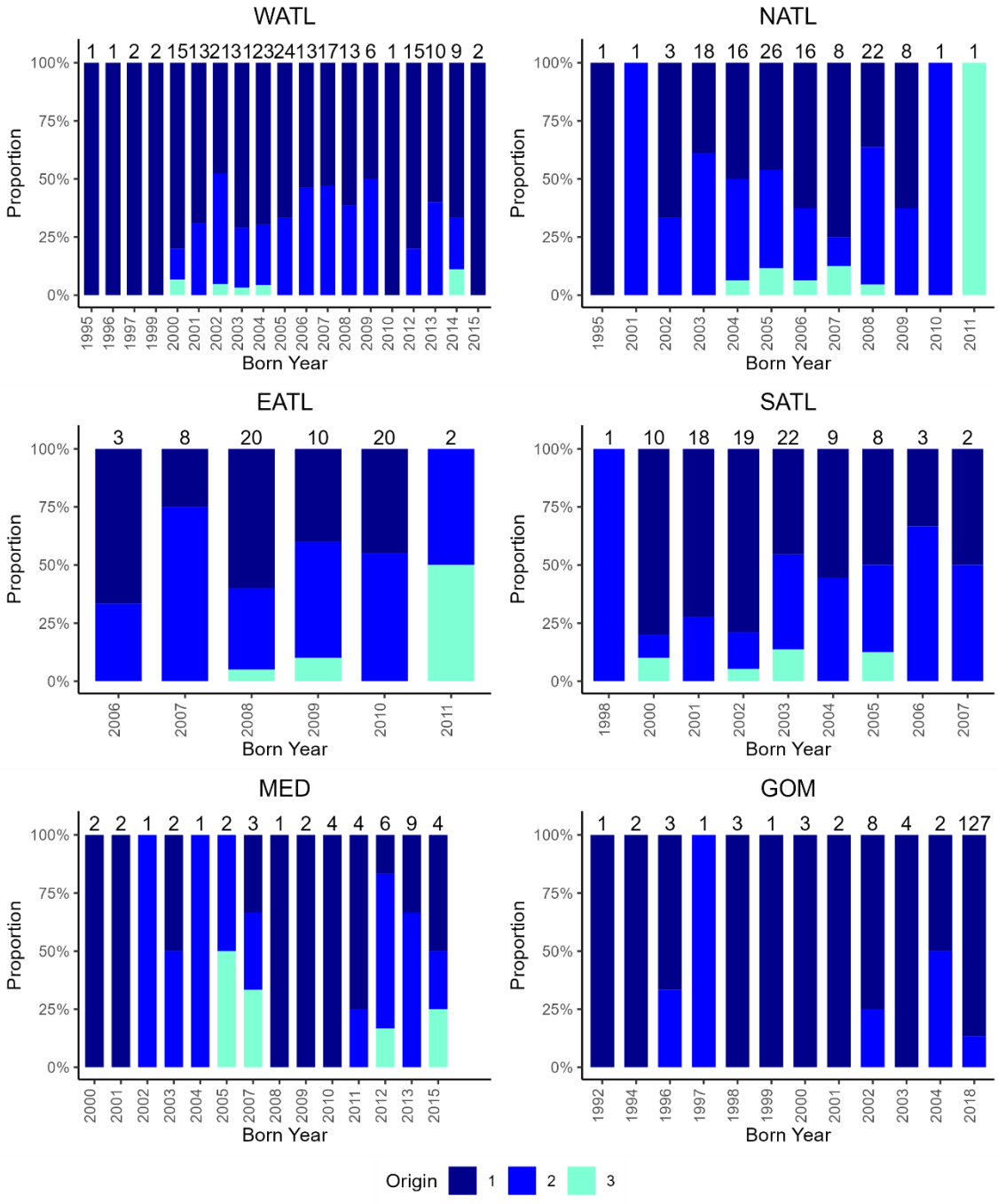

Figure 4.2.8. Histograms show the proportion of homozygous for the collinear (the not albacore-like) haplotype version (dark blue), homozygous for the inverted (of albacore origin) haplotype (blue) version, and heterozygous (light blue) individuals across the different ICCAT areas grouped per estimated born year.

4.2.4 Conclusions

Mixing of the different Atlantic bluefin tuna components along the North Atlantic:

- Genetic origin assignments of Atlantic bluefin tuna individuals from feeding aggregates captured at the different ICCAT areas genotyped with the 96 SNP

traceability panel from GBYP phase 6 to phase 11 are presented. The baseline wasfiltered based on the knowledge on the population structure acquired during the GBYP program and the assignments were performed based on the 86 common SNPs between the two different SNP datasets designed in phases 6 and 11 to include all available samples and the GBYP dataset has been updated with the results.

- New genetic origin assignments based on the genotypes obtained through the 96 SNP traceability tool of > 3,200 individuals captured at feeding aggregates showed varying mixing proportions of Mediterranean, Gulf of Mexico, and unassigned individuals across catch years, supporting the migratory patterns of Atlantic bluefin tuna are dynamic.
- The frequency of occurrence of the putative chromosomal inverted region of albacore origin was explored across the different ICCAT areas, being the introgressed version much more common in the North East and eastern Atlantic, where more than half of the individuals carried at least one copy, and less common in the Gulf of Mexico and the West Atlantic. The frequencies vary across catch year and year classes, but no clear pattern could be observed with the currently available sample size.

4.3 Subtask 3 - Developing methods in support to application of CKMR to Eastern ABFT

4.3.1 Introduction

The conservation of the ABFT relies on an adequate management of the species, for which biomass estimation of the stocks is necessary. Close-Kin-Mark-Recapture (CKMR) has been probed as a very useful tool for estimation of the abundance of southern bluefin tuna (Bravington et al. 2016) among other species. The successful application of this method relies on a good knowledge of the population structure of the species, the development of cost-effective genotyping tools for the genetic detection of kin pairs in the populations, and age and sex determination, among others. Efforts to understand the population structure of the species are making great progresses (see above) and development of an approach based on epigenetic analyses for age determination are ongoing. Therefore, here we focused on evaluating the minimum number of genetic markers needed to be included in

routinary genotyping for kin pair detection for CKMR analyses and on developing an efficient method to genetically identify sex in ABFT individuals.
During the execution of subtask 4.3, a total of 384 samples were prepared and sent for genotyping to ThermoFisher facilities in USA preserved in dry ice. The parcel was held within the shipment company facilities for more than a week without dry ice refilling due to extreme weather conditions. As a consequence, the samples were lost and the sample preparation and shipment had to be repeated. The second time the samples were sent to a closer facility in the UE, which made the shipment more efficient. This unfortunate event derived into consequent delay on this and other subtasks.

The objectives of this task are:

4. To assess the minimum number of genetic markers required for the **cost-effective identification of kin pairs** for future CKMR studies
5. To **evaluate the assignment accuracy of genetic markers** for sex determination in Atlantic bluefin tuna individuals.

4.3.2 Materials and methods

a) DNA extraction

DNA of 384 new samples was extracted. Among them 359 were larvae and 55 Young of the Year from the Mediterranean Sea. Regarding to the larvae, due to the small amount of tissue available, DNA was extracted from the entire specimen. All larvae were of less than 8mm, which corresponds with the category of preflexion or intermediate, and therefore these are not expected to have predated over other larvae of their same species which could be confounded with sample contamination during genetic analysis. DNA was extracted using the Wizard® Genomic DNA Purification kit (Promega, WI, USA) following manufacturer´s instructions for "Isolating Genomic DNA from Tissue Culture Cells and Animal Tissue". The starting material was approximately 20 mg of tissue or whole larvae and after extraction all samples were suspended in equal volumes of Milli-Q water. DNA quantity (ng/µl) was evaluated on the Qubit® 2.0 Fluorometer (Life Technologies) and DNA integrity was assessed by electrophoresis.

b) SNP Array genotyping and kinship analysis

In total, 384 DNA samples (all newly extracted) were genotyped with the 10,000 SNP array developed in Phase 10, including 359 larvae collected at three nearby stations from the Balearic Islands area an identifying within the GBYP phase (Table 4.3.2.2) and 55 young of the year from the Mediterranean Sea. Larvae were selected maximizing the number of samples included from the same station and if not possible from nearby stations.

Table 4.3.2.2. Number of larvae samples from each surveyed station genotyped using the SNP Array.

Station	n
Station 794	264
Station 882	23
Station 42	42
TOTAL	359

Genotypes were analyzed and assessed using Axiom Analysis Suite specific software setting default parameters. Individuals and genetic markers which did not met minimum quality standards were removed from the dataset following the Axiom Analysis Best Practices Workflow. The final genotype table including neutral markers informative for genetic origin and kinship analysis was exported to plink format and SNP markers with a minimum allele frequency lower than 0.02 were removed using PLINK software (Purcell et al. 2007) to avoid the presence of not informative markers. Different tables were then generated including random subset of 500, 1000, 1100, 1200, 1300, 1400, 1500, 1600, 1700, 1700, 1800, 1900, 2000, 3000, 4000, 5000, 6000 and all available markers. Pairs of half sibling pairs were identified using the R package kinference (Bravington, in prep.), based on the distribution of pairwise PLOD scores and their fit into the predicted values for unrelated and related pairs. Sampling individuals from the same cohort we expect to find either half or full sibling pairs. Therefore, genetic relatedness between pairs was calculated using PLINK software (Purcell et al. 2007) and pairs of samples with relatedness above 0.7 (expected relatedness between full sibling pairs would be 0.5) were suspicious from belonging to the same sample and were excluded from the analysis. Additionally, deviation from expected heterozygosity (F coefficient above 0.15) was estimated for all samples in order to detect cross contamination.

c) Evaluation of sex markers

Sex of 50 samples already genotyped using the new version of the 96 SNP traceability tool which includes three sex markers adapted from Suda et al. (2019) was confirmed through visual histological inspection of their gonads, which were previously preserved in formalin.

4.3.3 Results and discussion

a) Assessing the minimum number of markers for kinship analysis (subtask 3.1)

The final complete genotype dataset contained 359 individuals and 6,669 neutral markers. In total, 4 half and one full sibling pairs were detected using the complete dataset between larvae from the most sampled station. Two pairs of samples between two larvae from the same station and between two young of the year with high values of genetic relatedness (0.93 and 1.02 respectively) were likely to belong to the same sample and were excluded from the analysis, while no contaminated samples were detected. PLOD values estimated for the 4 half sibling pairs were 138, 185, 206 and 308, and for the full sibling pair was 553. The PLOD distribution plot suggested clean grouping of unrelated samples fitting the expected distribution, while detected kin pairs fall near the expected PLOD values for half and full sibling pairs, indicating accurate kin inference (Figure 4.3.1).

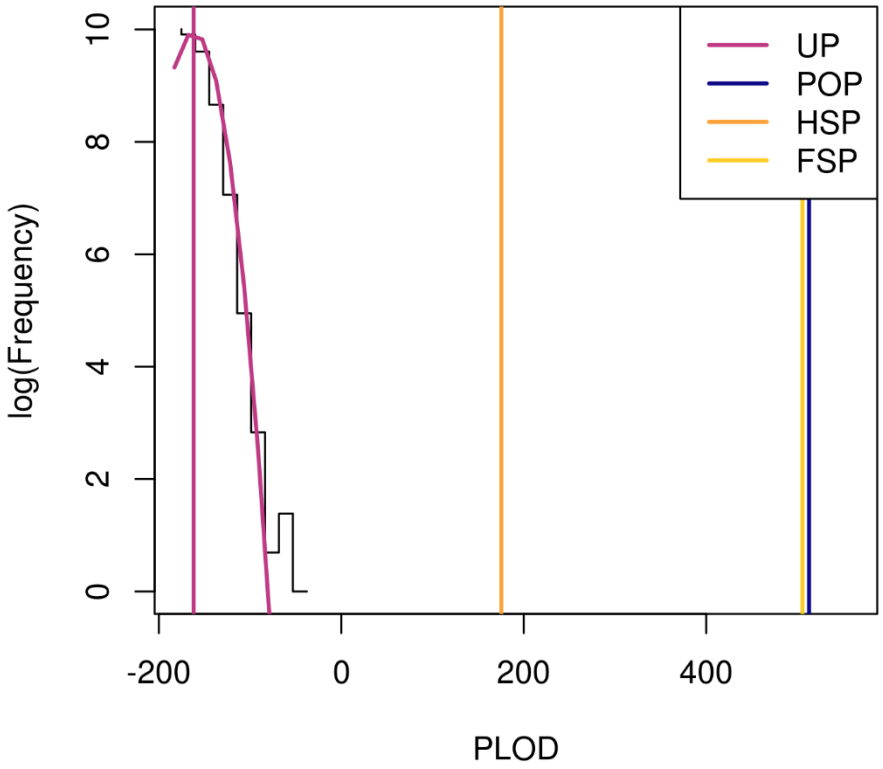

Figure 4.3.1. Histogram showing the distribution of the PLOD values estimated for each individual pair. The magenta line represents the expected distribution of unrelated pairs (UP), the orange, yellow and blue vertical lines show the expected PLOD value for half sibling pairs (HSP), full sibling pairs (FSP) and parent-offspring pairs (POP).

Kin detection with lower number of SNPs derived into increasing and inconsistent detection of kin pairs. While pairs inferred with datasets including 2,000 SNPs or more consistently provide with the same kin pairs, while datasets including lower number of SNPs resulted into different sets of detected pairs and higher number of detected relatives (Figure 4.3.2). These results suggest that 2,000 is the minimum recommendable number of SNPs for kin detection among eastern Atlantic bluefin tuna.

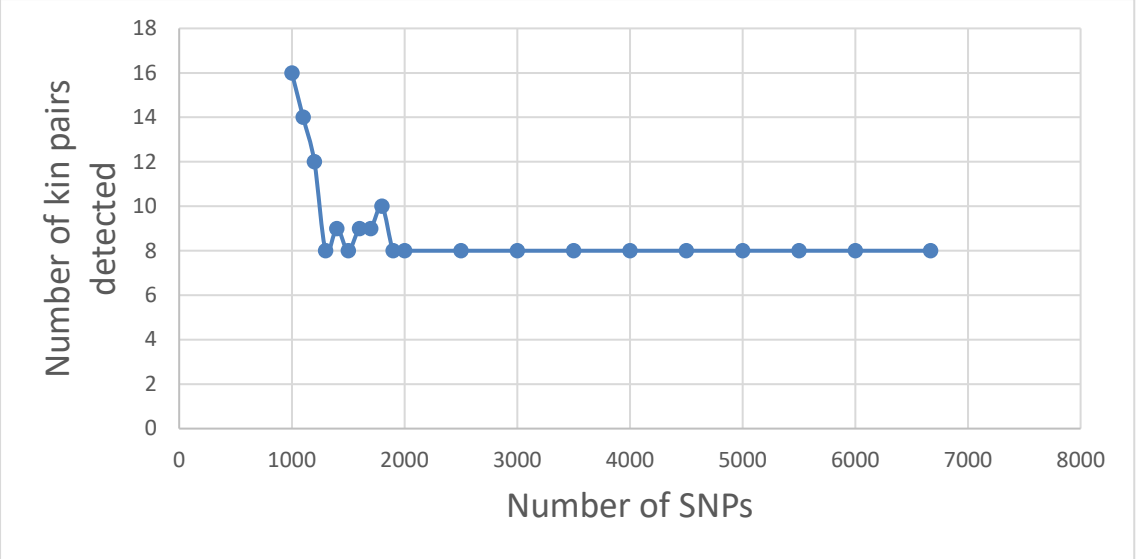

Figure 4.3.2. Plot showing the number of relatives detected (y axis) using sets of increasing number of SNPs (x axis). The dataset including 500 SNPs resulted in detection of 177 kin pairs.

b) High correct sex assignment rates based on genetic markers (subtask 3.2)

The markers included in the 96 SNP traceability panel correctly assigned the 94% of the samples for which sex has been confirmed through gonad histological inspection (Figure 4.3.3).

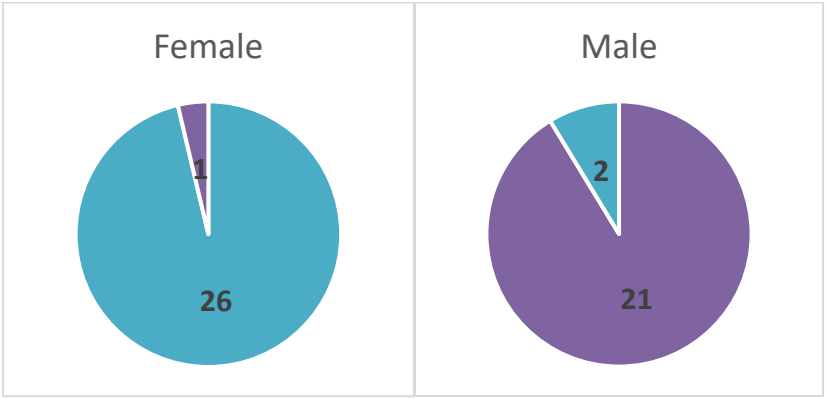

Figure 4.3.3. Pie charts show number of samples for which genetic sex was assigned as female (blue) and male (orange). Left and right plots include samples for which sex was assigned based on gonad histology inspection as female (left) and male (right).

These high correct assignment rates based on genetic markers will allow sex identification of Atlantic bluefin tuna individuals for which assignment based on visual inspection would be impossible, such as immature individuals, without necessity of accessing to the gonads. These markers, included in the 96 SNP traceability panel and in the SNP array, will allow to assign sex of individuals routinarily genotyped with these two approaches developed for origin assignment and kinship analysis among others, being of great relevance to improve the information available for CKMR models.

The percentages of correctly assigned male individuals estimated on samples for which phenotypic sex was confirmed through histological inspection improved compared to those referenced using sex data stored in the GBYP database improved from 80% (see report of Phase 11) to 91.3%, while the percentage of correctly assigned females remained similar, varying from 96.7% to 96.3% (see report of Phase 11). This could mean that the sex information of a small percentage of individuals of the GBYP database is wrong. However, these results are based on a small number of individuals and therefore it would be advisable to increase the sample size to obtain robust conclusions.

4.3.4 Conclusions

Cost-effective tools for kin pair identification for future CKMR studies:

- The custom SNP array designed to genotype more than 8,000 SNPs in Atlantic bluefin tuna samples for population structure, CKMR and genomic adaptation analyses was probed as a valid tool for kin pair detection among eastern samples. In total four half and one full sibling pairs were identified among 359 sample set, which mainly included larvae from the Balearic Island captured in 2020.
- The minimum number of SNP markers required to detect all sibling pairs present in the dataset was 2,000 SNPS. We therefore conclude that this is the minimum amount of SNPs among those included in the custom SNP array needed for effective kin finding among eastern individuals.
- The sex markers successfully included in the 96 SNP traceability panel and the custom SNP array will allow to correctly identify sex of all routinely analyzed samples at a 94% correct rate. This sex assignment rate was confirmed on 50 individuals; therefore we recommend it is validated in an higher number of samples.

References

Alexander, D. H., J. Novembre, and K. Lange. 2009. Fast model-based estimation of ancestry in unrelated individuals. Genome research 19:1655-1664.

Bolger, A. M., M. Lohse, and B. Usadel. 2014. Trimmomatic: a flexible trimmer for Illumina sequence data. Bioinformatics 30:2114-2120.

Bravington, M. V., P. M. Grewe, and C. R. Davies. 2016. Absolute abundance of southern bluefin tuna estimated by close-kin mark-recapture. Nature Communications 7:13162.

Danecek, P., A. Auton, G. Abecasis, C. A. Albers, E. Banks, M. A. DePristo, R. E. Handsaker, G. Lunter, G. T. Marth, S. T. Sherry, G. McVean, R. Durbin, and G. P. A. Group. 2011. The variant call format and VCFtools. Bioinformatics 27:2156-2158.

Garrison, E. P., and G. T. Marth. 2012. Haplotype-based variant detection from short-read sequencing. arXiv: Genomics.

Guan, Y. 2014. Detecting Structure of Haplotypes and Local Ancestry. Genetics 196:625-642.

Hernández, C. M., D. E. Richardson, I. I. Rypina, K. Chen, K. E. Marancik, K. Shulzitski, and J. K. Llopiz. 2022. Support for the Slope Sea as a major spawning ground for Atlantic bluefin tuna: evidence from larval abundance, growth rates, and particle-tracking simulations. Canadian Journal of Fisheries and Aquatic Sciences 79:814-824.

Jombart, T., and I. Ahmed. 2011. adegenet 1.3-1: new tools for the analysis of genome-wide SNP data. Bioinformatics 27:3070-3071.

Li, H. 2013. Aligning sequence reads, clone sequences and assembly contigs with BWA-MEM. arXiv preprint arXiv:1303.3997.

Li, H., B. Handsaker, A. Wysoker, T. Fennell, J. Ruan, N. Homer, G. Marth, G. Abecasis, R. Durbin, and G. P. D. P. Subgroup. 2009. The Sequence Alignment/Map format and SAMtools. Bioinformatics 25:2078-2079.

Marandel, F, Lorance, P, Berthelé, O, Trenkel, VM, Waples, RS, Lamy, J-B. Estimating effective population size of large marine populations, is it feasible?. *Fish Fish*. 2019; 20: 189– 198. https://doi.org/10.1111/faf.12338

Patterson, N., P. Moorjani, Y. Luo, S. Mallick, N. Rohland, Y. Zhan, T. Genschoreck, T. Webster, and D. Reich. 2012. Ancient Admixture in Human History. Genetics 192:1065-1093.

Piry, S., A. Alapetite, J.-M. Cornuet, D. Paetkau, L. Baudouin, and A. Estoup. 2004. GENECLASS2: A Software for Genetic Assignment and First-Generation Migrant Detection. Journal of Heredity 95:536-539.

Purcell, S., B. Neale, K. Todd-Brown, L. Thomas, M. A. R. Ferreira, D. Bender, J. Maller, P. Sklar, P. I. W. de Bakker, M. J. Daly, and P. C. Sham. 2007. PLINK: A Tool Set for Whole-Genome Association and Population-Based Linkage Analyses. The American Journal of Human Genetics 81:559-575.

Racimo, F., S. Sankararaman, R. Nielsen, and E. Huerta-Sánchez. 2015. Evidence for archaic adaptive introgression in humans. Nature Reviews Genetics 16:359-371.

Stapley, J., P. G. D. Feulner, S. E. Johnston, A. W. Santure, and C. M. Smadja. 2017. Variation in recombination frequency and distribution across eukaryotes: patterns and processes. Philosophical Transactions of the Royal Society B: Biological Sciences 372:20160455.

Suda, A., I. Nishiki, Y. Iwasaki, A. Matsuura, T. Akita, N. Suzuki, and A. Fujiwara. 2019. Improvement of the Pacific bluefin tuna (Thunnus orientalis) reference genome and development of male-specific DNA markers. Scientific Reports 9:14450.

van der Auwera, G., and B. D. O'Connor. 2020. Genomics in the Cloud: Using Docker, GATK, and WDL in Terra. O'Reilly Media, Incorporated.

5. DIRECT AGEING

Task leader: Enrique Rodriguez-Marín (IEO-CSIC)
Participants:
AZTI: Patricia Lastra Luque
IEO-CSIC: Pablo Quelle
SABS-FOC: Dheeraj S. Busawon

5.1 Review on current status of Atlantic bluefin tuna direct ageing.

5.1.1 Introduction

Atlantic bluefin tuna (Thunnus thynnus; ABFT) is a large scombrid that can reach nearly 4 meters in length and 700 kg in weight. It is capable of large migrations, being able to move from one side of the Atlantic Ocean to the other in less than a month and is distributed throughout much of the North Atlantic and the Mediterranean Sea (Rooker et al., 2007; Murua et al., 2017). The high value of fresh ABFT since the 1980s, with the rise of the sashimi market, has made this tuna of great commercial importance. Its fishing has been documented since before Christ and it is currently a fishery resource exploited by many countries. All these factors and the history of east Atlantic bluefin tuna stock overfishing and the recent improvement in stock status following the implementation of the rebuilding plan have turned this species into an icon whose management is receiving international attention (Mather et al., 1995; Fromentin et al., 2014).

Studies on fish growth are essential to describe their life cycle and to adopt correct fishery management measurements. The ABFT has a life span of about 40 years, it starts reproducing at 3 years of age, its movement capacity increases with age performing more extensive migrations both horizontally and vertically, and it is exploited in different age ranges depending on the type of gear and fishing area (Fromentin and Powers, 2005; Murua et al., 2017; Medina, 2020). The examination and reading of calcified structures (CS) including otoliths, spines (first spiny ray of the first dorsal fin), vertebrae and scales (Figure 5.1.1) has been one of the most frequent methods to estimate the age and growth of ABFT. The estimation of accurate, validated growth rates from CS has been used to identify overestimation of bluefin tuna population productivity, which has allowed more

accurate estimates of population size and mortality and, thus, availability for its exploitation (Kalish et al. 1996; Gunn et al. 2008; Neilson and Campana 2008).

Fisheries management for this species is carried out by the International Commission for the Conservation of Atlantic Tunas (ICCAT) in two management units: the western Atlantic and the eastern Atlantic Ocean and the Mediterranean Sea stocks. Growth studies of both stocks have historically been carried out independently and show small differences, but it is quite possible that these differences are due to sampling coverage, ageing techniques, and modeling methodologies. In fact, there are studies that have obtained almost identical growth parameters or show that there are no differences in the growth of both management units (Restrepo et al. 2010; Luque et al., 2014; Stewart et al., 2022).

There have been workshops in the past that have dealt with different methods for estimating ABFT growth (Hunt et al, 1978; Anon, 1983), but it has been in the last 20 years that direct ageing studies have been carried out in a coordinated manner among all the laboratories involved in the ageing of this species on both sides of the Atlantic. This coordination has definitely been favored by the ICCAT Atlantic Bluefin Tuna Research Program (GBYP) and has served to develop standardized protocols for the preparation and reading of CS, mainly on otoliths and spines, through several aging workshops and exchanges, which has allowed the readings performed in the different laboratories to apply the same methodology (Rodriguez-Marin et al., 2007; 2020; Busawon et al., 2020).

The aim of the present paper is to provide a comprehensive review on the methodology of direct age estimation and validation and represents a collation of the state-of-the-art scientific work on direct age estimation of ABFT.

5.1.2 Considerations to be applied for direct ageing: methodological issues to be considered with calcified structures.

Estimates of the annual age and growth of commercial species are necessary in the age structured models, which are applied to obtain catches at age from catches at length, and which are used in the assessment of the stock status. Using biased age or growth estimates in stock assessment will lead to biased estimates of stock biomass and mortality and will therefore cause a biased view of the dynamics and status of the stock, with consequent repercussions on resource management (Campana, 2001; Kolody et al., 2016).

Both different concepts, accuracy and precision of age data, are needed to avoid these subsequent problems in the stock assessment process and management (Beamish and Mcfarlane,1983; Campana, 2001). Errors in the age estimation can affect the accuracy, or the closeness of the age estimate to the true value, and the precision, or the reproducibility of repeated measurements on a given structure (Kalish et al., 1995; Campana, 2001). All age estimation methods aim to be accurate, precise and also practical. Reliable data are especially necessary when stock levels are low and errors in predictions can have devastating effects on the resources (Appelberg et al., 2005). The available methods for quantifying ageing accuracy and precision were detailed (Campana, 2001; Panfili et al., 2002) and the types of CS and the different methodologies of preparation, examination and conservation of the same were also explained in several works (Panfili et al., 2002).

In the case of the CS-based age estimation method, different aspects must be considered to successfully use it for age monitoring to support stock assessment. As follow: i) the initial having the appropriate age determination method, ii) its age validation, iii) have the reference collection of the CS and iv) a quality control monitoring (Campana & Thorrold, 2001; Campana et al., 2001).

a) Validation (accuracy) and corroboration.

Age validation is the process of affirming the temporal scale that opaque and translucent growth bands are deposited in fish CS to accurately determine age (Beamish and McFarlane, 1983). The positive result obtained after performing age validation studies is substantial, gaining accuracy and confidence in the age estimation (Appelberg et al., 2005), being the validation of the age estimation emphasized to be carried out since decades ago (Beamish and McFarlan, 1983; Casselman, 1989). Age validation should be a mandatory issue in all age estimation studies (Vitale et al., 2019). However, it certain requires time, valuable samples, and resources.

Age validation can be distinguished from age corroboration and, in turn, validating the periodicity of growth increment formation (VP) is also different than validating the absolute age (VA). Thus, validation of an absolute age is equivalent to determining the accuracy of an age estimate, that is, the closeness of the age estimate to the true value (Campana, 2001). Validating the periodicity of growth increment can be considered as a part of the validation process of the age, either referred to that the periodicity of some ages is validated, or that it refers to only a partial validation of the ageing method (Beamish and McFarlan, 1983; Kalish et al., 1995; Campana, 2001). On the other hand,

corroboration methods support or are correlated with a particular method of ageing, but are not directly or logically linked (Campana, 2001). The different methods of age validation and corroboration are grouped in other studies as methods of direct, semi-direct and indirect validation of age (Panfili et al., 2002).

Several age validation methods have been described (Campana et al., 2001), being of less general use than those of age corroboration and of which the following could be highlighted in tuna species: i) Marginal increment analysis: validates VP and requires samples from throughout year. It is the most commonly used validation method and provides that the pattern of alternating opaque and translucent growth zones observed in CS is seasonal and predictable (i.e. annual) (Vitale et al, 2019); ii) Bomb radiocarbon: validates VA and VP, but requires at least some of fish in sample must have been hatched before 1965, being it difficult and the method, expensive.

More age corroboration methods have been applied in tuna and other species, some of the most used being: i) Length frequency analysis: provides growth estimates mainly for the first age groups where the modal classes are more easily differentiated, but no age validation since there is no confirmation that the identified modes correspond to any age classes. Length information of fish is frequently available for many species. Size-selective migration into or out of the study area is not an allowable assumption, therefore having inconvenience for migratory species (Campana et al., 2001); ii) Tagging-recapture: provides growth estimates between the time of tagging and recapture for well-sampled ages, but no age validation since none of the recaptured fish are of known age; requires large-scale tagging to recapture enough fish that have been free for a long period to provide useful data (Campana et al., 2001); iii) Tracking strong year-classes over a long period of time, but strong (or weak) year-classes tend to disappear from the catches at age and year matrix, so it is more difficult to apply at older ages (Campana et al., 2001); iv) Daily increments between annuli: valuable for identifying 1st annulus and presupposes knowledge of dates of hatch and annulus formation. Daily increment formation must also be usually assumed (Campana et al., 2001); v) Microchemistry corroborates the seasonal frequency of CS macrostructure features through tracking the seasonally varying incorporation rates of different microconstituents and stable isotopes (Vitale et al., 2019).

Regarding the back-calculation, it consists in estimating fish length at an earlier time on the basis of a set of measurements of CS size and fish length made at a single point in time (Francis, 1990). It is useful for estimating lengths at ages that are rarely observed (e.g. not recruited young ages) (Francis, 1990). It is not a method of age validation or

corroboration, but it shows consistency in the interpretation of the sequence of growth increments, independent of whether or not the interpretation is correct (Campana et al., 2001).

b) Standardization (protocols for preparing and reading & reference collections)

The routine age estimation in several stocks still depends on skills and experience of individual age readers, and standardized age estimation criteria lacks. However, significant progress has been made in those mainly studied within international organizations such as ICCAT or ICES in recent decades (Appelberg et al., 2005; Luque et al., 2014; Rodriguez-Marin et al., 2020).

Precision is defined as the reproducibility of repeated measurements on a given structure, whether or not those measurements (age readings) are accurate (Campana et al., 2001). Several measures of aging precision are used, the first two being the most widely used and having a direct relationship between them: i) Average percent error (APE); ii) Coefficient of variation (CV) is the ratio of the standard deviation over the mean; iii) Percent agreement (PA) among readers, is the ratio between the number of coincident readings and the total number of readings, that varies widely among ages, not being considered an index as adequate as both previous ones (Beamish & Fournier, 1981; Chang, 1982)

Quality control (QC) monitoring is the process of inspection and measurement used to detect ageing errors or inconsistencies in a timely manner during the age estimation process (Campana et al., 2001). The precision in the routine age estimation process is improved by QC monitoring: establishing protocols, reference CS collections, repeated age readings by the same reader or group of readers, and comparison among age readers and with experts in otolith exchanges and workshops (Vitale et al, 2019).

Reference CS collection of prepared ageing structures, of known or agreed estimate ages (from age validation studies or agreed among international experts), representative of all factors (age, sex, season, area, etc.), which might influence the appearance or relative size of the growth increments. A reference collection is relevant for: i) monitoring age estimation consistency over both the short and long term, as well as among age readers; ii) training of new age readers (Campana et al., 2001). The use of a collection of digital images facilitates CS ageing exchanges.

Age verification: exchanges of CS and workshops. Verification confirms the consistency of the age estimation, i.e. the repeatability or precision of a numerical interpretation that may be independent of age (Panfili et al., 2002). Aforementioned indices of precision (CV, APE and PA) among age readers participating are estimated both globally and for each factor analyzed, such as the type of CS used, preparation methodologies, areas, quarters, etc are analyzed in the CS exchanges and workshops. Another measure related to accuracy, usually the relative bias, is also estimated. It is the systematic over- or underestimation of age relative to the modal age (Eltink et al., 2000).

5.1.3 Calcified structures used.

The premise is that hard parts grow proportionally to fish length and that periodic marks (e.g. daily and yearly) are deposited at regular intervals. In general, otoliths are the preferred CS for ageing as they are not subject to vascularization (fin spines), regeneration/demineralization (scales) and indistinguishable banding (vertebrae).

a) Otoliths

This section will review the state of knowledge of otolith direct ageing for Atlantic bluefin tuna (ABFT). Validation of periodicity of marks are essential for accurate age determination. Direct validation methods include known age fish, marking of hard parts and radiocarbon dating. Furthermore, three levels of validation have been suggested to better describe the term "validation" (Francis 1995, Murua et al., 2017). Murua et al. 2017 summarized the published studies which validated daily or annual increment formation in hard parts of tuna species and noted that accuracy of annual age estimates derived from ABFT otoliths were validated with bomb radiocarbon (Neilson and Campana 2008) and by examining the periodicity of annulus formation (Siskey et al. 2016). Radiocarbon dating validated ages from 5 to 32 years old and had the highest validation level-based Francis's criteria (Francis 1995). Marginal increment analysis has been used recently, to establish the timing of band deposition (Rodriguez-Marin et al., 2022).

The use of non-standardized processing and ageing methods could also be an important source of bias, as different laboratories and readers could have varying interpretations. Therefore, reliable growth estimates must involve standardized methods and inter-laboratory comparisons with reference collections. Several workshops and calibration exercises addressing otolith processing methods and direct ageing protocols for ABFT have been carried out in order to reduce ageing bias and standardize otolith ageing for

ABFT (Hunt et al. 1978; Prince and Pulos 1983, Rodriguez-Marin et al. 2007, Secor et al. 2014, Busawon et al. 2015, Busawon et al. 2018, Rodriguez-Marin et al. 2019 and Rodriguez-Marin et al. 2020).

Standardization of otolith processing examined various potential sources of bias: 1) Section location, thickness and type (V vs. Y sections): A number of calibration exercises showed an ageing bias when using different section location, thickness and type along the otolith. 2) Light type (transmitted vs. reflected): no ageing bias was found between light types. However, it was found that edge type agreement was higher when using transmitted light. And 3) Standard imaging protocols: varying magnifications were found to be a potential source of ageing bias.

Standard otolith reading protocols were developed to limit interpretation bias: 1) Development of aids (yardstick and a template): Age estimations of younger fish was highly uncertain due to the diffuse nature of the otolith marks and high frequency of false annuli. These aids were developed based on annual band measurements of young of the year otoliths to identify the approximate location of the first annuli. The template identifying the first 5 annuli was derived from measured growth increments on expert agreed annotated images. 2) Annuli identification: description of what would constitute an annulus (e.g., annulus has to span the whole ventral arm) in each zone of the otolith was described. 3) Edge type: edge type identification was identified as a source of bias, as readers have little agreement during the various calibration exercises. 4) Standard measurement/reading lines: Standard landmarks and methods were developed to measure annual growth increments which facilitate identification of ageing bias and growth analysis (e.g., back calculation). 5) Development of an annotated image reference collection for reader calibration.

Standardization of age estimates has allowed for improved growth estimates for ABFT. Ailloud et al. (2017) were the first to use standardized age estimates and tagging data which resulted in improved fitting of the Western Atlantic bluefin tuna growth curve. However, at the 2017 ABFT stock assessment a bias in juvenile age estimates was detected in the age length data used by Ailloud et al. (2017). To address this issue, a workshop was held and resulted in updated standardized protocols (Rodriguez-Marin et al. 2020). In 2022, Stewart et al. (2022) developed a back-calculation method using age estimates on standardized otolith sections, and applied mixed-effects growth models to derive an updated growth curve for ABFT. Since back-calculation estimates fish length at age prior to capture, this method has the advantage of providing estimates of fish not

commonly observed and providing increased quantity of length at age data (Murua et al. 2017). It should be noted that the derived growth coefficient (k) from Stewart et al. (2022) is similar to Butler et al. (1977 females) and Neilson & Campana (2008) but lower than most studies using otoliths with Restrepo et al. (2010) having the lowest k. In terms of $L\infty$, Stewart et al. (2022) has the second highest asymptotic size with Restrepo et al. (2010) having the highest.

Recently, standardization protocols were further improved by addressing the remaining controversy regarding seasonality of growth band deposition which influences age estimations and conversion of annuli count to age. Rodriguez-Marin et al. (2022) applied marginal increment analysis to examine timing of band formation. The study indicated that opaque band formation begins in June and is completed by the end of November which resulted in a change in the adjustment criterion from July 1st to November 30th to convert annuli count to age estimates.

Over the past decades, standardization of protocols to process and age ABFT otoliths has made some significant strides which should result in direct age estimates being incorporated in population dynamic models in the near future. However, it is essential to maintain inter-laboratory and inter-reader calibrations to ensure that standards are maintained and assess if further standardization are required.

b) First fin spine of the dorsal fin.

Direct ageing using the fine spine remain to be directly validated in ABFT and certainly limits its use for aging purposes in this species. Direct validated estimates of ages using fin spines are limited to few tuna species including the Atlantic and Mediterranean albacore (Ortiz de Zarate et al., 1996; Megalofonou, 2000) and more recently the South Pacific Albacore (Farley et al., 2013), using oxytetracycline mark–recapture method. Besides, age validation studies employing bomb radiocarbon method, one of the most reliable approaches currently available as a dated mark, have preferentially applied on otolith whereas the suitability of this method in fin spines has been only explored in ABFT (Rodriguez-Marin et al. 2013). Results of this study showed that fin spines certainly contained radiocarbon at concentrations consistent with expectation and hence fin spine radiocarbon chronology was consistent with an accurate age interpretation. However, the results should be viewed with caution, as they are only based on a single fin spine available from an ABFT captured in 1984 that was valuable for C14 analysis. In this regard, further validation studies of fin spines would be needed, either by increasing the

sample size or exploring alternative methods such as the post-bomb radiocarbon method (Ishihara et al. 2017).

Given this limitation, progress has been made to validate indirectly fin spine age estimates using other methods such as marginal increment and edge type analysis (Morales and Panfili, 2002). This has been documented in different tuna species such as Atlantic yellowfin tuna (Lessa and Duarte-Neto, 2004) and bigeye tuna (Duarte-Neto et al. 2012), Pacific bigeye tuna (Sun et al. 2001), and Atlantic bluefin tuna (Luque et al. 2014). In the later, seasonal periodicity of annuli formation showed that the appearance of the translucent band occurs from September to May, with a 50% of occurrence between mid-October and May, indicating an annual periodicity in the formation of the translucent bands and hence confirming a yearly periodicity of annulus formation. Besides, tracking cohort have contributed to the indirect validation, such as the exceptionally abundant 1994 cohort in different Atlantic Spanish fisheries, where few differences were found between age key lengths (ALK) built by age estimates from fin spines and the growth curve currently used for the eastern ABFT stock (Cort, 1991; Rodríguez-Marín et al., 2009, ICCAT 2013).

Another approach that serves as an indirect validation method involves comparing age estimates from fin spines and otoliths from the same specimen, since age readings in otoliths are validated (Neilson and Campana 2008). This alternative approach provides useful information on the accuracy and bias of age estimating structures (Clear et al., 2000; Sylvester and Berry, 2006; Gunn et al., 2008). Rodriguez-Marin et al. (2015) study indicated that the comparison of otoliths and fin spines age interpretations coming from the same ABFT specimen showed a good fit to a linear relationship between both age estimations up to 10 years, and from this age it is observed that the spine age interpretations are lower than that of the corresponding otoliths.

In the last 40 years, fin spines have become a valuable skeletal hard part alternative to otoliths for fishery scientists. As such, the examination of growth increments in fin spines is a widely accepted method for estimating age and growth parameters used in stock assessment models for economically important tuna species (see for review in Murua et al. 2017). The approach simply assumes that as fish increase in length, there will also be proportional increases in the size of the fin spine and that the deposition of periodic marks occurs at fixed intervals that can be interpreted as yearly (annuli) growth increments. Following this up, the estimation of age is based on counting the number of these growth marks, usually called annuli (i.e., yearly formed) that are interpreted as periodic events

(e.g., Compean-Jimenez and Bard, 1983). However, its use is difficult because the earliest growth marks are replaced by vascular tissue, which increases with age or body length (Drew et al. 2006; Luque et al. 2014; Santamaria et al. 2015).

The first spine of the first dorsal fin is a suitable calcified structure for ageing small- and medium-sized ABFT because its transverse sections display well-defined growth marks (Rooker et al., 2007; Santamaria et al., 2009; Luque et al., 2014). This is mainly because of fin spine sampling is easier than otoliths or vertebrae and has the advantage that it does not require damaging or processing the body of the fish, thus minimizing possible impacts on commercial value. Hence, fin spine sampling represents a non-lethal and minimally invasive sampling method (Zymonas and McMahon, 2006) particularly attractive for fish species that cannot be sacrificed for their otoliths such as endangered (threatened) fish or those of management concern (e.g., protected), or commercially valuable species such as ABFT, since it greatly affects the appearance of a fish, diminishing its market value. Ease of collection is also important when sampling on-board fishing vessels, or in port, as there is little time to collect samples.

The fin spine preparation method is less time-consuming than other calcified structures such as vertebrae, as only transverse sections are needed and staining is not necessary (Rodriguez-Marin et al., 2012). In contrast, the main drawback of using fin spines for estimating "annual age" is the vascularization or resorption of the fin spine nucleus. This process known as nucleus vascularization starts at the center of the fin spine and proceeds outward as the fish grows. Thereby, the fin spine nucleus is reabsorbed obscuring the earliest growth marks (i.e., annuli associated with early life history) that are replaced by vascular tissue (Drew et al. 2006; Luque et al. 2014; Santamaria et al. 2015). In this context, nucleus vascularization, is the greatest disadvantage of using this calcified structure for ageing purposes, as it might result in significant age underestimation and growth overestimation (Panfili et al., 2002). It is especially prevalent in epipelagic species such as the billfishes (e.g., Kopf et al. 2010) and tunas (see Murua et al. 2017 for review), possibly due to their elevated metabolic activity. This loss of growth marks has been overcome in several tuna species by estimating the positions of these marks in younger fishes (Hill et al., 1989), although this method remains non-validated for T. thynnus. This method relies on the assumption that the annulus of a particular age class forms at approximately the same radius for each individual in the population; nevertheless, very little has been published regarding the quantification of obscured annuli due to

vascularization in most of these species including T. thynnus (Luque et al., 2014; Santamaria et al., 2015).

Despite of the fin spine nucleus vascularization reduces the reliability of age determination for large individuals, fin spines have proven useful in direct age determination for the eastern Atlantic and Mediterranean ABFT stock (Rooker et al. 2007). Indeed, the accepted growth curve for the eastern ABFT stock used for population assessments is based on length frequency analysis and fin spines direct ageing (Cort 1991; ICCAT, 2013). Besides they can be rapidly extracted, and easily processed, comparative analysis has also shown that fin spine ages are in close agreement with otolith ages collected from same specimen (Rodríguez-Marín et al., 2015).

Luque et al. (2014) study represent the most comprehensive study achieved up to date addressing important caveats in methodological issues that affect age estimates of eastern ABFT using dorsal fin spines such as: definition of the spine in terms of its biometric relationships, sectioning location and the quantification of spine nucleus vascularization as well as the annual periodicity of annulus formation and evaluation of levels of agreement, precision and relative accuracy among readers.

Fin spine sections display well-defined growth marks at regular intervals as an ordered series of alternate opaque and translucent bands based on their relative translucency. In ABFT, age is estimated by counting the translucent bands. An annulus is defined as a bipartite structure consisting generally of a wide opaque band followed by a narrow translucent band, presumably formed on a yearly basis. However, these annuli are not always a bipartite structure and sometimes multiple opaque and translucent pair banding appeared. The optical differences between translucent and opaque bands are related to different calcium concentrations, with higher concentrations in the translucent ones (Leonor et al. 1999). However, the physiological mechanisms that cause the formation of these growth marks are not fully understood and have been associated with periodic seasonal changes in the environment, such as cycles in temperature and food availability (Morales- Nin 1992; Jobling 2002) as well as have been linked to migrations pattern, trophic and spawning events (Compeán-Jimenez and Bard 1983; Sun et al. 2001. Despite of Luque et al. (2014) study provided the standardization of protocols to process and age ABFT fin spines, it is essential however, to maintain inter-laboratory and inter-reader calibrations to ensure that standards are maintained and assess if further standardization are required.

c) Vertebrae

Currently, the vertebra is a structure that is not used to determine ABFT age. The most recent studies are consistent with previous results supporting the use of vertebrae up to 11 years of age, at which age they begin to underestimate age compared to the otolith (Lee et al. 1983, Prince et al. 1985, Rodríguez-Marín et al. 2007).

Recent studies using vertebrae in the ABFT are not aimed at constructing growth curves, but at other research related to length and age of tunas in different historical periods (Andrews et al. 2022, Andrews et al. 2023). Or in other species, such as Pacific bluefin tuna (PBFT), where the most recent use has been to identify the natal origin of individuals through differences in the measurements of the first ring rays (Uematsu et al. 2017).

Growth studies on bluefin tuna vertebrae began at the beginning of the 20th century with Sella in the eastern stock (Rodriguez-Marin et al. 2007), although it was not until the 1960s that most were carried out in both stocks. In 1978 (Hunt et al. 1978) the first ABFT ageing workshop was held and studies on vertebrae were discussed. A methodology for sample selection (which vertebrae to use), collection, storage, preparation and interpretation of the "ridges and grooves" found on the surface of the vertebrae was detailed. With the exception of one paper from the last decade (Milatou & Megalofonou, 2014), the last studies using these structures date back to the 2000s, when the last comparison between CSs using this structure was carried out (Rodriguez-Marin et al. 2007), in which it was recommended to continue using vertebrae because they can be an easily obtained structure, depending on the fishery.

In the East, growth studies using vertebrae have used both caudal and precaudal vertebrae, of which the latter have been the least used. The maximum age dated in these studies was 18 years by Milatou & Megalofonou (2014) with samples from farms in the Mediterranean. The most common maximum age found in these studies was 13 or 14 years. For $L\infty$ there is also a large variation in results from 258.4 cm in the study conducted in the Icelandic fishery by Olafsdottir & Ingimundardottir (2003) to 472.4 cm SFL by Vilela (1960). This has implications for growth rate by varying growth rates (K) from 0.154 to 0.051 in the Von Bertalanffy equation. Within the vertebral work carried out on this stock, Olafsdottir & Ingimundardottir (2003) compared whole vertebrae with vertebral sections and found a difference of between 0 and 2 years. Regarding the comparison with other structures, there is a paper (Rodriguez-Marin et al. 2006) on samples of the same specimens collected in the Icelandic fishery that compares the

readings of vertebrae with spines. Between 5 and 11 years, the readings based on both CS are very similar.

In the western stock, fewer studies have attempted to construct a growth curve using combined methods, the only one using vertebrae alone being from Faber and Lee (1981). The most common maximum age results were maximum values of 14 years, and $L\infty$ ranged from 371 to 428.2 cm SFL (Mather & Schuck 1960). The maximum value of K in these studies reaches only 0.08 (Faber and Lee, 1981). In this stock, however, more comparative studies have been carried out with other structures, such as with the otolith (Lee et al. 1983) or the study by Prince et al. (1985), where in addition to the whole vertebra, readings are performed in the sections of the vertebra.

Among the advantages of this structure are the ease of extraction, both in terms of identification of the identification of the cut area and of the corresponding vertebrae, and conservation (refrigerated) (Berry et al. 1977). The other major advantage is that it maintains the linear relationship between the growth of the structure and the size of the fish throughout its life (e.g. Lee et al. 1983, Prince et al. 1985...).

On the other hand, the main handicaps (Rodriguez-Marin et al. 2007) are that it requires a long cleaning time and that the vertebrae have to be stained in order to be read. When it comes to reading the vertebrae, there are several problems. The identification of the first ring and its restructuring in larger individuals (Berry et al. 1977, Rodriguez-Marin et al. 2007), and the problems of interpreting the distal part of the cone, are the most important (Prince et al. 1985). For this reason, existing studies do not recommend its use beyond the age of 10 years. Cutting the vertebrae may improve the reliability of the counts in the distal part of the cone, while the interpretation of the bands in the area of the structure´s focus is more difficult. The combined method may help to overcome these problems in larger individuals, but may lead an overestimation of age in small and medium-sized individuals (Prince et al. 1985).

Vertebra 35 of the caudal region (Sella 1929, Hamre 1960, Mather & Schuck 1960) has been the most commonly used piece of the vertebral column and there have been comparative studies between this and 36, giving different results in ring size between them from age 6 on (Lee et al. 1983), but no significant differences were found in independent counts.

The sampling method most commonly used in studies is that of Berry et al 1977. It should be noted that the vertebrae should be refrigerated and separated only at the time of staining. Care should be taken during cleaning, especially in the cone area. Staining

should be carried out within a short time of cleaning to avoid deterioration (Berry et al. 1977) and the time spent in the stain should be appropriate to the size of the vertebra (Rodriguez-Marin et al. 2007). Alizarin staining is best for subsequent reading of growth structures.

For the reading of this structure, the “ridges” are identified, which are thought to form at the end of the growing season (boreal summer), followed by “grooves”, which are thought to form in winter. It should be noted that there are false rings which can lead to error in the interpretation of age. When vertebra are sectioned to perform the readings. A cut is made in the transverse plane of the vertebra to remove the posterior cone and a second cut is made in the frontal plane over the lateral processes. A section of 1-1.5 mm is made. This is polished until it is translucent and at this point internal banding readings are done on the vertebra. Using both methods of processing the vertebra, a combined reading is obtained, which allows the larger pieces to be read with greater confidence.

d) Scales

Scales have never been validated but have been used mainly in comparison with length frequency methods and vertebrae for young adults (Mather et al. 1995). Fish scales were among the first structures to be used for species direct ageing. The first published work on BFT CS was that of Corson in 1923 using scales. In 1932, at a conference of experts, it was already stated that scales were only useful for young individuals (Mather et al 1995). This is again the conclusion of later workshops and comparative studies for ABFT and other tuna species (Casselman, J.M., 1983; Gunn et al. 2008). Studies have used scales in both ABFT management units, but mostly in the younger segment of the population (Mather et al., 1995).

The main advantages of scales are ease of collection and simplicity of processing (Casselman, J.M., 1983) and although methods have improved over time, cellulose printing for subsequent reading with a magnifying glass is an improvement in methodology (Mather & Schuck, 1960). Age reading is based on the interpretation of checks, areas where the "circuli" are more compact versus other areas where they are more spaced out (Mather et al. 1995). The most recent work with tuna scales (Gunn et al. 2008) compares age readings between structures from the same individual, concluding that they are useful up to 4 years for southern bluefin tuna. The reasons are the high incidence of regenerated scales and the compression of the “circuli” at the scale margin.

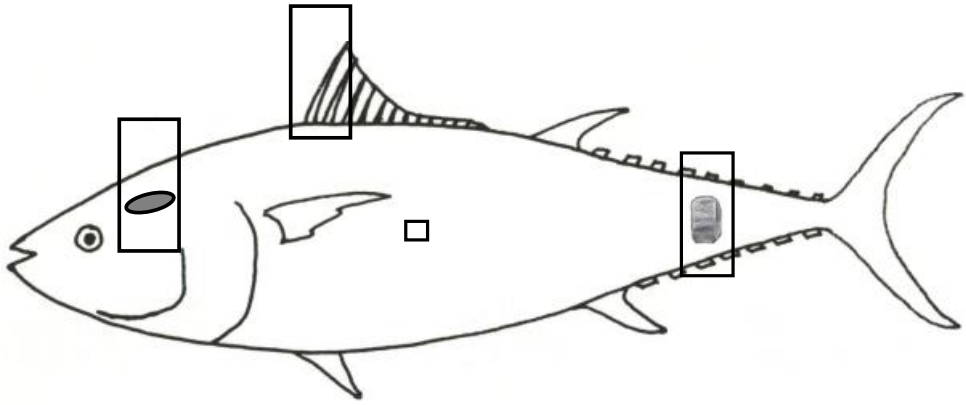

Figure 5.1.1. Scheme of a bluefin tuna with the calcified structures involved in direct ageing. From left to right: otolith, fin spine, scale and vertebra.

5.2 Develop of a reference collection of calcified structures.

Reference collections for direct ageing are very important as they serve as quality control of the readings to detect errors in ageing. These collections help maintain consistency in readings and avoid gradual bias in ageing precision. The use of reference collections also allows readings by various readers to be comparable. Another important use of collections is that they serve as training sets for new readers. Reference collection readings should be based on a validated or at least corroborated methodology and have been made by the consensus of experienced readers (Campana, 2001).

The collections consist of approximately 200 images of otoliths and spines (first radius of the first dorsal fin) provided in Appendix 1 and 2. These structures had readings that were either agreed by several experienced readers or by several readings by one experienced reader. Attempts were made to address all potential factors that can affect reading interpretation, such as tuna size, month and year of capture, geographic location and fishing gear. A wide temporal and size coverage was prioritized for its effect on age estimation and identification of the marginal edge of the structure. Selected images, which are of high quality and include a reference scale, contain samples with good readability and confidence in the identification of the marginal edge.

In the otolith collection, 210 images of otolith sections that were read under transmitted light and following the standardized preparation and reading protocols described in

Rodriguez-Marin et al. (2020) were chosen. The number of bands ranged from 0 to 18 bands, with at least 10 specimens in the 0 to 13 band categories (Table 5.2.1). The size frequency distribution (Straight Fork Length, SFL) of the specimens used for both reference collections is depicted in Figure 5.2.1.

In the spine reference collection, 180 samples were selected read under transmitted light and cut at 1.5 the reference diameter of the spine base, following standardized protocols for spine preparation and reading (Luque et al., 2014). The age range covered is from 1 to 23 years, being about 10 specimens for ages 1 to 14 years (Table 5.2.2).

Both collections are accompanied with information on the sampling of calcified structures and an excel sheet for reading, with specific fields for each structure and automated calculation of the coefficient of variation (CV). In the case of new readers, it is recommended to follow the standard procedure of two readings (Rodriguez-Marin et al., 2020), but if the collections are used by experienced readers who perform discontinuous readings, a single reading can be carried out. The number of samples to be read should be at least 100 randomly selected images, and for the readings to have a valid precision, the CVs should be less than 10 %. A new selection and reading of samples are necessary if this value is higher.

Table 5.2.1. Reference collection of otoliths. Number of samples by band number and month.

	Month												
Number of bands	1	2	3	4	5	6	7	8	9	10	11	12	Total
0									2	6	2		10
1					2	1	5	2					10
2						6		2	1				9
3						7		1			3	2	13
4	2				1			3		2	1	1	10
5						1	3	2	1		1	2	10
6						2	1	1			4	2	10
7	1					6	1				4	2	14
8	2				1	1					8	2	14
9	2			1	1	1	1				7	4	17
10			1	1							6	5	13
11	3		3			2					8		16
12	4		3	1	3					2	7		20
13			1	2							13	8	24
14	3		2								2		7
15										1	1	2	4
16		1		2	2						1	1	7
17										1			1
18				1									1
Total	17	1	10	8	10	27	11	11	4	12	68	31	210

Table 5.2.2. Reference collection of spines. Number of samples by age and month.

	Month												
Adjusted age	1	2	3	4	5	6	7	8	9	10	11	12	Total
1					3		2	4	1				10
2						3	2	4				1	10
3						1	2	3	4		2		12
4						1	3	4	3	1	2		14
5				1	1		4	3	1	1	3		14
6	1			2	2	1	2	2	1	2	1		14
7			1		2	3	2	3	1	2			14
8		1		2	3	2		2		2	2		14
9			1		2	4	1	1	1	1	2		13
10					4	2		1	1	1			9
11					2	2			2	1			7
12					2	2	1	1	1		1		8
13					1	3		1	1		1		7
14			1		2	5		1	1	1			11
15						1		1	1	2			5
16						4		2	3				9
17					1	2		2					5
18								2					2
19									1				1
20													
21													
22													
23								1					1
Total	1	1	3	5	25	36	19	38	23	14	14	1	180

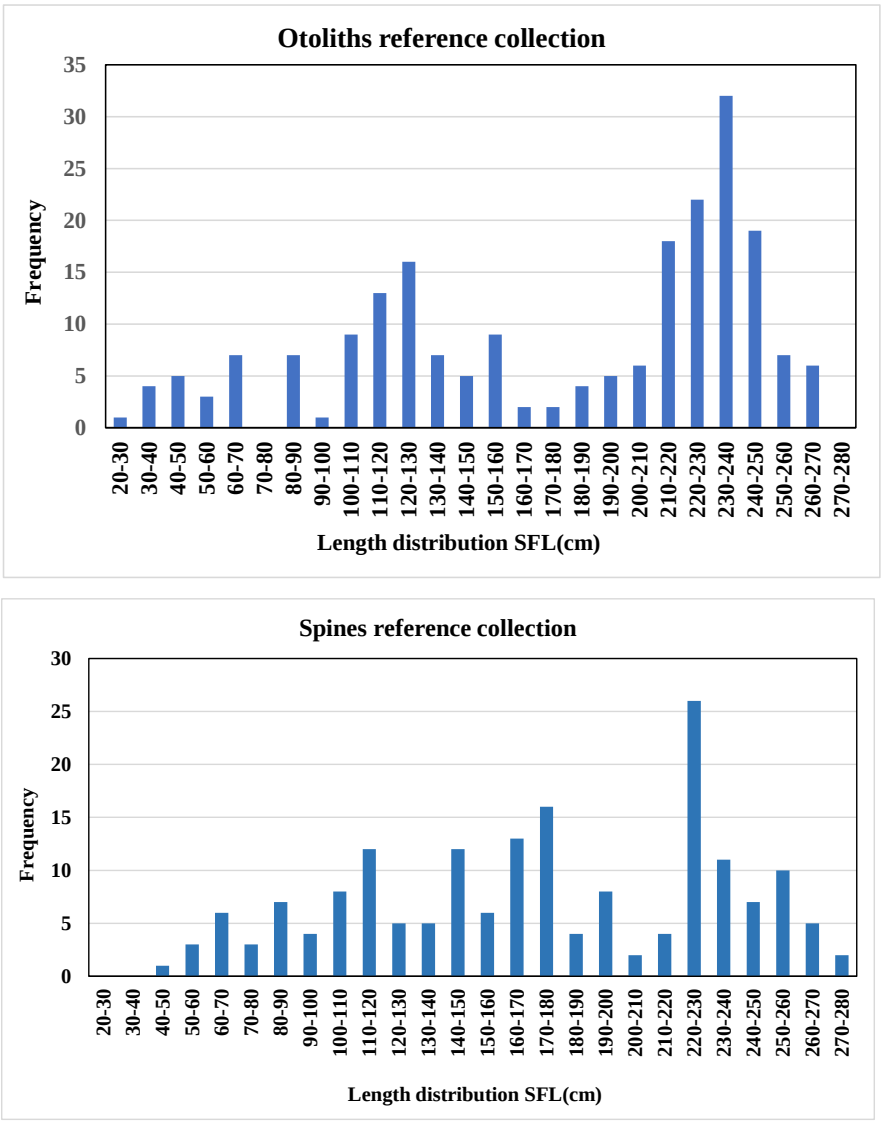

Figure 5.2.1. Length distribution (Straight Fork Length, SFL) of reference collection specimens by 10 cm size bin. Reference collections of otoliths top and spines bottom.

5.3 Selection of otolith samples to perform the epigenetic ageing study for east Atlantic bluefin tuna.

Epigenetic age analysis will be performed using east Atlantic bluefin tuna (EABFT) muscle tissue. DNA methylation age will be compared with chronological age in calcified structures, such as otoliths, whose use for age interpretation has been validated (Neilson and Campana, 2008; Siskey et al., 2016). Otoliths already aged will be used in order to be able to select readings with high confidence in the age reading, and to cover the whole age range. In addition, attention has been paid to factors that may influence the analysis of the application of the epigenetic clock for the EABFT, the selection was made with the following criteria: otoliths with a high reading confidence, with good confidence in the

marginal edge identification and if possible, with agreement in the identification of the marginal edge type between readings of the same otolith sample. At least 15 samples per sex and age were selected and fishing areas and months of the year were covered as representatively as possible.

A total of 250 specimens have been selected with otolith and muscle samples, and an additional 159 specimens have been pre-selected to have replacement options in case the specimen's muscle sample is not available. A selection of 2 to 16 annual bands has been obtained, with adequate sex coverage and number of specimens in the range of 2 to 14 annual bands (Table 5.3.1). Most of the selected specimens come from the Mediterranean Sea.

Table 5.3.1. Sample sizes by number of annual bands (from otolith readings) of Atlantic bluefin tuna captured in the eastern Atlantic and within the Mediterranean Sea for use in epigenetic age calibration.

Number of bands	Atlantic		Mediterranean		Total
	Females	Males	Females	Males	
2			8	9	17
3	1		7	8	16
4		1	10	9	20
5		2	10	8	20
6	3	1	7	7	18
7	2	2	8	9	21
8	1	3	9	7	20
9	3	1	7	8	19
10	1	1	9	8	19
11	4	5	5	6	20
12	3	3	5	7	18
13	1	2	8	7	18
14		1	10	7	18
15			2	3	5
16			1		1
Total	19	22	106	103	250

References

Ailloud, L.E., Lauretta, M.V., Hanke, A.R., Golet, W.J., Allman, R.J., Siskey, M.R., Secor, D.H. & Hoenig, J.M. 2017. Improving growth estimates for Western Atlantic bluefin tuna using an integrated modeling approach. Fish Res, 191: 17-24.

Andrews, A. J., Mylona, D., Rivera-Charún, L., Winter, R., Onar, V., Siddiq, A. B., Tini, F. & Morales-Muniz, A. 2022. Length estimation of Atlantic bluefin tuna (*Thunnus thynnus*) using vertebrae. Int J Osteoarchaeol, 32(3): 645-653.

Andrews, A. J., Di Natale, A., Addis, P., Piattoni, F., Onar, V., Bernal-Casasola, D., Aniceti, V., Carenti, G., Gomez-Fernandez, V., Garibaldi, F., Morales-Muñiz, A. & Tinti, F. 2023. Vertebrae reveal industrial-era increases in Atlantic bluefin tuna catch-at-size and juvenile growth. ICES J Mar Sci, 0: 1-12.

Beamish, R. J. & Fournier, D. A. 1981. A method for comparing the precision of a set of age determinations. Can J Fish Aquat Sci 38: 982–983.

Beamish, R.J. & McFarlane, G.A., 1983. The forgotten requirement for age validation in fisheries biology. Trans. Am. Fish. Soc. 112: 735–743.

Berry, F. H. 1977. Age estimates in Atlantic bluefin tuna-An objective examination and an intuitive analysis of rhythmic markings on vertebrae and in otoliths. Col. Vol. Sci. Pap. ICCAT, (2): 306-316.

Busawon D.S., Rodriguez-Marin, E., Luque, P.L., Allman, R., Gahagan, B., Golet, W., Koob, E., Siskey, M., Ruiz, M. & Quelle, P. 2015. Evaluation of an Atlantic bluefin tuna otolith reference collection. Col Vol Sci Pap ICCAT 71: 960–982

Busawon, D., Rodriguez-Marin, E.& Quelle, P. 2018. Protocol for the preparation of Atlantic bluefin tuna otoliths. SABS, IEO Working doc.

Busawon, D.S., Addis, P., Allman, R., Bellodi, A., Garibaldi, F., Ishihara, T., Karakulak, S., Luque, P.L., Quelle P. & Rodriguez-Marin, E. 2020. Evaluation of Atlantic bluefin tuna otolith ageing protocols. Collect. Vol. Sci. Pap. ICCAT, 76 (2): 147-171.

Butler, M.J.A., Caddy, J.F., Dickson, C.A., Hunt, J.J. & Burnett, C.D. 1977. Apparent age and growth, based on otolith analysis, of giant bluefin tuna (*Thunnus thynnus thynnus*) in the 1975–76 Canadian catch. Coll Vol Sci Pap ICCAT, 6: 318–330.

Campana, S. E. 1999. Chemistry and composition of fish otoliths: Pathways, mechanisms and applications. Mar. Ecol. Prog. Ser. 188: 263–297. doi:10.3354/meps188263.

Campana SE. 2001. Accuracy, precision and quality control in age determination, including a review of the use and abuse of age validation methods. J Fish Biol, 59: 197–242

Campana, S. E. & Thorrold, S. R. 2001. Otoliths, increments and elements: keys to a comprehensive understanding of fish populations? Can J Fish Aquat Sci, 58: 30–38.

Campana, S. E. 2005. Otolith science entering the 21st century. Mar Freshw Res, 56: 485–495. doi:10.1071/MF04147

Casselman, J.M., 1983. Age and Growth Assessment of Fish from Their Calcified Structures-Techniques and Tools. In: Prince, E. D., & Pulos, L. M. (eds.). Proceedings of the International Workshop on age determination of oceanic pelagic fishes: Tunas, billfishes, and sharks., Miami, Florida, February 15-18, 1982

Casselman, J.M., 1987. Determination of age and growth. In: Weatherley, A.H., Gill, H.S. (eds.), The Biology of Fish Growth. Academic Press Ltd., London, Chapter 7, pp. 209–242.

Chang, W. Y. B. 1982. A statistical method for evaluating the reproducibility of age determination. Can J Fish Aquat Sci 39, 1208–1210.

Compeán-Jimenez, G. & Bard, F. X. 1983. Growth increments on dorsal spines of Eastern Atlantic bluefin tuna, *Thunnus thynnus*, and their possible relation to migrations patterns. In Prince, E. D., & Pulos, L. M. (eds.). Proceedings of the International Workshop on age determination of oceanic pelagic fishes: Tunas, billfishes, and sharks., Miami, Florida, February 15-18, 1982.

Corriero, A., Karakulak, S., Santamaria, N., Deflorio, M., Spedicato, D., Addis, P., Desantis, S., Cirillo, F., Fenech-Farrugia, A., Vassallo-Agius, R., de la Serna, J. M., Oray, I., Cau, A., Megalofonou, P. & De Metrio, G. 2005. Size and age at sexual maturity of female bluefin

tuna (*Thunnus thynnus* L. 1758) from the Mediterranean Sea. J Appl Ichthyol, 21: 483–486.
Cort, J.L. 1991. Age and growth of the bluefin tuna (*Thunnus thynnus*) in the Northeast Atlantic. Coll Vol Sci Pap ICCAT 35:213–230
Drew, K., Die, D.J. & Arocha, F. 2006. Understanding vascularization in fin spines of white marlin (*Tetrapturus albidus*). Bull Mar Sci 79:847–852.
Duarte-Neto, P., Higa, F.M. & Lessa, R.P. 2012. Age and growth estimation of bigeye tuna, *Thunnus obesus* (Teleostei: Scombridae) in the southwestern Atlantic. Neotrop Ichthyol, 10:149–158
Eltink, A. T. G. W., Newton, A. W., Morgado, C., Santamaria, M. T. G. & Modin, J. 2000. Guidelines and Tools for Age Reading Comparisons. (PDF document version 1.0, October 2000.) European Fish Ageing Network (EFAN) Report 3-2000. 56 pp.
Farber, M.I. & Lee, D.W. 1981. Ageing western Atlantic Bluefin Tuna, *Thunnus thynnus*, using tagging data, caudal vertebrae and otoliths. Col. Vol. Sci. Pap. ICCAT, 15: 288-301.
Farley, J.H., Williams, A.J., Clear, N.P., Davies, C.R. & Nicol, S.J. 2013. Age estimation and validation for South Pacific albacore *Thunnus alalunga*. J Fish Biol 82:1523–1544.
Francis, R., 1990. Back-calculation of fish length: a critical review. J. Fish Biol, 36 (6): 883–902.
Francis, R.I.C.C. 1995. The analysis of otolith data—a mathematician's perspective (what, precisely, is your model?). In: Secor DH, Dean JM, Campana SE (eds) Recent developments in fish otolith research. Belle W. Baruch Library in Marine Science 19, University of South Carolina Press, Columbia, pp 81–95
Fromentin, J.-M., Bonhommeau, S., Arrizabalaga, H. & Kell, L.T. 2014. The spectre of uncertainty in management of exploited fish stocks: The illustrative case of Atlantic bluefin tuna. Mar Policy, 47: 8-14.
Fromentin, J.-M., Powers, J.E. 2005. Atlantic bluefin tuna: population dynamics, ecology, fisheries and management. Fish Fish, 6: 281-306.
Garbin, T. & Castello, J.P. 2014. Changes in population structure and growth of skipjack tuna, *Katsuwonus pelamis* during 30 years of exploitation in the southwestern Atlantic. Lat Am J Aquat Res, 42(3): 434-446.
Gunn, J.S., Clear, N.P., Carter, T.I., Rees, A.J., Stanley, C.A., Farley, J.H., Kalish, J.M. 2008. Age and growth in southern bluefin tuna, *Thunnus maccoyii* (Castelnau): Direct estimation from otoliths, scales and vertebrae. Fish Res, 92: 207-220. doi:10.1016/j.fishres.2008.01.018.
Hill, K. T., Cailliet, G. M. & Radtke, R. L. 1989. A comparative analysis of growth zones in four calcified structures of Pacific blue marlin, Makaira nigricans. Fish Bull 87, 829–843.
Hunt, J.J., Butler, M.J.A., Berry, F.H., Mason, J.M. & Wild, A. 1978. Proceedings of Atlantic Bluefin Tuna ageing workshop. Col. Vol. Sci. Pap. ICCAT 7: 332-348.
ICCAT, 2013. Report of the 2012 Atlantic bluefin tuna stock assessment session. Coll. Vol. Sci. Pap. 69: 1–198.
ICCAT. 2017. Report of the 2017 ICCAT Bluefin Stock Assessment Meeting. Madrid, Spain. Available from https://www.iccat.int/Documents/SCRS/DetRep/BFT_SA_ENG.pdf
Jobling, M. 2002. Environmental factors and rates of development and growth. In: Hart PJB, Reynolds JD (eds). Handbook of fish biology and fisheries, vol 1., fish biology. Blackwell Science Ltd, Malden, pp 97–122.
Kalish, J. M., Beamish, R. J., Brothers, E. B., Casselman, J. M., Francis, R. I. C. C., Mosegaard, H., Panfili, J., Prince, E. D., Thresher, R. E., Wilson, C. A. & Wright, P. J. 1995. Glossary for otolith studies. In Secor, D. H., Dean, J. M. & Campana, S. E., (eds). Recent Developments in Fish Otolith Research pp. 723–729. Columbia: University of South Carolina Press.
Kalish, J.M., Johnston, J.M., Gunn, J.S. & Clear, N.P. 1996. Use of the bomb radiocarbon chronometer to determine age of southern bluefin tuna *Thunnus maccoyii*. Marine Ecology Progress Series, 143, 1-8.
Kerr, L.A. & Campana, S.E., 2014. Chemical composition of fish hard parts as a natural marker of fish stocks. In: Cardin, S.X., Friedland, K. D.& Waldman, J.R. (eds). Stock Identification Methods. Academic Press, pp. 205–234.
Kolody, D.S., Eveson, J.P. & Hillary, R.M. 2016. Modelling growth in tuna RFMO stock assessments: current approaches and challenges. Fish Res 180:177–193.

Kopf, R. K., Drew, K. & Humphreys, R. L. 2010. Age estimation of billfishes (Kajikia spp.) using fin spine cross-sections: the need for an international code of practice. Aquat Living Resour, 23, 13–23. doi: 10.1051/alr/2009045.

LeGeros RZ. 1991. Calcium phosphates in oral biology and medicine. Monographs in Oral Science 15: 1-201 DOI 10.1159/000419232.

Lee, D.W., Prince, E.D. & Crow, M.E. 1983. Interpretation of growth bands on vertebrate and otoliths of Atlantic Bluefin Tuna, *Thunnus thynnus*. In: Prince, E. D., & Pulos, L. M. (eds.). Proceedings of the International Workshop on age determination of oceanic pelagic fishes: Tunas, billfishes, and sharks., Miami, Florida, February 15-18, 1982.

Lessa, R. & Duarte-Neto, P. 2004. Age and growth of yellowfin tuna (*Thunnus albacares*) in the western equatorial Atlantic, using dorsal fin spines. Fish Res 69:157–170.

Loewen, T.N., Carriere, B., Reist, J.D., Halden, N.M. & Anderson, W.G., 2016. Linking physiology and biomineralization processes to ecological inferences on the life history of fishes. Comp. Biochem. Physiol. A. Mol. Integr. Physiol. 202: 123–140.

Luque, P., Rodriguez-Marin, E., Landa, J., Ruiz, M., Quelle, P., Macias, D. & Ortiz De Urbina, J. 2014. Direct ageing of *Thunnus thynnus* from the eastern Atlantic Ocean and western Mediterranean Sea using dorsal fin spines. J. Fish Biol. 2014, 84, 1876-1903.

Mather, F.J. & Schuck, H.A. 1960. Growth of Bluefin tuna of the western north Atlantic. Fish Bull Fish Wildlife Service, 61.

Mather, F.J., Mason, J.M. & Jones, A.C. 1995. Historical document: Life history and fisheries of Atlantic bluefin tuna. NOAA Technical Memorandum NMFS-SEFSC, 370, 165 pp.

Medina, A. 2020. Reproduction of Atlantic bluefin tuna. Fish Fish, 21(6): 1109-1119.

Megalofonou, P. 2000. Age and growth of Mediterranean albacore. J Fish Biol 57:700–715.

Megalofonou, P. & De Metrio, G. 2000. Age estimation and annulus formation in dorsal spines of juvenile bluefin tuna, *Thunnus thynnus*, from the Mediterranean Sea. J Mar Biol Ass U K, 80: 753–754.

Milatou, N., & Megalofonou, P. 2014. Age structure and growth of bluefin tuna (*Thunnus thynnus*, L.) in the capture-based aquaculture in the Mediterranean Sea. Aquaculture, 424: 35-44.

Morales-Nin, B. 1992. Determination of growth in bony fishes from otolith microstructure FAO Fish Tech Pap, 322. Rome, FAO.

Morales-Nin, B. & Panfili, J. 2002. Indirect validation. In: Panfili J, Pontual HD, Troadec H, Wright PJ (eds) Manual of fish sclerochronology, Ifremer-IRD coedition: Brest, France, pp 31–57.

Murua, H., Rodriguez-Marin, E., Neilson, J.D., Farley, J.H., Juan-Jordá, M.J. 2017. Fast versus slow growing tuna species: age, growth, and implications for population dynamics and fisheries management. Rev Fish Biol Fish, 27: 733-773. doi:10.1007/s11160-017-9474-1.

Neilson, J.D., Campana, S.E. 2008. A validated description of age and growth of western Atlantic bluefin tuna (*Thunnus thynnus*). Can J Fish Aquat Sci, 65: 1523-1527.

Olafsdottir, D. & Ingimundardottir, T. 2003. Age-size relationship for bluefin tuna (*Thunnus thynnus*) caught during feeding migrations to the northern N-Atlantic. Collect. Vol. Sci. Pap. ICCAT, 55: 1254-1260.

Ortiz de Zárate, V., Megalofonou, P., De Metrio, G. & Rodríguez-Cabello, C. 1996. Preliminary age validation results from tagged-recaptured fluorochrome label albacore in North East Atlantic. Coll Vol Sci Pap ICCAT 43:331–338

Panfili, J., de Pontual, H., Troadec, H. & Wright, P.J. (Eds.), 2002. Manual of fish sclerochronology. Brest, France: Ifremer-IRD coedition, 464 pp.

Prince, E. D., & Pulos, L. M. 1983. Proceedings of the International Workshop on age determination of oceanic pelagic fishes: Tunas, billfishes, and sharks, Miami, Florida, February 15-18, 1982.

Prince, E. D., Lee, D. W., & Javech, J. C. 1985. Internal zonations in sections of vertebrae from Atlantic bluefin tuna, *Thunnus thynnus*, and their potential use in age determination. Can J Fish Aquat Sci, 42(5): 938-946.

Restrepo, V.R., Diaz, G.A., Walter, J.F., Neilson, J.D., Campana, S.E., Secor, D. & Wingate, R.L. 2010. Updated estimate of the growth curve of Western Atlantic bluefin tuna. Aquat Living Resour 23: 335-342. doi:10.1051/alr/2011004.

Rey, C., Combes, C., Drouet, C. & Glimcher, M.J. 2009. Bone mineral: update on chemical composition and structure. Osteoporos Int, 20: 1013-1021. doi:10.1007/s00198-009-0860-y.

Rodríguez-Marín, E., Clear, N., Cort Basilio, J.L., Megalofonou, P., Neilson, J.D., Neves dos Santos, M., Olafsdottir, D., Rodríguez-Cabello, C., Ruiz, M. & Valeiras, J. 2007. Report of the 2006 ICCAT Workshop for bluefin tuna direct ageing. Collect. Vol. Sci. Pap. ICCAT, 60: 1349-1392.

Rodríguez-Marín, E., Ortiz de Urbina, J. M., Alot, E., Cort, J. L., De la Serna, J. M., Macias, D., Rodríguez-Cabello, C., Ruiz, M. & Valeiras, X. 2009. Following bluefin tuna cohorts from east Atlantic Spanish fisheries since 1980s. Collect. Vol. Sci. Pap. ICCAT,63, 121–132

Rodriguez-Marin, E., Luque, P. L., Ruiz, M., Quelle, P. & Landa, J. 2012. Protocol for sampling, preparing and age interpreting criteria of Atlantic bluefin tuna (*Thunnus thynnus*) first dorsal fin spine sections. Collect. Vol. Sci. Pap. ICCAT, 68: 240–253.

Rodriguez-Marin, E., Luque, P. L., Busawon, D., Campana, S., Golet, W., Koob, E., Neilson, J., Quelle, P. & Ruiz, M. 2013. An attempt of validation of Atlantic bluefin tuna (*Thunnus thynnus*) ageing using dorsal fin spines. In: Porch, C. & Fromentin, J. M. (eds). Report of the 2013 Bluefin Tuna Meeting on Biological Parameters Review. 11–12. Tenerife.

Rodriguez-Marin E., Quelle P., Busawon, D., & Hanke, A. 2019. New protocol to avoid bias in otolith readings of Atlantic bluefin tuna juveniles. Collect. Vol. Sci. Pap. ICCAT, 75(6): 1301-1314.

Rodriguez-Marin, E., Quelle, P., Addis, P., Alemany, F., Bellodi, A., Busawon, D., Carnevali, O., Cort, J., Di Natale, A. & Farley, J. 2020 Report of the ICCAT GBYP international workshop on Atlantic bluefin tuna growth. Collect. Vol. Sci. Pap. ICCAT, 76: 616-649.

Rodriguez-Marin, E., Busawon, D., Luque, P.L., Castillo, I., Stewart, N., Krusic-Golub, K., Parejo, A., Hanke, A. Timing of Increment Formation in Atlantic Bluefin Tuna (*Thunnus thynnus*) Otoliths. Fishes 2022, 7, 227. https://doi.org/10.3390/fishes7050227

Rooker, J.R., Alvarado Bremer, J.R., Block, B.A., Dewar, H., DeMetrio, G., Corriero, A.,Kraus, R.T., Prince, E.D., Rodriguez-Marin, E., Secor, D.H., 2007. Life history and stock structure of Atlantic bluefin tuna (*Thunnus thynnus*). Rev. Fish. Sci. 15,265–310.

Santamaria, N., Bello, G., Corriero, A., Deflorio, M., Vassallo-Agius, R., Bök, T. & De Metrio, G. 2009. Age and growth of Atlantic bluefin tuna, *Thunnus thynnus* (Osteichthyes: Thunnidae), in the Mediterranean Sea. J Appl Ichthyol 25:38–45.

Santamaria, N., Bello, G., Pousis, C., Vassallo-Agius, R., de la Gándara, F. & Corriero, A. 2015. Fin spine bone resorption in Atlantic Bluefin Tuna, *Thunnus thynnus*, and comparison between wild and captive-reared specimens. PLoS ONE 10:e0121924.

Santiago, J. & Arrizabalaga, H. 2005. An integrated growth study for North Atlantic albacore (*Thunnus alalunga*, Bonn. 1788). ICES J Mar Sci 62:740–749.

Sardenne, F., Dortel, E., Le Croizier, G., Million, J., Labonne, M., Leroy, B., Bodin, N. & Chassot, E. 2015. Determining the age of tropical tunas in the Indian Ocean from otolith microstructures. Fish Res 163: 44–57.

Secor, D.H., Allman, R., Busawon, D., Gahagan, B., Golet, W., Koob, E., Luque, P.L., & Siskey, M. 2014. Standardization of otolith-based ageing protocols for Atlantic bluefin tuna. Collect. Vol. Sci. Pap. ICCAT, 70(2): 357-363.

Siskey, M., Lyubchich, V., Liang, D., Piccoli, P. & Secor, D. 2016. Periodicity of strontium: calcium across annuli further validates otolith-ageing for Atlantic bluefin tuna (*Thunnus thynnus*). Fish Res 177: 13–17

Stewart, N.D., Busawon, D.S., Rodriguez-Marin, E., Siskey, M. & Hanke, A.R. 2022. Applying mixed-effects growth models to back-calculated size-at-age data for Atlantic bluefin tuna (*Thunnus thynnus*). Fish Res, 250, 106260, doi:https://doi.org/10.1016/j.fishres.2022.106260.

Soares, B.J., Monteiro-Neto, C., Costa, M.R., Martins, R.R.M., Vieira, F. C. S., Andrade-Tubino, M.F., Bastos, A.L. & Tubino, R.A. 2019. Size structure, reproduction, and growth of skipjack tuna (*Katsuwonus pelamis*) caught by the pole-and-line fleet in the southwest Atlantic. Fish Res, 212: 136-145. https://doi.org/10.1016/j. fishres.2018.12.011.

Sun, C.L., Huang, C.L. & Yeh, S.Z. 2001. Age and growth of the bigeye tuna *Thunnus obesus* in the western Pacific Ocean. Fish Bull, 99:502–509.

Tzadik, O.E., Curtis, J.S., Granneman, J.E., Kurth, B.N., Pusack, T.J., Wallace, A.A., Hollander, D.J., Peebles, E.B. & Stallingset, C.D. 2017. Chemical archives in fishes beyond otoliths: A review on the use of other body parts as chronological recorders of microchemical constituents for expanding interpretations of environmental, ecological, and life-history changes. Limnol Oceanogr Methods, 15:238-263. doi:10.1002/lom3.10153.

Uematsu, Y., Ishihara, T., Hiraoka, Y., Shimose, T., & Ohshimo, S. 2018. Natal origin identification of Pacific bluefin tuna (*Thunnus orientalis*) by vertebral first annulus. Fish Res, 199, 26-31.

Ugarte, A., Unceta, N., Pecheyran, C., Goicolea, M.A. & Barrio, R.J. 2011. Development of a matrix matching hydroxyapatite calibration standards for quantitative multi-element LA-ICP-MS analysis: application to the dorsal spine of fish. J Anal At Spectrom, 26:1421-1427. doi: 10.1039/c1ja10037h.

Vitale, F., Worsøe Clausen, L., & Ní Chonchúir, G. (Eds.) 2019. Handbook of fish age estimation protocols and validation methods. ICES Cooperative Research Report No. 346. 180 pp. http://doi.org/10.17895/ices.pub.5221

Zymonas ND & McMahon TE. 2006. Effect of pelvic fin ray removal on the survival and growth of bull trout. North Am J Fish Manage, 26: 953-959, doi: 10.1577/M05-119.

6. OTOLITH CHEMISTRY

Task Leader:

Igaratza Fraile (AZTI), Jay Rooker (TAMUG) and Deirdre Brophy (GMIT)

Participants:

AZTI: Naiara Serrano, Iraide Artetxe-Arrate, Patricia Lastra-Luque

CNRS: Christophe Pecheyran, Fanny Claverie, Gaelle Barbotin

UNIVERSITY OF ARIZONA: David D. Dettman

GMIT: Elizabeth Tray, Louise Vaughan

6.1 Task 1: Temporal evolution of ABFT mixing proportions

6.1.1 Introduction

The Atlantic bluefin tuna (ABFT, *Thunnus thynnus*) is a large pelagic migratory species that lives mainly in the temperate ecosystem of the North Atlantic Ocean and adjacent seas. The management plan for ABFT considers two management units (stocks) separated by the 45°W meridian, assuming that the western stock spawns in or near the Gulf of Mexico and the eastern stock in or near the Mediterranean Sea. Challenging this assumption, several studies have shown that mixing occurs between the two management areas, which results in uncertainties about the degree of connectivity between the two stocks with implications for stock assessment and management advice (e.g., Kerr et al. 2020; Rodriguez-Ezpeleta et al. 2019; Rooker et al. 2008; Block et al. 2005). Over the last 11 Phases of GBYP ABFT individuals have been routinely analyzed for otolith carbon and oxygen stable isotope ($\delta^{13}C$ and $\delta^{18}O$) composition to investigate the degree of eastern and western population contribution to different mixing areas in the north Atlantic Ocean. The results so far have suggested that mixing of the eastern and western stocks occurs both sides of the 45ºW management boundary foraging grounds at variable rates. This routine task has provided a database with ~3000 individuals captured between 2009 and 2021 from different regions of the species distributional range. The aim of this task is to compile and summarize all otolith stable isotope data generated in GBYP, and to investigate the temporal evolution of ABFT mixing proportions over the last decade.

6.1.2 Material and Methods

In GBYP Phase-10, classification accuracy of age-0, age-1 and adult baselines was compared, and concluded that the baseline of adult spawners from the Mediterranean Sea and Gulf of Mexico performed the best as reference set for eastern and western stocks. Here, we have re-assigned the individual origin of all available carbon and oxygen stable isotope data analyzed in the GBYP framework to date (N=2711), combined with ABFT individuals from the Bay of Biscay sampled and analyzed in previous projects (N=212). The baseline used to characterize the GOM and MED spawning populations was based on samples (N=173) from mature adults (>185 cm FL in the GOM, >135 cm in the MED) collected during the spawning season at each ground: from April to June in the GOM, and from May to June in the eastern MED and from Jun to July in the central and western MED (Table 6.1.1). Besides, only individuals with MED or GOM genetic profile confirmed in Task 4.1.2.1 were selected for the baseline. Classification accuracy of this baseline was tested using different classification methods and based in Leave-One-Out cross validation (LOOCV) results. The classification method that scored highest at classification accuracy was then used to predict the origin of 2923 ABFT individuals captured outside spawning areas (Figure 6.1.1). These methods of classification differ from HISEA (used in previous GBYP phases) in the sense that they allow for estimating the individual probability of belonging to each of the populations as a function of $\delta^{13}C$ and $\delta^{18}O$. Assuming that the origin of tuna cannot be perfectly predicted from $\delta^{13}C$ and $\delta^{18}O$ values, individuals were assigned to a population (GOM or MED) when their probability was > 70%, when not, they were classified as unassigned (UNASS). A test of equal proportions was used (Pearson's chi-squared test statistic) to see whether they were differences in origin proportions between different catch years. Additionally, a test for trend in proportions (Mann Kendall trend test) was performed to see whether there was a linear trend in the proportion of cases across years or not.

Table 6.1.1 ABFT individuals used as reference baseline for this task.

Stock	N	Catch month	Catch year	SFL range	Estimated age range	Represented time period
GOM	81	Apr-Jun	2010-2014	199-281	9-18	1992-2005
MED	92	May-Jul	2010-2015	141-272	5-17	1995-2009

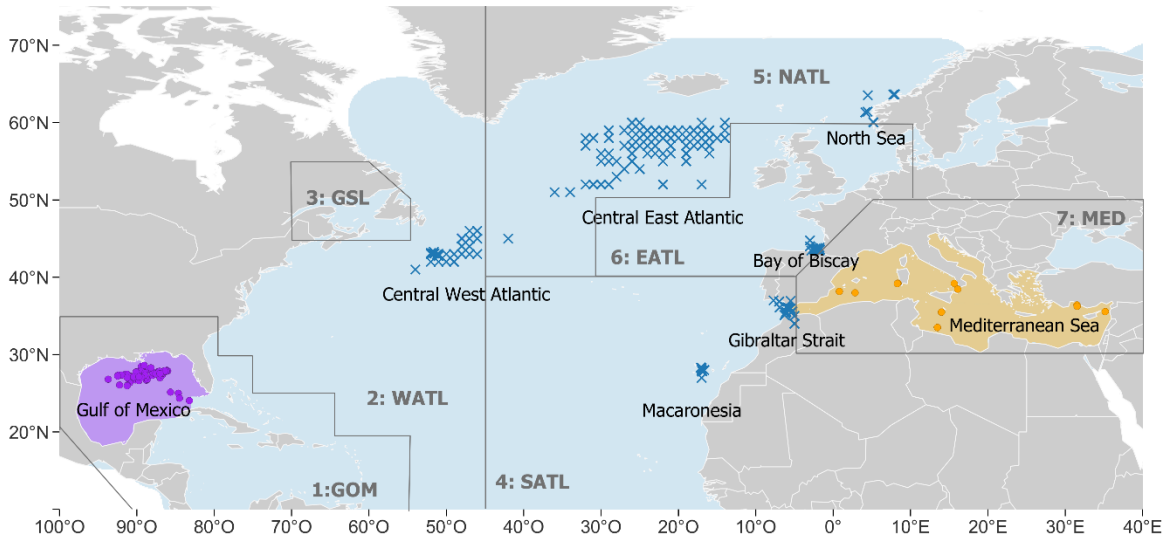

Figure 6.1.1 Map of individuals with stable isotope data analyzed in this study. Adults collected from the two main spawning areas, the Gulf of Mexico (GOM, purple area) and the Mediterranean Sea (MED, orange area) are shown as purple and orange dots, respectively. Approximate capture locations of individuals of unknown origin are shown as blue crosses, while grey squares represent the spatial definitions of seven areas used in this analysis: West Atlantic (WATL), Gulf Saint Lawrence (GSL), South Atlantic (SATL), North Atlantic (NATL) and East Atlantic (EATL). ABFT distribution range in light blue.

6.1.3 Results and Discussion

The adult spawner stable isotope baseline used as reference set (Figure 6.1.2), had a mean accuracy assigning fish to their spawning area (Mediterranean vs Gulf of Mexico), that ranges between 88.4% to 94.2% (k value 0.77 to 0.88) depending on the classifier chosen (Table 6.1.2). Multinomial logistic regression (MLR) was chosen to assign the origin of each fish in the mixed sample and its associate levels of probability to belong to one of the two populations (GOM or MED) based on their otolith $\delta^{13}C$ and $\delta^{18}O$ values. Previous studies have shown that projections of populations composition derived from MLR classification were generally in agreement with maximum likelihood estimates from HISEA, but that predicted contributions for the GOM were occasionally higher with MLR (Rooker et al. 2019).

Table 6.1.2. Accuracy of different classification methods in assigning individuals to their spawning area after leave-one-out cross validation.

Classifier	Mean accuracy %	Kappa index	% Correct GOM	% Correct MED
Naive Bayes	93.0	0.86	92	94
Multinomial Logistic Regression	94.2	0.88	93	95
Random Forest	88.4	0.77	88	89
Quadratic discriminant function	94.2	0.88	93	96
Neural Network	94.2	0.88	88	95

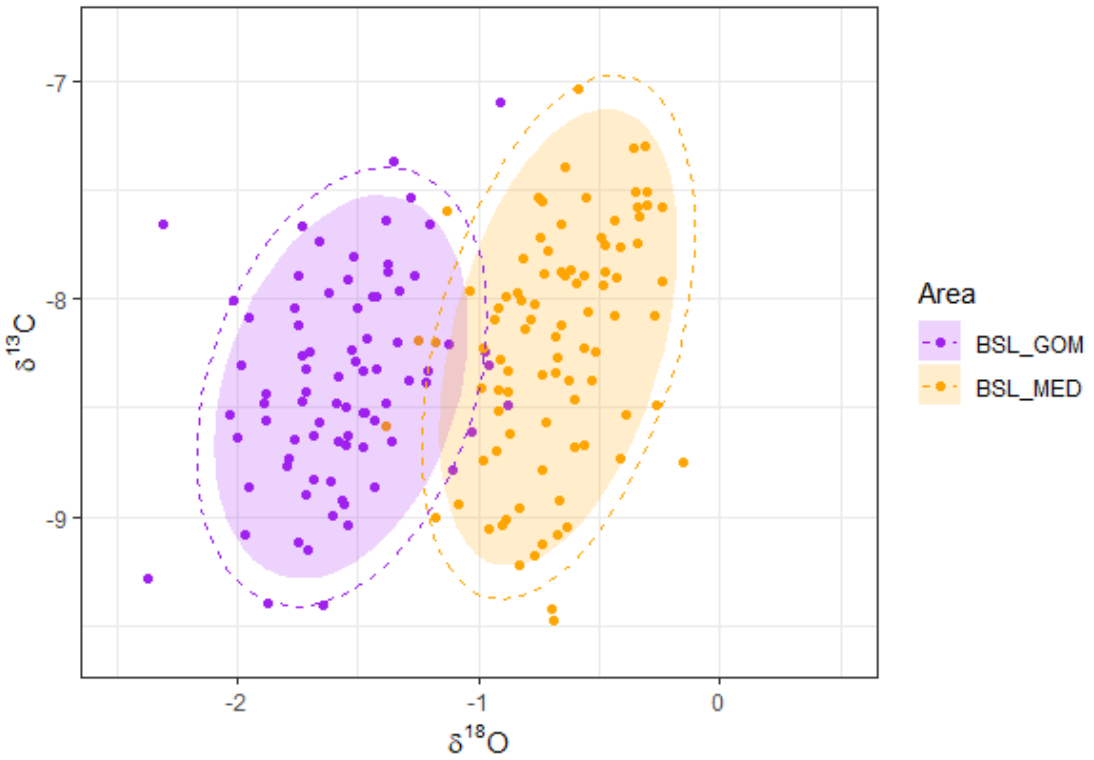

Figure 6.1.2. Oxygen ($\delta^{18}O$) and carbon ($\delta^{13}C$) values in otoliths of adult ABFT captured from the Gulf of Mexico (GOM, purple) and Mediterranean Sea (MED, orange) spawning areas and used as a baseline set (N=173). Ellipses show 90%(shaded) and 95% (dotted) confidence interval for each population.

For ABFT captured west of 45°W (i.e., WATL), the origin proportions of the assigned individuals varied significantly between years (MED; Chi squared=33.4, df=7, $p<0.001$), with some years being more abundant in those individuals assigned as GOM and others

in those individuals assigned as MED (Figure 6.1.3A): In 2011, 2012, 2017 and 2018, 43.5%, 66.7%, 37.9% and 44.0% of the fish analyzed were assigned as GOM, respectively, 39.6%, 68,.6%, 44.4% and 57.1% of fish caught in 2013, 2014, 2015 and 2016, were assigned as MED, respectively. The number of unassigned fish was ≥25% in 2013, 2015 and 2017.

In all other areas east of 45°W (i.e., NATL, EATL, SATL) most of the fish were assigned to the MED origin, with a smaller contribution of GOM origin fish regardless of the year analyzed. Proportions of MED origin fish significantly differ between years in the case of NATL (chi-squared=28.1, df=10, p=0.002), EATL (chi-squared=21.1, df=3, p<0.001), and SATL (chi-squared=33.8, df=11, p<0.001). In the NATL (Figure 6.1.3B), fish assigned to the MED ranged from 54.2% in 2013 to 100% in 2019 (in 2009 no fish were assigned to the MED origin but only 3 fish were available). As to the GOM assigned fish, excluding 2009, proportion of fish ranged from 9.8% to 19.2% until 2015, with proportion of GOM origin fish being <10% from 2016 onwards. In the EATL (Figure 6.1.3C), proportion of fish assigned to the MED origin ranged between 86.5 to 100%, with little apparent contribution of GOM origin fish (<10.0%). In the SATL (Figure 6.1.3D), fish assigned to the MED ranged from 65.5% in 2014 to 100% in 2017. There were few fish assigned to the GOM in all years analyzed, except in 2017, 2020 and 2021 (when fewer samples were available), contributing between 5.8-13.7% of the captured fish depending on the year. Finally, proportions of unassigned fish were higher in the WATL (16.7 to 34.8%, excluding 2010) and NATL (15.2% to 30.8%, excluding 2009) than in the EATL (0% to 25.0%) and SATL (9.0% to 23.4%).

Results suggest that both individuals originated in the GOM and MED cross the 45°W management boundary, mixing with the other population in feeding aggregates of the Atlantic Ocean, this rate being different among years. Variability in eastern or western origin ABFT commonly coring into the other management area has already been reported using otolith microchemistry results but with a shorter time representation than the one presented in this report (Rooker et al. 2019; Brophy et al. 2020). The proportion of fish from GOM origin found to cross to the east, is smaller than the proportion of MED origin fish found that cross to the west. There may be two explanations for this finding or be a combination of both; (1) fish originating in the GOM tend to move less, and (2) being a smaller stock in terms of production, the chances of finding a fish from the GOM are lower.

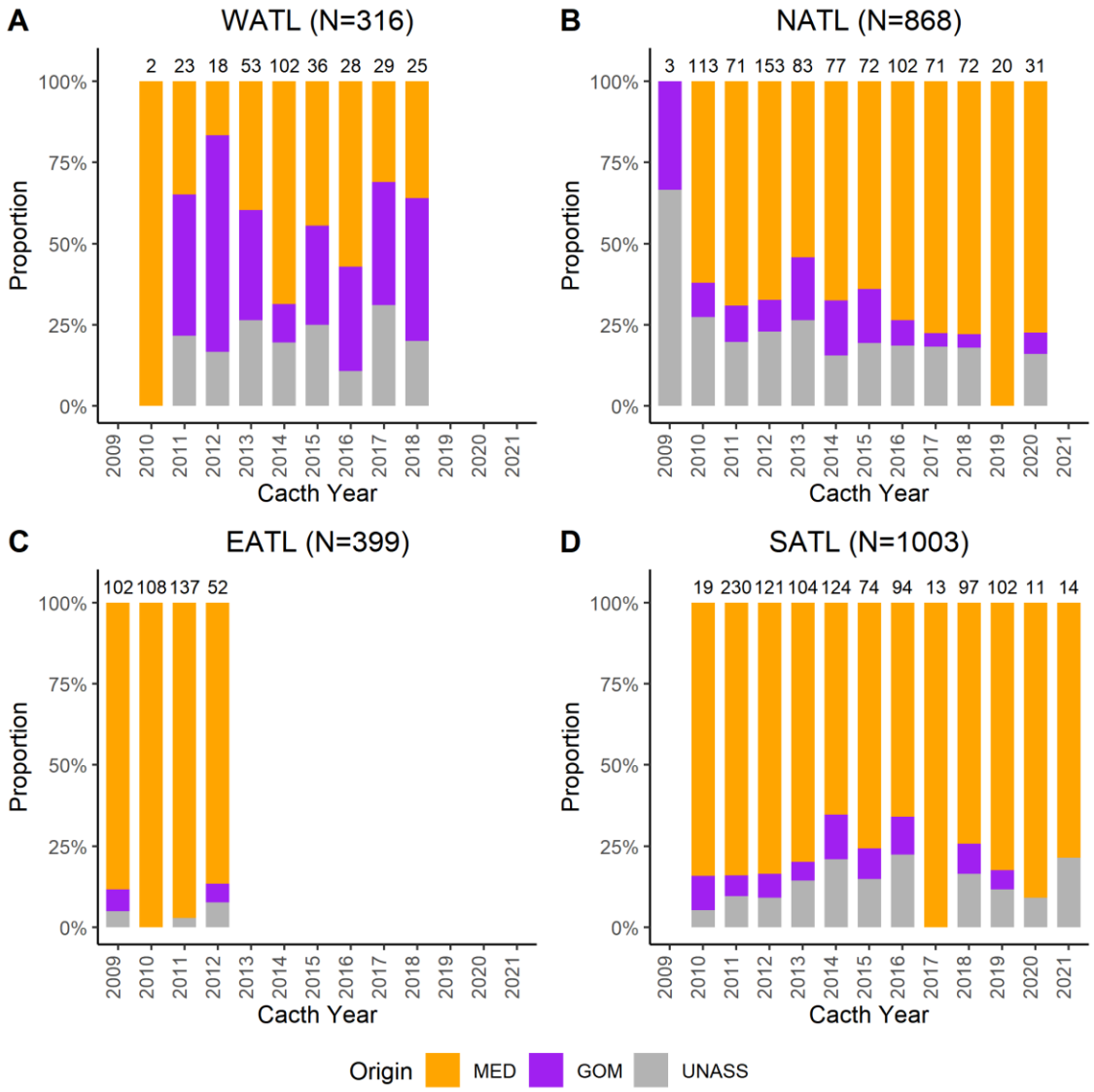

Figure 6.1.3. Estimated proportions of MED (orange), GOM (purple) and unassigned (grey) origin of Atlantic bluefin tuna samples collected from 2009 to 2021 in the West (WATL), North (NATL), East (EATL) and South (SATL) Atlantic Ocean.

In terms of yearly trends, we show that there was not a significant linear temporal trend in the proportions of MED origin for fish captured in WATL (tau=0.14, p=0.711) and SATL (tau=-0.09, p=0.730). Years with relatively higher contribution of MED origin fish in the WATL, coincide with years of relatively lower contribution of MED origin fish in the SATL (Figure 6.1.4A and C). A significant linear trend in MED origin proportions of fish captured from NATL was found (tau=0.61, p=0.012), with the proportion of MED origin fish significantly increasing with years (Figure 6.1.4B). Further research would be needed in order to combine knowledge on ABFT connectivity together with hydroclimatic and human pressures effects that could impact on the observed year to year variability.

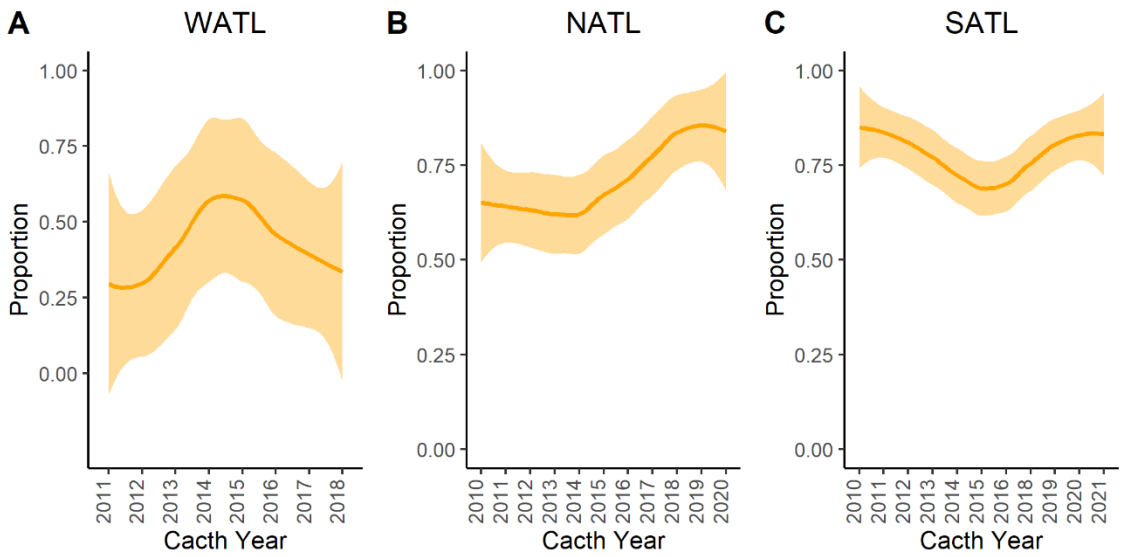

Figure 6.1.4. Temporal evolution of estimated proportions of MED origin of Atlantic bluefin tuna samples collected in the West (WATL), North (NATL) and South (SATL) Atlantic Ocean

6.1.4 Conclusions

- Reference baseline of otolith carbon and oxygen stable isotope ($\delta^{13}C$ and $\delta^{18}O$) composition confirmed with genetic data, allow to determine the origin of adult ABFT captured in feeding aggregates of the Atlantic Ocean with high precision.

- The two populations (MED origin and GOM origin) of ABFT mix in feeding grounds of the Atlantic Ocean, and mixing proportions vary with years in all regions.

- The proportion of fish from GOM origin found to cross to the east, is smaller than the proportion of MED origin fish found that cross to the west.

- There is an increasing linear trend in the presence of MED origin relative to GOM origin fish in the NATL. In other areas, observed year to year variations in origin composition did not follow a linear trend.

6.2 Task 2: Analyses of carbon and oxygen isotope ration ($\delta^{13}C$ and $\delta^{18}O$) in otolith of bluefin tuna captured in the potential mixing zones

6.2.1 Introduction

Understanding the degree of connectivity between eastern and western populations of Atlantic bluefin tuna is essential for the management of the species. Prior research has shown that stable carbon and oxygen isotopes ($\delta^{13}C$ and $\delta^{18}O$), are valuable for discriminating bluefin tuna from Gulf of Mexico and Mediterranean nurseries (e.g., Rooker et al. 2008). During the previous GBYP phases, otolith $\delta^{13}C$ and $\delta^{18}O$ analyses suggested that western origin contributions were negligible in the Mediterranean Sea, Bay of Biscay and Strait of Gibraltar, but mixing rates could be considerable, in some years, in the central North Atlantic, Canary Islands and western coast of Morocco (Rooker et al. 2014; Fraile et al., 2015). To further assess and monitor the spatial and temporal variability of mixing proportions throughout the North Atlantic Ocean, a total of 127 otoliths were analyzed for $\delta^{13}C$ and $\delta^{18}O$. The selection included otoliths from the central North Atlantic (N=71) and Norwegian Sea (N=31) and Canary Island (N=25) regions. This task builds on prior research carried out under the GBYP program, where otoliths of bluefin tuna have been chemically analyzed for origin determination. By increasing the sample size and temporal coverage, we aim to better understand the dynamics of mixing rates in the North Atlantic Ocean. The results presented here have been incorporated in the stable isotope dataset, which currently includes more than 3000 $\delta^{13}C$ and $\delta^{18}O$ data. We demonstrated the great potential of this catalogue in bluefin tuna monitoring and reinforce the need of updating the dataset by including new $\delta^{13}C$ and $\delta^{18}O$ analyses.

6.2.2 Material and Methods

In this section, we investigate the origin of bluefin tuna collected in the central North Atlantic Ocean (east and west of the 45ºW management boundary), Norwegian Sea and Canary Island using stable $\delta^{13}C$ and $\delta^{18}O$ isotopes in otoliths. Samples utilized for this study (N=127) were collected between 2012 and 2018 by Japanese longliners operating in the central North Atlantic, by the Norwegian fleet in September 2020, and the artisanal bait boat fishery in the Canary Island between October 2020 and March 2021 (Figure 6.2.1).

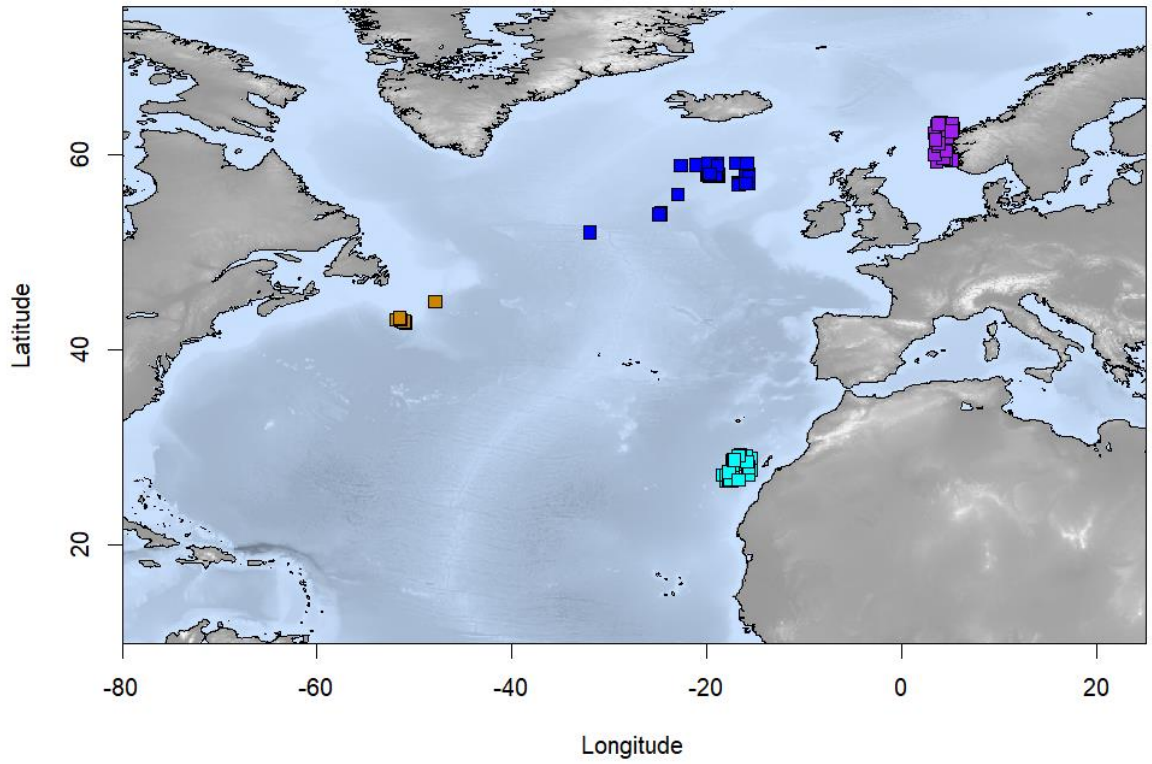

Figure 6.2.1: Sample distribution in the North Atlantic Ocean.

Otolith handling followed the protocols previously described in Rooker et al. (2008). Briefly, following extraction by GBYP participants, sagittal otoliths of bluefin tuna were cleaned of excess tissue with nitric acid (1%) and deionized water. One sagittal otolith from each bluefin tuna specimen was embedded in Struers epoxy resin (EpoFix) and sectioned using a low speed ISOMET saw to obtain 1.2 mm transverse sections that included the core. Following attachment to a sample plate, the portion of the otolith core corresponding to approximately the yearling periods of bluefin tuna was milled from the otolith section using a New Wave Research MicroMill system. A two-vector drill path based upon otolith measurements of several yearling bluefin tuna was created and used as the standard template to isolate core material following Rooker et al. (2008). The pre-programmed drill path was made using a 500 µm diameter drill bit and 15 passes each at a depth of 50 µm was used to obtain core material from the otolith. Powdered core material was transferred to silver capsules and later analyzed for $\delta^{13}C$ and $\delta^{18}O$ on an automated carbonate preparation device (KIEL-III) coupled to a gas-ratio mass spectrometer (Finnigan MAT 252). Stable $\delta^{13}C$ and $\delta^{18}O$ isotopes are reported relative to

the PeeDee belemnite (PDB) scale after comparison to an in-house laboratory standard calibrated to PDB.

Stable isotope signals of mixed stocks were compared with yearling samples from Mediterranean and Gulf of Mexico nurseries revised in GBYP-Phase 3 and presented in Rooker et al. (2014). HISEA software (Millar 1990) was used to generate direct maximum likelihood estimates (MLE) of mixed-stock proportions in each of the mixing zones. HISEA computes the likelihood of fish coming from a nursery area with characterized isotopic signature. MLE estimator is defined as the composition that maximizes the likelihood of the entire mixed fishery sample (Millar 1990). Uncertainty in estimation is addressed by re-sampling the baseline data 500 times with replacement and bootstrapping the mix data (n=1000).

Additionally, otolith $\delta^{13}C$ and $\delta^{18}O$ values were statistically analyzed and individuals were assigned to source populations with associated levels of probability. The identification of individual origin is needed for at least two main reasons: the construction of stock-age-length-keys, and the comparison/improvement of individual assignments based on different types of markers (i.e., genetic, otolith shape and stable isotopes). Among the classification methods tested with the yearling baseline dataset, it has been shown that Quadratic Discriminant Function Analysis (QDFA) performs the best attaining the highest classification accuracy (Fraile et al. 2015). Thus, QDFA was used to provide posterior probabilities for each pair of $\delta^{13}C$ and $\delta^{18}O$ values. Individual probabilities of origin were estimated after comparing the stable isotopic values with the reference otoliths from the Mediterranean Sea and Gulf of Mexico (Rooker et al., 2014)

6.2.3 Results and Discussion

Two of the 127 otoliths analyzed in the current phase were removed from the dataset as they were considered measurement errors. The remaining 125 samples were successfully analyzed for $\delta^{13}C$ and $\delta^{18}O$, and resulting values were compared to baseline populations from the Mediterranean Sea and Gulf of Mexico (Figure 6.2.2).

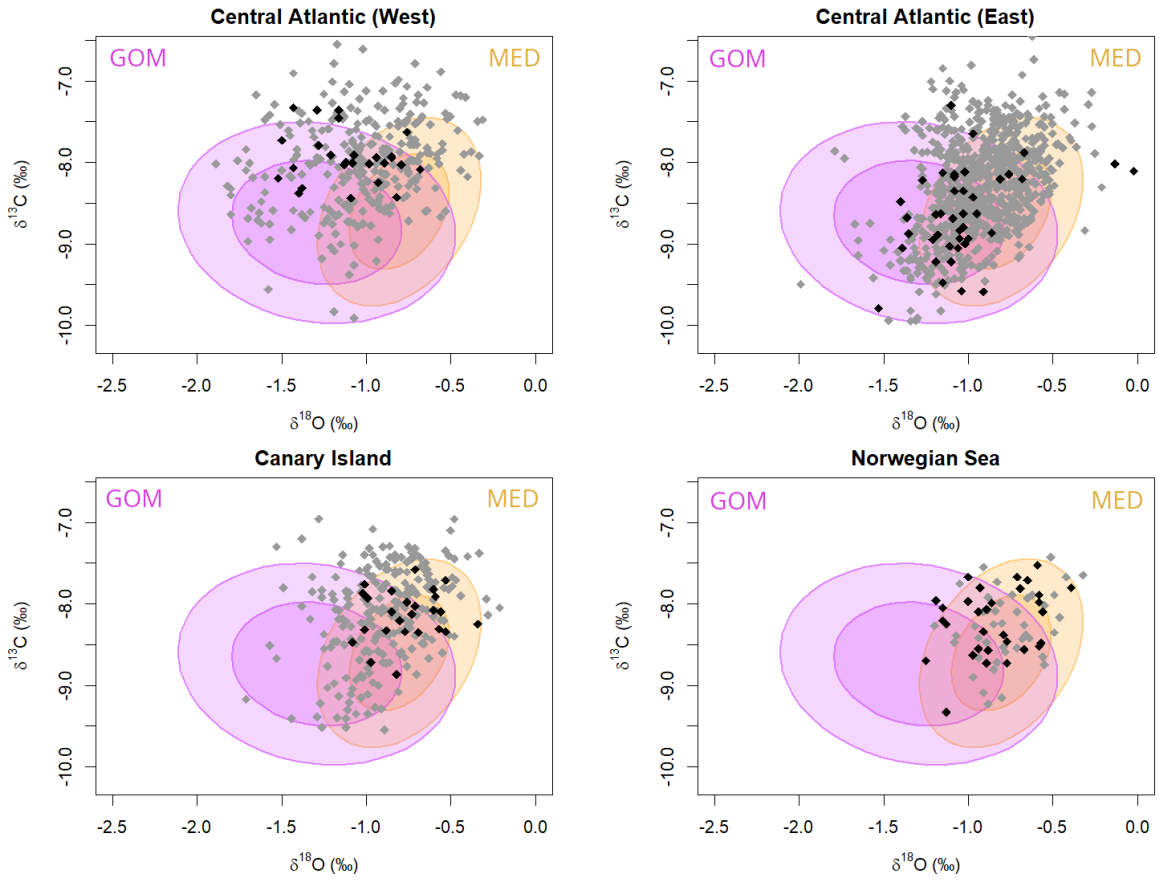

Figure 6.2.2: Confidence ellipses (1 and 2 SD or ca. 68% and 95% of sample) for otolith $\delta^{13}C$ and $\delta^{18}O$ values of yearling bluefin tuna from the east (MED orange) and west (GOM purple) nurseries along with the $\delta^{13}C$ and $\delta^{18}O$ values (grey & black circles) for otolith cores of bluefin tuna of unknown origin collected from the central North Atlantic (east and west of the 42°W boundary), Canary Island and Norwegian Sea. Otolith $\delta^{13}C$ and $\delta^{18}O$ values generated under the current GBYP Phase-12 are plotted in bold. Stable isotope data from previous Phases are shown for comparison (grey dots).

Otolith $\delta^{18}O$ and $\delta^{13}C$ values analyzed during the current Phase corresponded well with those measured in previous GBYP Phases (black and grey dots respectively in Fig. 6.2.2). Previous otolith chemical analyses indicated that individuals from both production zones readily cross the 45°W management boundary and mixing of the eastern and western population occurs throughout the North Atlantic Ocean. In the current Phase, otoliths from the central North Atlantic collected between 2012 and 2018 and stored within the GBYP biobank were analyzed to enlarge the stable isotope dataset and improve the reliability of mixing proportions. Samples analyzed in the current phase were combined with $\delta^{13}C$ and $\delta^{18}O$ measurements performed so far and compared with reference values. The results were concordant with previous findings, suggesting a high degree ox mixing in the central North Atlantic (west of the 45°W), moderate mixing in the central North

Atlantic (east of 45ºW) and catches in the Norwegian Sea and Canary Island dominated by the Mediterranean population.

Mixing proportions using Maximum Likelihood Estimates (MLE) were computed for samples analyzed during the current phase alone and merged with the analyses from previous GBYP Phases (Table 6.2.1). The results showed that mixing of individuals arising from the Mediterranean Sea and Gulf of Mexico production areas seems to take place in the central North Atlantic feeding grounds. Samples analyzed in the current phase indicated high mixing ratios at both sides of the 45ºW management boundary. However, combining the data from the current and previous phases suggested that mixing has been particularly important in the western side of the Atlantic Ocean, where 66% of the catches were from the Gulf of Mexico production zone and 34% were migrants from the Mediterranean Sea. Besides, population mixing east of the 45ºW boundary was moderate, as most of the bluefin tuna catches (90%) by the Japanesse fleet operating in this area were found to be originated in the Mediterranean Sea.

Table 6.2.1: Maximum likelihood estimates of the origin of bluefin tuna from the central North Atlantic (east and west of the 45ºW boundary), Canary Island and Norwegian Sea analyzed under the current (shaded in blue) and previous contracts. Estimates are given as percentages. The mixed-stock analysis (HISEA program) was run under bootstrap mode with 1000 runs to obtain standard deviations around estimated percentages (± %).

Area	Years	West (%)	East (%)	SD	N
Central North Atl. (west of 45ºW)	2014-2018	54%	46%	18%	26
	2010-2018	34%	66%	5%	316
Central North Atl. (east of 45ºW)	2012-2017	46%	54%	14%	43
	2012-2017	10%	90%	3%	792
Canary Island	2020-2021	0%	100%	0%	25
	2013-2021	3%	97%	2%	302
Norwegian Sea	2020	0%	100%	0%	31
	2018-2020	0%	100%	0%	74

Mixed-stock analyses by MLE indicated that individuals sampled in the Norwegian Sea and Canary Island in the current and previous phases were connected to the

Mediterranean population, based on their $\delta^{13}C$ and $\delta^{18}O$ values (Table 6.2.1). Mixing proportions were calculated using the Hisea mixture model, and 100% of the tuna captured in both areas were assigned to the eastern population. Based on these results, Mediterranean population would be the only contributor to the Norwegian and Canary Island fisheries. The Canary Island region has been identified as a putative mixing area of eastern and western populations, since considerable western contribution was found in some years (e.g. 2013, 2015 and 2016). The contribution of western individuals to the east Atlantic fisheries is of particular interest to resource managers because of the strong asymmetrical production between the two populations (Secor, 2015). The combination of $\delta^{13}C$ and $\delta^{18}O$ values analyzed under the GBYP program during the last decade suggested that the Mediterranean population is the main contributor of the catches in the Canary Island, and that the contribution of western migrant in this region may be a sporadic phenomenon.

Samples analyzed in this task were also assigned to Gulf of Mexico (GOM) and Mediterranean Sea (MED) populations individually, with associated levels of probability. The identification of individual origin is needed for at least two main reasons: the construction of stock-age-length-keys, and the comparison/improvement of individual assignments based on different types of markers (i.e., genetic, otolith shape and stable isotopes). Moreover, it allows for tabulation of the results according to any stratification that might be used during the stock assessment or MSE process. Individual origin assignments were computed using Quadratic Discriminant Analysis Function, and results were overall concordant with MLE method.

The results are presented in Fig.6.2.3, which shows the probability of each individual to be assigned to either Gulf of Mexico or Mediterranean Sea source populations, considering these two possible origins to assign the dataset. Full posterior probabilities of the bluefin tuna otoliths analyzed in the current phase have been included in the Appendix 3 of the current report. Probabilities between 30% and 70% were considered as unassigned.

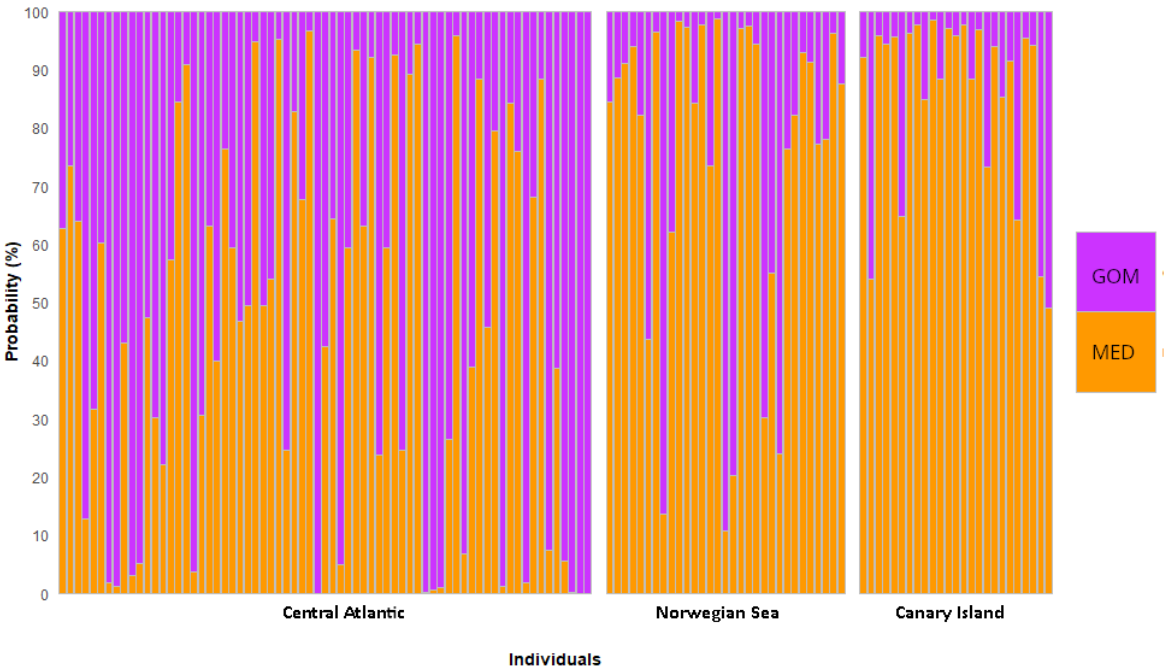

Figure 6.2.3: Bar plot representing individual assignment probability to GOM or MED nursery areas using Quadratic Discriminant Function Analysis on $\delta^{13}C$ and $\delta^{18}O$ data. Each vertical bar represents an individual and the different colors are the probability that each individual was assigned to the Gulf of Mexico (purple) or Mediterranean Sea (orange) populations. Samples analyzed under GBYP-Phase 12 were captured in the central North Atlantic, Norwegian Sea and Canary Island.

Individual origin has also been evaluated geographically to get an overview of the last decade. The probability of western origin has been mapped in catch locations between 2009 and 2022 (Figure 6.2.3). When several fish from the same catch locations were analyzed, the mean probability value was used to represent that location. The results showed a spatial separation of catches within the North Atlantic Ocean: fisheries operating in the eastern North Atlantic dominated by the Mediterranean origin fish, western Atlantic coast dominated by the Gulf of Mexico origin fish, and central North Atlantic catches composed by a mixture of stocks.

Our results provide strong evidence of longitudinal population structuring of bluefin tuna in the North Atlantic Ocean, and demonstrate the capacity of otolith chemistry to determine their natal origin, at both spatial and interannual time-scales. Here, we enhance the importance of monitoring temporal variations in mixing ratios for an effective stock management, especially in the current scenario of changing environment.

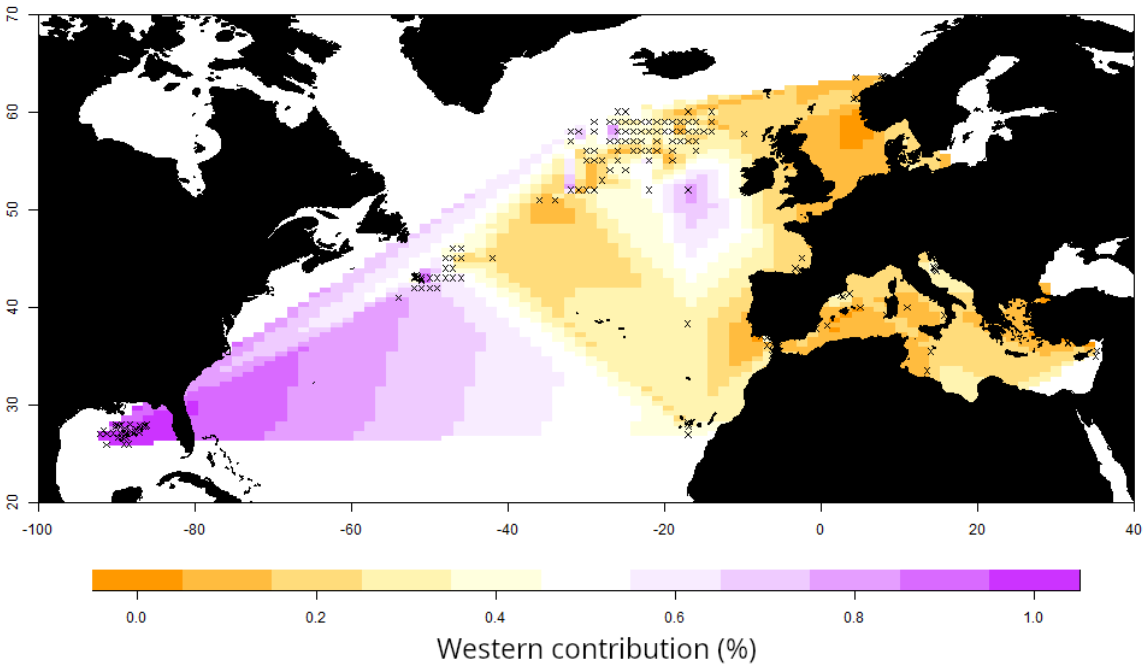

Figure 6.2.3: Western contribution estimated by individual origin assignment using Quadratic Discriminant Analysis. Data from 2019 to 2022 were combined and interpolated among the sampled positions (represented by "x"). Mean values were estimated for data from the same catch location.

6.3 Task 3: Refine microchemistry-based methodologies for determining the timing of relevant biological traits

6.3.1 Introduction

Previous phases of GBYP have progressed the development of otolith microchemistry methods for reconstructing environmental histories in Atlantic bluefin tuna. Current techniques, secondary ion mass spectrometry (SIMS), and isotope ratio mass spectrometry (IRMS) have been cross calibrated and the linear relationship between water temperature and oxygen stable isotopes ($\delta^{18}O$) in the otolith has been demonstrated using bluefin held in sea pens for three years. High resolution $\delta^{18}O$ profiles captured using SIMS show fluctuations that most likely reflect movements between areas of different water chemistry overlaid on seasonal temperature changes. Two patterns are evident among the Mediterranean population: in some fish otolith $\delta^{18}O$ values show regular annual fluctuations between widely divergent extremes after the 2nd year of life, while in

others $\delta^{18}O$ values are more stable across the otolith transect. This may reflect alternative migratory and resident behaviours, which have previously been proposed to occur in this stock (Aranda et al. 2013, Cermeño et al. 2015).

This task aimed to build on progress made in previous phases by further developing otolith microchemistry-based approaches for reconstructing migration histories and determining the timing of important events in the life history of Atlantic bluefin tuna. This can add value to the GBYP tissue bank by enabling new analyses of previously collected material and data.

Objective

- Compare otolith trace element profiles between ABFT with distinct otolith $\delta^{18}O$ profiles to develop otolith chemistry indicators of migrant and resident behaviors.
- Refine fractionation equation for Atlantic bluefin tuna.

6.3.2 Materials and Methods

a) Two-dimensional otolith trace element imaging.

During phase 11 and 12, otolith trace elemental maps were generated for 15 sagittal otoliths of bluefin tuna which had previously been analyzed using SIMS (as described in phase 10 and phase 11 reports). Fourteen of these individuals were from the Mediterranean population. One was captured off the coast of Morocco and its stock origin was uncertain due to disagreement between otolith chemistry and genetic based assignments.

Prior to the SIMS analysis the otoliths were embedded in two-part epoxy resin (Araldite 2020) and polished with silicon carbide sandpapers of a range of grit sizes under running water until the core was exposed. After the SIMS analysis the otolith sections were polished again and were cleaned with deionized water and dried under laminar air flow. Otoliths sections were analyzed with laser ablation inductively coupled mass spectrometry (LA-ICPMS) (available at the Institut des Sciences Analytiques et de Physico-Chimie pour l'Environnement et les Matériaux, Université de Pau et des Pays de l'Adour/CNRS, Pau, France) to create two dimensional maps of trace element concentration. To correct for short-term instrumental drift, two standards (NIST-610 and NIST-612) were measured at the beginning and the end of each session. Measurement

accuracy was determined based on an otolith certified reference material for trace elements (FEBS-1). The laser beam was set to scan in a raster pattern mode over the surface of the ventral arm of the otolith. 2-dimensional image were built from the fs-LA-HR-ICPMS signal resulting from the samples ablation according to a series of horizontal lines. Sr, Ba, Mn and Mg concentrations were converted to colour images to visualize trace element patterns. 2D images were filtered using the Ca concentration as a reference to remove all the signals corresponding to epoxy and crystalbond.

b) Alignment of $\delta_{18}O$ and trace element profiles

The trace elemental images were aligned with images of the ablations made using SIMS and where available, images of the second otolith that were annotated for age estimation. In ImageJ, the PAMAL ratio 2.2 plug in and the line profiling tool were used to extract Sr, Ba, Mg and Mn concentrations from a transect corresponding to the SIMS ablations (Figure 6.3.1). Scaled trace element concentrations and $\delta^{18}O$ values from each transect and the positions of annual bands were overlaid in a series of plots. The $\delta^{18}O$ profiles were characterised according to the level of fluctuation in $\delta^{18}O$ values observed across the adult portion of the transects (age 3 onwards) using the range (maximum-minimum) of the scaled $\delta^{18}O$ values. Profiles with fluctuations in $\delta^{18}O$ greater than 3 were classed as *variable* and those with fluctuations in $\delta^{18}O$ less than 3 were classed as *stable*. This categorisation corresponded with the previous visual interpretation of the profiles.

Second order differencing with a lag of 3 was used to produce a stationary time series for each chemical variable along each transect. This reduced the influence of ontogenetic changes in otolith chemical composition and allowed for closer alignment of the $\delta^{18}O$ and trace element profiles.

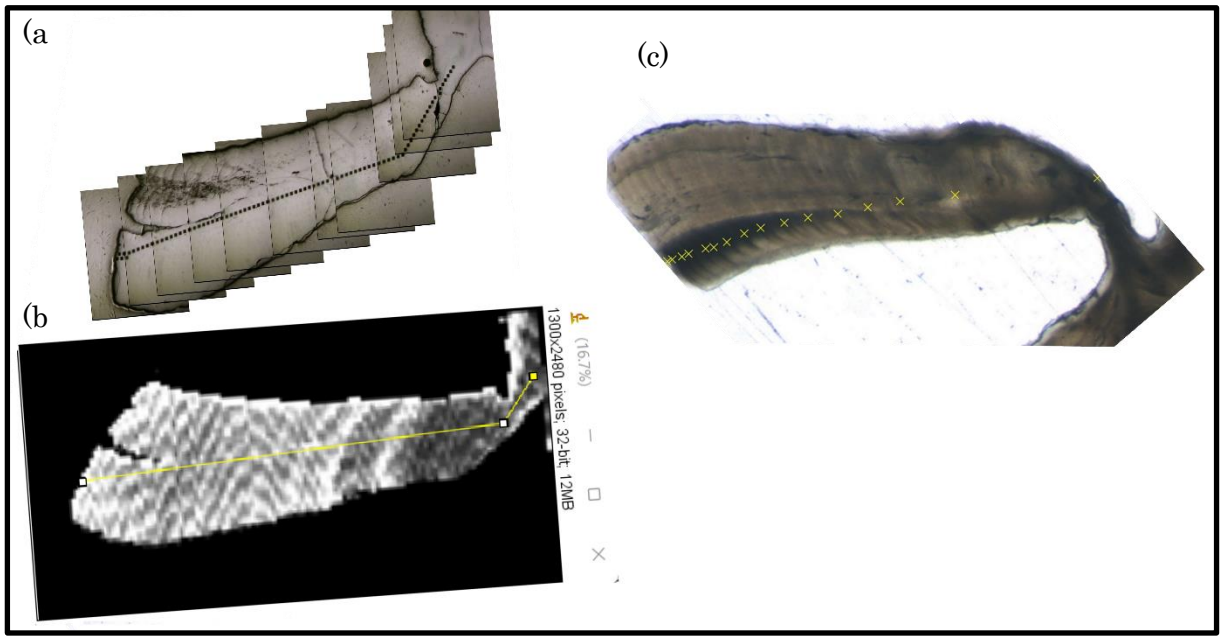

Figure 6.3.1. (a) Stitched microscope image of a bluefin tuna otolith section showing the ablations from the SIMS analysis. (b) Two-dimensional image of Sr concentrations from the La ICPMS analysis of the same otolith section showing the transect used to extract the trace element profiles. (c) Section of the second otolith from the same fish showing the position of the annual growth bands.

c) Quantifying synchrony in the chemical profiles

Similarity in the shapes of the standardised and differenced $\delta^{18}O$ and trace element profiles were examined for each individual using the shape-based distance measure (SBD) in the dtwclust package in R (Sardá-Espinosa 2019). This measure is based on coefficient-normalized cross-correlation (Paparrizos and Gravano 2015). Values vary from 0 to 2 with 0 indicating perfect similarity in shape. In addition, the Pearson correlation coefficient was calculated for each pair of differenced profiles.

d) Trace element variability as a potential marker of movement between water masses

The cyclical fluctuations observed in the $\delta^{18}O$ profiles are likely to reflect a combination of seasonal temperature changes as well as horizontal and vertical movements of fish between water masses with different chemistry. Large scale fluctuations in $\delta^{18}O$ within the adult portion of the transect may indicate migratory behaviour while stable $\delta^{18}O$ with the same otolith region suggests residency within a more restricted area. Each of the $\delta^{18}O$ and trace element profiles was truncated to isolate the region corresponding to ages 4 to 7, where pronounced fluctuations in $\delta^{18}O$ were most apparent. Points on the $\delta^{18}O$ transect

were categorised as *high* or *low* relative to the mean of the scaled values for that portion of the transect (*high* >= 0.1; *low* <=-0.1; intermediary values were excluded). Points on each trace element transect were categorised according to whether the corresponding $\delta^{18}O$ values were high or low.

Multidimensional scaling was used to visualise multivariate difference in trace element concentrations between the *high* $\delta^{18}O$ and *low* $\delta^{18}O$ regions of the transect for each individual and across all individuals combined.

e) Refinement of Fractionation equation for Atlantic bluefin tuna

During GBYP phase 10, a fractionation equation for Atlantic bluefin tuna was estimated, using SIMS measurements of $\delta^{18}O$ from three adult fish (total length ~160cm) held within pens for 3 years. During phase 11, IRMS and SIMS measurements of $\delta^{18}O$ in the same otoliths were combined to produce an equation for converting SIMS estimates of $\delta^{18}O$ to the equivalent IRMS measurement. This task built on these advances by reanalysing IRMS measurements of $\delta^{18}O$ from young of the year Atlantic bluefin tuna in combination with SIMS estimates of $\delta^{18}O$ from the ranched fish. The aim was to determine if there was a consistent relationship between $\delta^{18}O$ in the otolith and seawater temperature across the two life stages which could be used to generate a more robust fractionation equation.

The reanalysis included IRMS measurements of $\delta^{18}O$ from the whole otoliths of 123 young of the year collected at various locations in the central, western and eastern Mediterranean and the East Atlantic in 2011, 2012, 2013, 2015 and 2017. The age of each fish was estimated based on fish length to derive an estimated birth date. Estimates of sea surface temperature were obtained from the Copernicus Climate Service (2019) and the gridded dataset of Legrande and Schmidt (2006) was used to derive estimates of seawater $\delta^{18}O$ for each location where the young of the year were collected. SIMS $\delta^{18}O$ values along the transects of the three adult tuna corresponding to the period of captivity were converted to equivalent IRMS measurements using the conversion equation presented in the GBYP phase 11 report and combined with corresponding seawater temperature and $\delta^{18}O$ estimates (as described in the GBYP phase 10 report). The young of the year and adult datasets were combined and the relationship between temperature and $\delta^{18}O$ fractionation ($\delta^{18}O_{otolith}$ - $\delta^{18}O_{seawater}$) was plotted.

6.3.3 Results

a) Alignment of $\delta_{18}O$ and trace element profiles

Plots of the trace element profiles overlaid on $\delta^{18}O$ transects showed evidence of synchronous cycles across trace elements and stable isotopes (see example in Figure 6.3.2). The extent of the overlap varied between individuals and between elements. Fluctuation in strontium often corresponded with annual bands, as has previously been reported (Siskey et al. 2016), however sub-annual cycles were also observed.

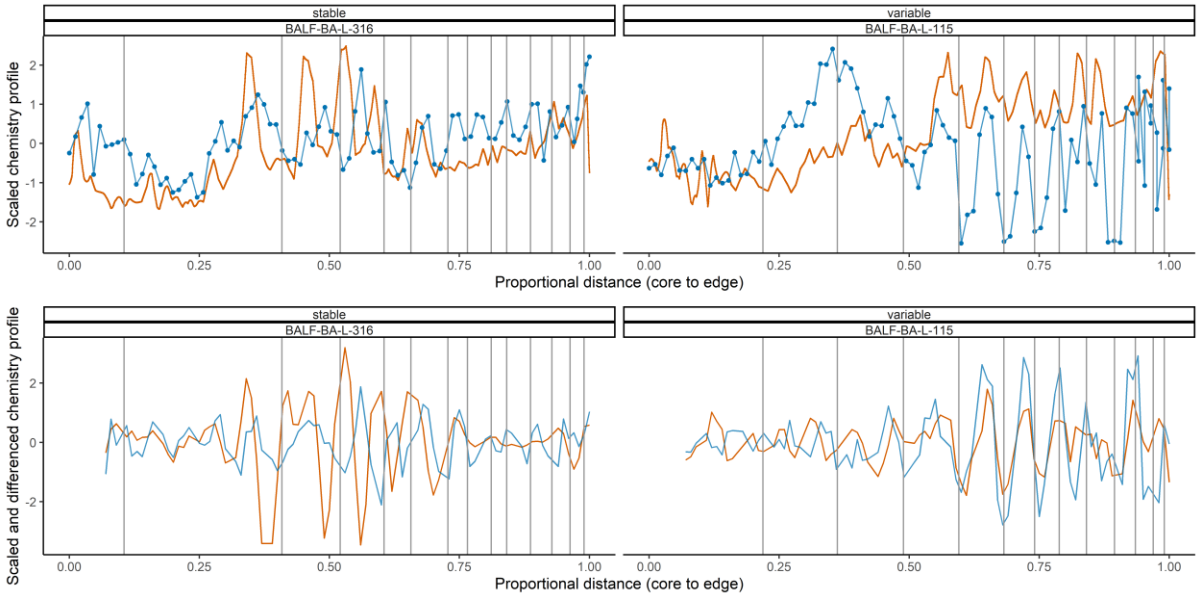

Figure 6.3.2: Strontium concentration (orange) along otolith transects from two bluefin tuna overlaid on $\delta_{18}O$ values (blue) from the same transects. The profiles in the upper panels have been scaled. The lower panels show the same scaled profiles after applying 2nd order differencing to remove ontogenetic trends. The profiles on the left are an example of a stable $\delta_{18}O$ profile those on the right are variable (the difference between the minimum and maximum $\delta_{18}O$ values in the adult portion of the otolith exceeds 3).

b) Measures of synchronicity in the chemical profiles

The SBD measures showed overlap in the shape of the profiles across all pairwise combinations of elements and $\delta^{18}O$ for individuals in both the *variable* and the *stable* $\delta^{18}O$ groups (Figure 6.3.3). Significant correlations were detected between the $\delta^{18}O$ and trace element profiles and between pairs of trace elements (Figure 6.3.4). The strongest correlations were observed between Mg and Mn profiles and between $\delta^{18}O$ and Sr profiles. For two out of the 15 individuals, no significant correlations were detected between the $\delta^{18}O$ and trace element profiles.

c) Multivariate differences in trace elements between areas of high and low $\delta_{18}O$ along adult profiles

When individuals were combined, the MDS plot showed complete overlap in the trace elemental signatures of the *high* and *low* $\delta^{18}O$ (Figure 6.3.5) transect portions for both the *variable* and *stable* groups. There was therefore no evidence that the pronounced fluctuations in $\delta^{18}O$ correspond to a common migration route between water masses with distinct chemistry. However, when trace element variation was plotted for each individual separately, trace elemental variation between *high* and *low* $\delta^{18}O$ portions of the transect was observed in some individuals (BALF-BA-L-115; BALF-BA-L-176; BALF-BA-L-358 and BALF-BA-L-461). This may reflect individual variation in migration behaviour or physiological responses to spatial and temporal changes in temperature and water chemistry.

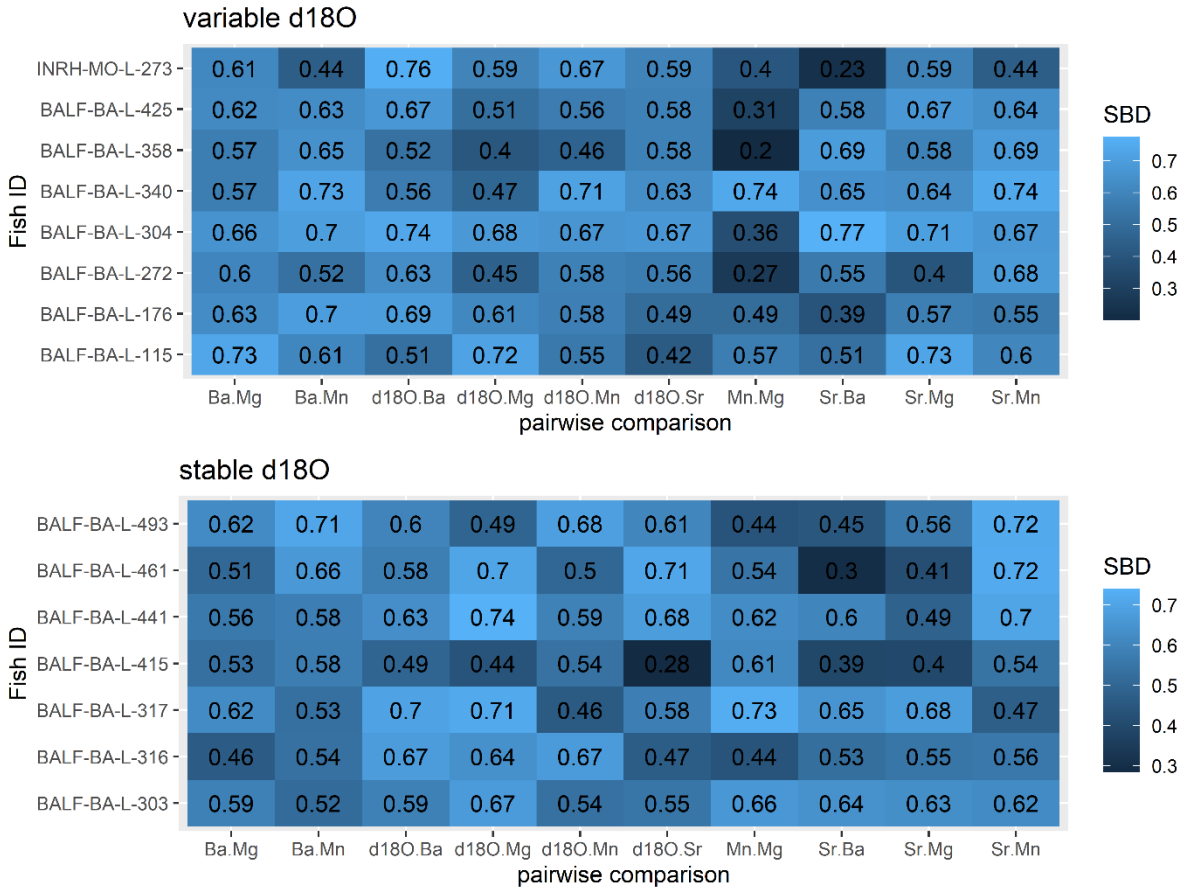

Figure 6.3.3: Shape based distance measures for each pair of scaled and differenced otolith chemistry profiles from each individual in the variable and stable $\delta^{18}O$ groups. SBD values can range from 0 to 2 with 0 indicating identically shaped time series.

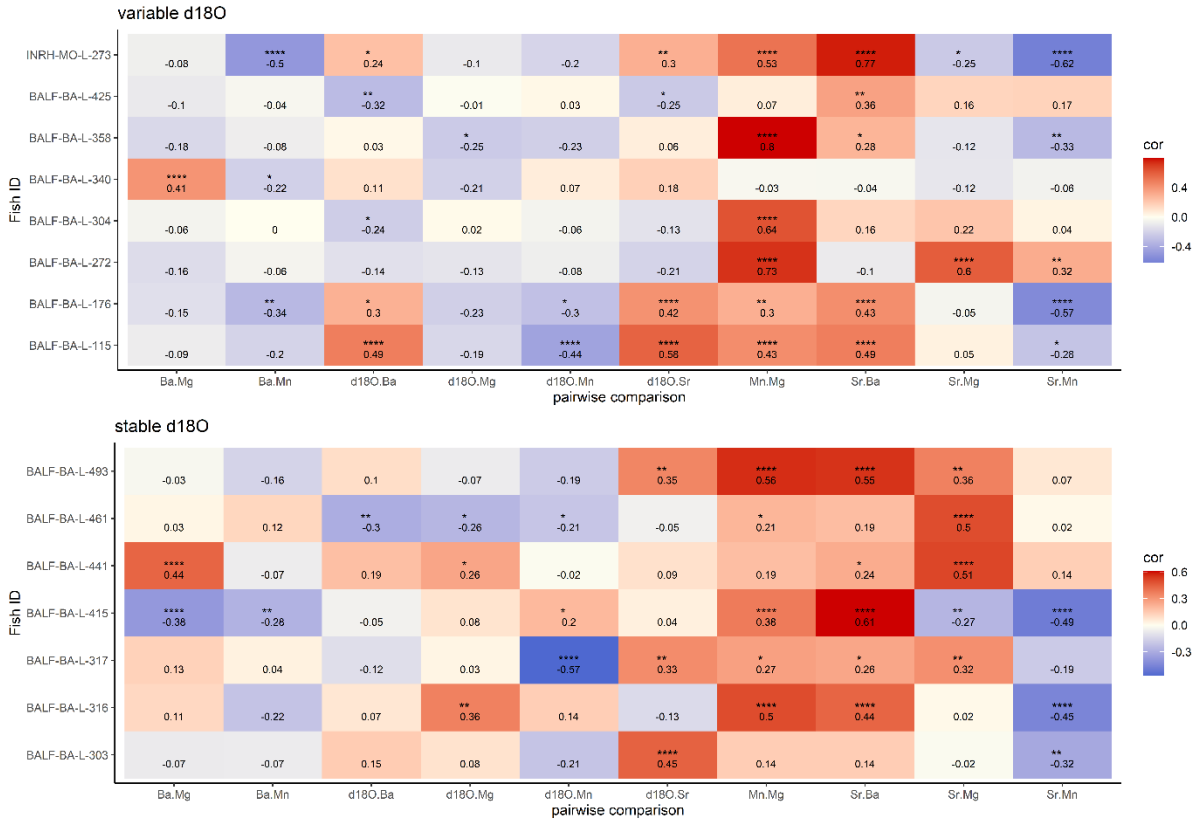

Figure 6.3.4: Pearson correlation test results for each pair of scaled and differenced otolith chemistry profiles from each individual in the variable and stable $\delta_{18}O$ groups. The figures in each cell and the colour gradient indicate the correlation coefficients. Statistical significance is shown with an asterisk (<0.05, <0.01**, <0.001***, significant after Bonferroni adjustment for 150 pairwise comparisons ****).*

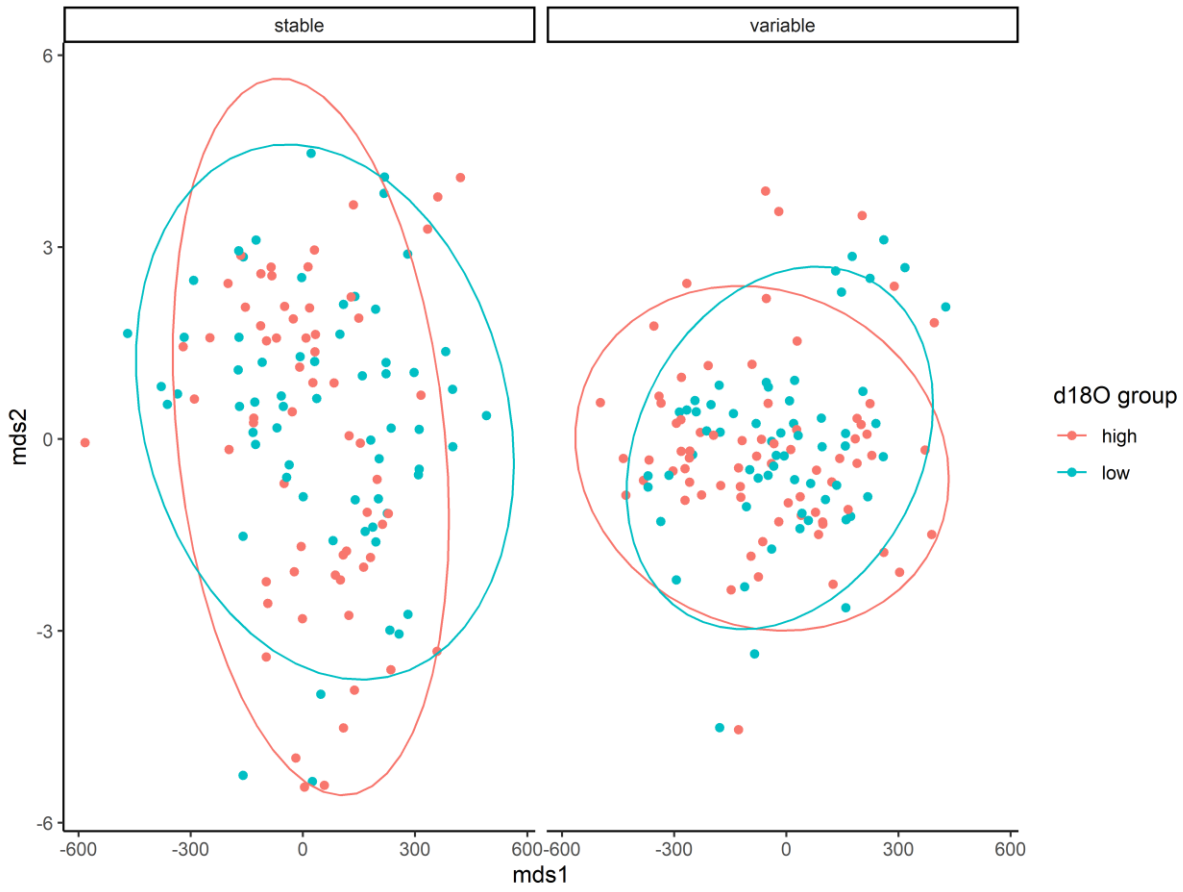

Figure 6.3.5: Multidimensional scaling (MDS) plot showing variation in trace elements (Sr, Ba, Mg, Mn) between areas of high and low $\delta_{18}O$ values within the adult portion of the transect (age 4-7) within the variable and stable $\delta_{18}O$ groups.

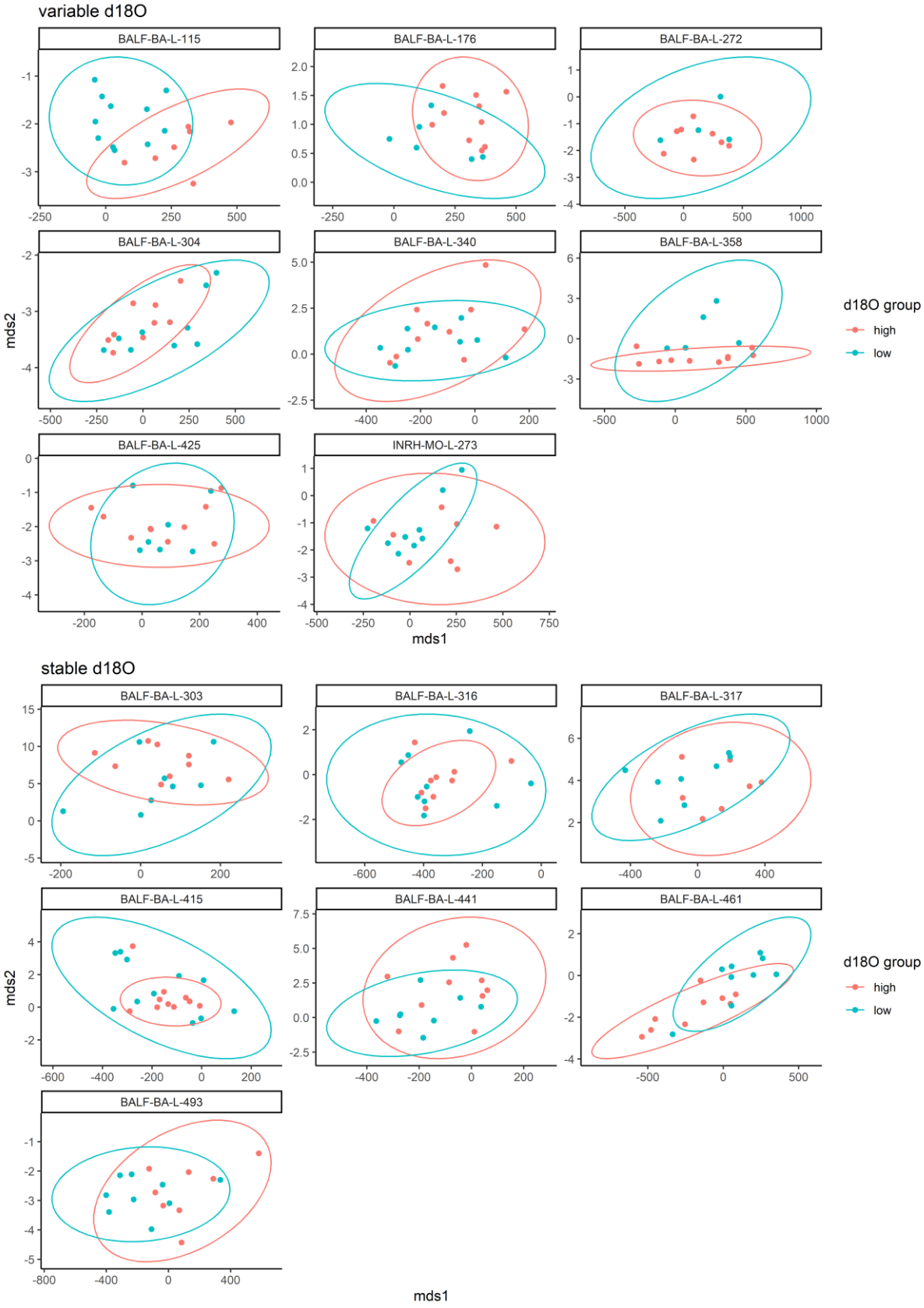

Figure 6.3.6: Multidimensional scaling (MDS) plot showing variation in trace elements (Sr, Ba, Mg, Mn) between areas of high and low $\delta_{18}O$ values within the adult portion of the transect (age 4-7) at the individual level.

d) Refinement of Fractionation equation for Atlantic bluefin tuna

The reanalysis showed a strong relationship between $\delta^{18}O$ fractionation and seawater temperature which was reasonably consistent across the adults and young of the year (R^2 =0.8). The resulting fractionation equation spans a wide range of temperatures (15-27.5 °C) and a greater fish size range than previously derived equations (Figure 6.3.7). The fractionation equation could be used to reconstruct temperature histories using existing $\delta^{18}O$ data from the GBYP database.

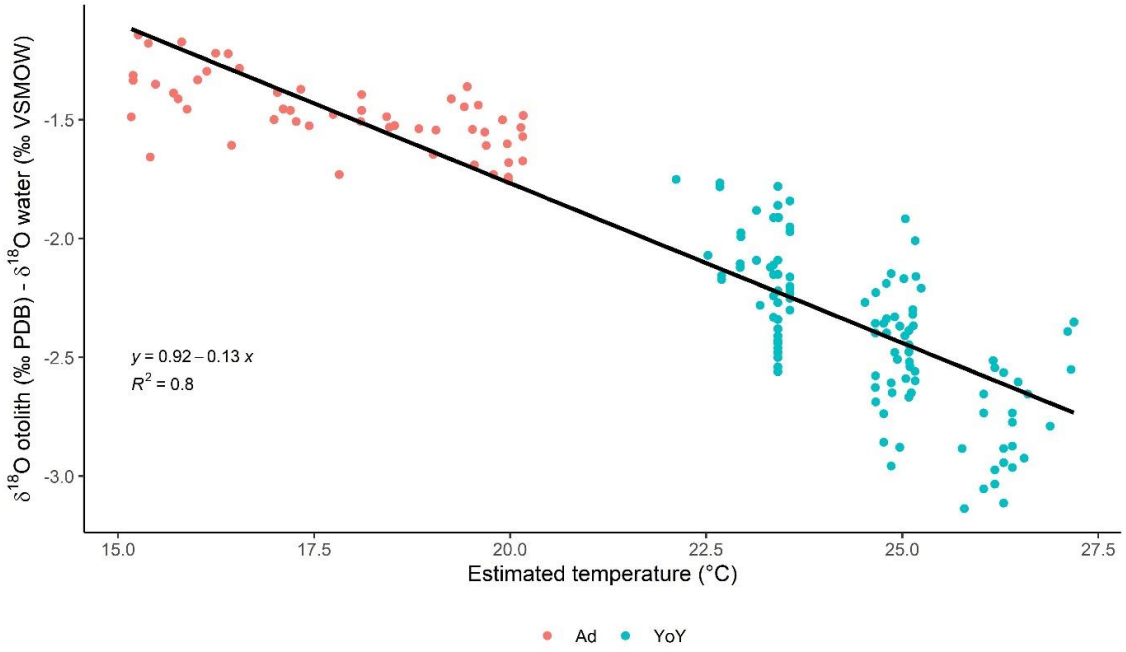

Figure 6.3.7: $\delta_{18}O$ fractionation plotted against the estimated mean seawater temperature during the period of otolith growth for adult bluefin held at a fish farm in the central Mediterranean (43.19° latitude, 15.24° longitude) between June 2013 and January 2016 (Ad, red points) and young of the year collected at various locations in the central, western and eastern Mediterranean and the East Atlantic in 2011,2012, 2013, 2015 and 2017 (YoY, blue points). Regression parameters are shown in colour for individual fish and in black for the three fish combined.

6.3.4 Conclusions

The combined analysis of trace element and $\delta^{18}O$ profiles from the same otolith transects showed that cyclical patterns in $\delta^{18}O$ values often coincided with fluctuations in trace elements. Synchronicity with $\delta^{18}O$ was most pronounced for Sr and may be attributed to the direct and indirect influence of temperature on the uptake of Sr into the otolith (Seyama et al. 1991, Siskey et al. 2016). Significant

correlations between $\delta^{18}O$ and Ba, Mg and Mn were also observed in some individuals.

Multivariate comparison of trace element signatures between otolith regions with high and low $\delta^{18}O$ signatures showed no evidence of common migration route between distinct water masses and reflect high levels of individual variability in horizontal and vertical movement and physiological responses to changes in temperature.

Combining SIMS with two-dimensional trace elemental mapping and visual interpretation of annual growth bands provides highly resolved data integrating the temperature and environmental history of the fish across its life span. Application of this approach to fish of known environmental history (e.g., from tagging studies) would build understanding of the various interacting factors that influence the otolith chemistry profiles. Otolith profiles between fish from the Western Atlantic and Mediterranean stocks may show more distinct signatures than groups within the Mediterranean. Integrated analysis of these profiles (e.g., using time series clustering approaches) could be used to discriminate between fish with distinct life histories. There is also scope to use this approach for verifying interpretations of annual bands in the otolith.

The combined fractionation equation for young of the year and adult Atlantic bluefin tuna demonstrates that $\delta^{18}O$ closely reflects the temperature and isotopic composition of the water throughout life. This equation provides a means to reanalyse existing datasets in order to reconstruct environmental histories and detect movement between water masses.

References

Aranda, G., F. J. Abascal, J. L. Varela, and A. Medina. 2013. Spawning Behaviour and Post-Spawning Migration Patterns of Atlantic Bluefin Tuna (Thunnus thynnus) Ascertained from Satellite Archival Tags. PLoS One 8:e76445.

Block, B., Teo, S., Walli, A., & Boustany, A. (2005). Electronic tagging and population structure of Atlantic bluefin tuna. Nature, 434, 1121–1127.

Brophy, D., Rodríguez-Ezpeleta, N., Fraile, I., & Arrizabalaga, H. (2020). Combining genetic markers with stable isotopes in otoliths reveals complexity in the stock structure of Atlantic bluefin tuna (Thunnus thynnus). Nature Scientific Reports, 10(1), 1–17. https://doi.org/10.1038/s41598-020-71355-6

Cermeño, P., G. Quílez-Badia, A. Ospina-Alvarez, S. Sainz-Trápaga, A. M. Boustany, A. C. Seitz, S. Tudela, and B. A. Block. 2015. Electronic Tagging of Atlantic Bluefin Tuna (Thunnus thynnus, L.) Reveals Habitat Use and Behaviors in the Mediterranean Sea. PLoS One 10:e0116638.

Fraile, I., Arrizabalaga, H. and Rooker, J.R., 2015. Origin of Atlantic bluefin tuna (Thunnus thynnus) in the Bay of Biscay. ICES Journal of Marine Science: Journal du Conseil 72: 625-634.

Kerr, L., Whitener, Z., Cadrin, S., Morse, M., Secor, D., & Golet, W. (2020). Mixed stock origin of Atlantic bluefin tuna in the US rod and reel fishery (Gulf of Maine) and implications for fisheries management. Fisheries Research, 224, 10.1016/j.fishres.2019.105461. https://doi.org/10.1016/j.fishres.2019.105461

LeGrande, A. N., and G. A. Schmidt. 2006. Global gridded data set of the oxygen isotopic composition in seawater. Geophysical Research Letters 33.

Millar, R.B., 1990. Comparison of methods for estimating mixed stock fishery composition. Canadian Journal of Fisheries and Aquatic Sciences 47: 2235-2241.

Paparrizos, J., and L. Gravano. 2015. k-Shape: Efficient and Accurate Clustering of Time Series. Pages 1855–1870 Proceedings of the 2015 ACM SIGMOD International Conference on Management of Data. Association for Computing Machinery, Melbourne, Victoria, Australia.

Rodríguez-Ezpeleta, N., Díaz-Arce, N., Walter, J. F., Richardson, D. E., Rooker, J. R., Nøttestad, L., Hanke, A. R., Franks, J. S., Deguara, S., Lauretta, M. V., Addis, P., Varela, J. L., Fraile, I., Goñi, N., Abid, N., Alemany, F., Oray, I. K., Quattro, J. M., Sow, F. N., … Arrizabalaga, H. (2019). Determining natal origin for improved management of Atlantic bluefin tuna. Frontiers in Ecology and the Environment, 17(8), 439–444. https://doi.org/10.1002/fee.2090

Rooker, J. R., H. Arrizabalaga, I. Fraile, D. H. Secor, D. L. Dettman, N. Abid, P. Addis, S. Deguara, F. S. Karakulak, A. Kimoto, O. Sakai, D. Macias, and M. N. Santos. 2014. Crossing the line: migratory and homing behaviors of Atlantic bluefin tuna. Marine Ecology Progress Series 504:265-276.

Rooker, J. ., Fraile, I., Liu, H., Abid, N., Dance, M. A., Itoh, T., Kimoto, A., Tsukaraha, Y., Rodriguez-Marin, E., & Arrizabalaga, H. (2019). Wide-Ranging Temporal Variation in Transoceanic Movement and Population Mixing of Bluefin Tuna in the North Atlantic Ocean. Frontiers in Marine Science, 6(398), 1–13. https://doi.org/10.3389/fmars.2019.00398

Rooker, J. R., D. H. Secor, G. De Metrio, R. Schloesser, B. A. Block, and J. D. Neilson. 2008a. Natal Homing and Connectivity in Atlantic Bluefin Tuna Populations. Science 322:742-744

Sardá-Espinosa, A. 2019. Time-Series Clustering in R Using the dtwclust Package. The R Journal 11:22.

Secor, D. H. 2015. Migration Ecology of Marine Fishes. Baltimore: Johns Hopkins University Press

Seyama, H., J. S. Edmonds, M. J. Moran, Y. Shibata, M. Soma, and M. Morita. 1991. Periodicity in Fish Otolith Sr, Na, and K Corresponds With Visual Banding. Experientia 47:1193-1196.

Siskey, M. R., V. Lyubchich, D. Liang, P. M. Piccoli, and D. H. Secor. 2016. Periodicity of strontium: Calcium across annuli further validates otolith-ageing for Atlantic bluefin tuna (Thunnus thynnus). Fisheries Research 177:13-17.

7. STOCK MIXTURE ANALYSIS WITH OTOLITH CHEMISTRY AND GENETIC MARKERS

Task Leader: Iraide Artetxe-Arrate (AZTI) & Natalia Diaz (AZTI)

Participants:

AZTI: Igaratza Fraile, Naiara Rodriguez-Ezpeleta

7.1 Introduction

The fisheries for Atlantic bluefin tuna are managed considering two management units, conventionally separated by the 45°W meridian (ICCAT, 2020). However, efforts to understand the population dynamics through tagging, genetic and microchemistry studies indicate that mixing of both units occurs at variable rates across the two management areas. Over the last 10 Phases of the GBYP programme ABFT individuals have been routinely analyzed to assign stock of origin based on otolith microchemistry and genetic markers to investigate the degree of eastern and western population contribution to different mixing areas in the Atlantic Ocean. These results have been routinely presented separately; however, the use of both methods together can provide further insights into the complexity of the stock structure of the species and enhance the understanding of ecological and evolutionary processes that may help to identify stock units with a high degree of confidence (Brophy et al. 2020). The aim of this task is to use carbon and oxygen stable isotopes and 86 SNPs available for the same individuals, to estimate the origin of ABFT captured outside spawning areas in the Atlantic Ocean and assess the level of mixing in the different areas.

7.2 Material and Methods

Two different approaches were followed: (1) Individual origin was re-assigned using an integrated classification model that includes both genetic and stable isotope data (i.e., Integrated approach) and (2) genetic and stable isotope data was used complementarily (i.e., Combined approach). Both approaches were applied to ABFT captured outside two spawning areas (Mediterranean Sea, MED, and Gulf of Mexico, GOM) in the Atlantic Ocean (Figure 7.1).

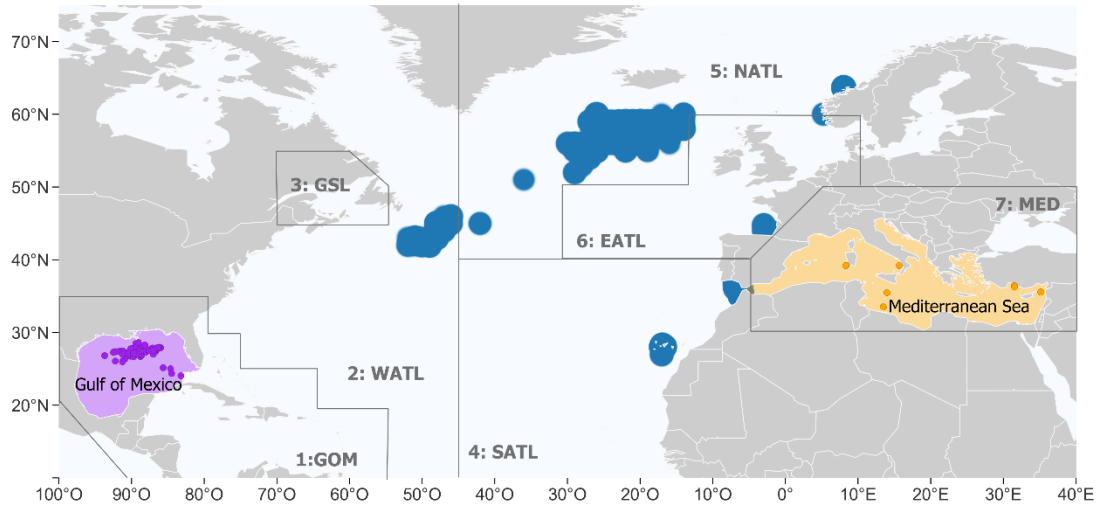

Figure 7.1. Map of individuals with both stable isotopes and genetic data analyzed in this study. Adults collected from the two main spawning areas, the Gulf of Mexico (GOM, purple area) and the Mediterranean Sea (MED, orange area) are shown as purple and orange dots, respectively. Approximate capture locations of individuals of unknown origin are shown as dark blue locations. Grey delimited squares represent the spatial definitions of seven areas used for ABFT MSE by ICCAT where; 1: Gulf of Mexico (GOM), 2: West Atlantic (WATL), 3: Gulf Saint Lawrence (GSL), 4: South Atlantic (SATL), 5: North Atlantic (NATL), 6: East Atlantic (EATL) and 7: Mediterranean Sea (MED).

7.2.1 Integrated approach

The most likely population of origin of individuals with both otolith stable isotope data and genetic data available (with SNP missing <5%) in the GBYP framework (N=1519) was assigned following the random forest (RF, ntree=200) approach described in Brophy et al., (2020). Genotype data from 96 newly analyzed individuals were included to increase the number of samples with combined otolith microchemistry values and genetic assignment estimation. The baseline (N=161) used to characterize the Gulf of Mexico (GOM) and Mediterranean (MED) spawning populations was built based on mature adults (>185 cm FL in the GOM, >135 cm in the MED) collected during the spawning season at each spawning ground: from April to June in the GOM, and from May to June in the eastern MED and from June to July in the central and western MED. Besides, only individuals with MED or GOM genetic profile confirmed in Task 4.2 were selected to conform the baseline (Table 7.1). Baseline classification accuracy was tested estimated, whilst Cohen's kappa (κ) coefficient was calculated as an additional metric of classifier performance statistic (Jones et al., 2017). Values of κ range from 0 to 1, where 0 indicates that the RF

resulted in no improvement over chance, and 1 indicates perfect agreement. Variable importance was determined based on the mean decrease in accuracy and mean decrease in the Gini Coefficient, where higher values indicate greater importance of the variable in the model (Cutler et al. 2017).

Table 7.1. ABFT individuals used as reference baseline for integrated analyses.

Stock	N	Catch month	Catch year	SFL range	Estimated age range	Represented time period
GOM	81	Apr-Jun	2010-2014	199-281	9-18	1992-2005
MED	80	May-Jul*	2011-2015	163-250	6-14	1999-2009

* May to June in the eastern MED and from Jun to July in the central and western MED

When an individual showed a probability of belonging to GOM or MED populations <70%, it was classified as unassigned (UNASS). Contribution of each origin was assessed by catch locations, and differences in proportions by catch year and sex were analyzed by areas used for ABFT MSE by ICCAT (see Figure 7.1). A test of equal proportions was used (Pearson's chi-squared test statistic) to see whether there were differences in origin proportions between different catch years. Additionally, a test for trend in proportions (Mann Kendall trend test) was performed to see whether there was a linear trend in the proportion of cases across years or not.

7.2.2 Combined approach

Individuals with origin estimated by for both stable isotope data only in Task 6.1 and genetic markers only in Task 4.2 captured in feeding aggregates (N=1809), were compared and combined to create profiles that fit one of the nine possible combinations: (1) GOM-like otolith and GOM-like genetics, (2) MED-like otoliths and MED-like genetics, (3) unassigned otolith origin and unassigned genetic origin, (4) GOM-like otolith and MED-like genetics, (5) MED-like otolith and GOM-like genetics, (6) MED-like otolith and unassigned genetic origin, (7) GOM-like otolith and unassigned genetic origin, (8) unassigned otolith origin and GOM-like genetics, and (9) unassigned otolith origin and MED-like genetics.

7.3 Results and Discussion

7.3.1 Integrated approach

Random forest model of the integrated baseline has an overall accuracy of 99.1% of correctly assigning fish to their area of origin, showing an almost perfect agreement (k=0.98) between observed and predicted origins (Table 7.2). In this model, 30 variables accumulated >85% of the sum of mean decrease in Gini coefficient (Figure 7.2). Most important variables in distinguishing between the GOM and MED inviduals was $\delta^{18}O$, followed by RAD 213, RAD 35 and RAD 26. These variables were also highlighted as most important variables in the model of Brophy et al., (2020), although in different order. Comparing to single approaches (Tasks 6.1 and 4.2), the integrated model proved to increase the resolving power of stock discrimination.

Table 7.2. Random Forest model output assigning individuals included in the baseline to their area of origin, GOM or MED (n=161). OOB: Out of bag error.

Measure	Value
OOB%	0.93
GOM classification accuracy%	82
MED classification accuracy%	100
Overall classification accuracy %	99.1
Kappa index	0.98
95% Confidence Interval	0.95-1.00
Sensitivity	0.98
Specifity	1.00
Balanced accuracy	0.99

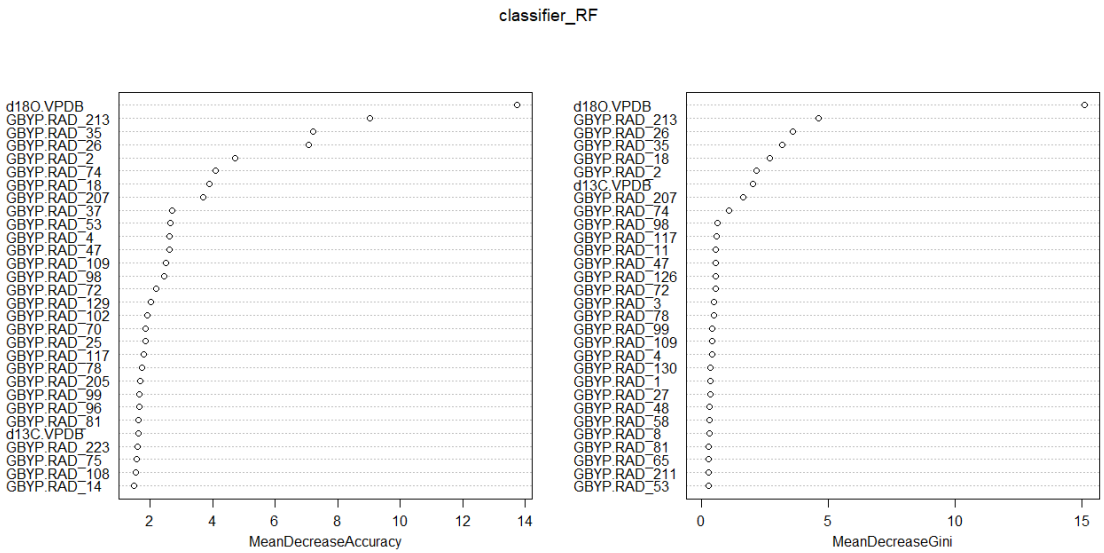

Figure 7.2. Variable importance, shown as Mean Decrease in Accuracy (left panel) and Mean Decrease in Gini coefficient (right panel) from random forest model applied to the baseline samples (N=161).

Overall, the integrated method resulted in lower numbers of unassigned individuals than otolith stable isotope only and genetic markers only models (Figure 7.3). Many of the fish that were unassigned when the techniques were used separately were classified as MED origin fish using the integrated approach. The integrated method also reduced the proportion of fish assigned to the GOM origin in all areas.

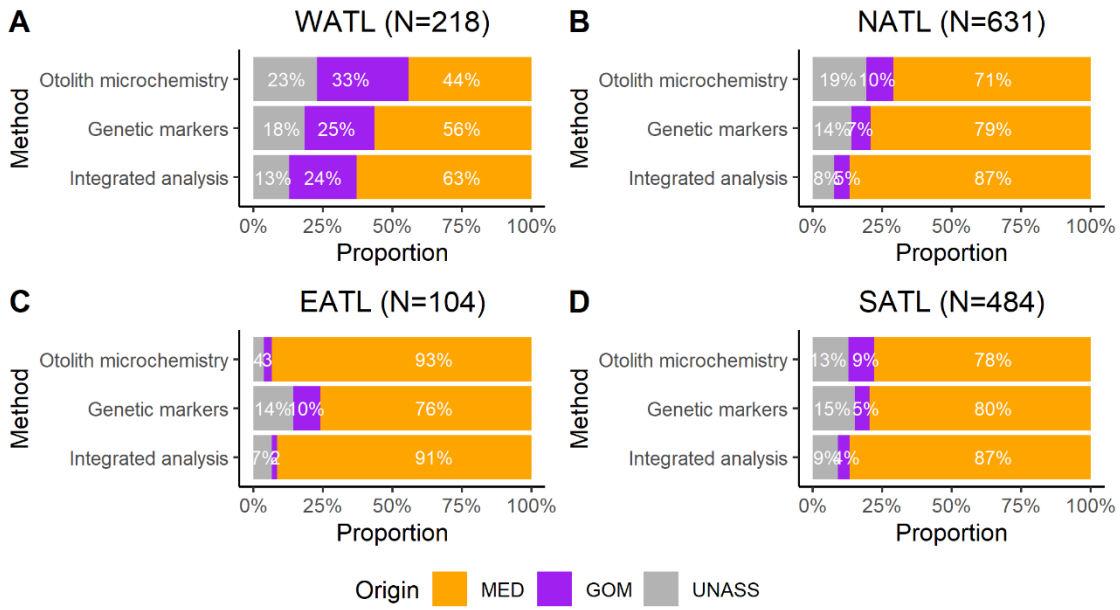

Figure 7.3. Estimated proportions of MED (orange), GOM (purple) and unassigned (grey) origin of ABFT captured in the West (WATL), North (NATL), East (EATL) and South (SATL)

Atlantic Ocean by method; (1) otolith stable isotope data, (2) genetic markers and (3) integrated approach.

Origin assignment of individuals captured outside spawning areas revealed that the proportion of MED origin ABFT was higher in all areas (Figure 7.4). In the WATL the proportion of fish assigned to the GOM origin with the integrated approach was higher (>50%) in 2011 and 2012, but as of 2013 the proportion of individuals from the MED origin increased (Figure 7.4A). In the NATL, the proportion of fish assigned to the MED origin was above 80% in every year analyzed except of 2013 (Figure 7.4B). Every year but 2019 and 2020 (when only samples from easternmost EATL, that is the Norwegian Sea, were available) a small proportion of fish was assigned to the GOM origin also, ranging between 3% to 14%. In the EATL most individuals (>70%) were assigned to the MED origin also, with a small proportion (2%) of fish assigned as GOM in 2011 (Figure 7.4C). The proportion of unassigned fish was noticeably higher in 2012 compared to 2011. In the SATL most fish were assigned to the MED origin, except in 2014, when the number of fish assigned to the MED and to the GOM was the same (Figure 7.4D). Besides, this year the number of unassigned individuals was particularly high (45%). These results suggest that both individuals originated in the GOM and MED can be found at both sides of the 45°W management boundary. The fact that the proportion of fish of MED origin was higher in all analyzed locations, may be because (1) fish originating in the MED tend to move more, and/or (2) the chances of finding fish from the GOM are lower, as this stock is smaller in terms of production. Unfortunately, no ABFT with integrated data were available from additional western feeding grounds such Gulf St Lawrence, Newfoundland, Gulf of Maine, the US coast or the Slope Sea, where previous studies based on genetic markers had shown higher proportion of GOM individuals relative to MED individuals Rodríguez-Ezpeleta et al., (2019) but a study based on otolith stable isotope composition revealed that most of the fish caught in the Gulf of Maine were assigned to MED origin (Kerr et al., 2020). Unifying in one study all the stable isotope and genetic marker data available to date would help to get a more complete picture of the puzzle regarding ABFT mixing on both sides of the Atlantic Ocean.

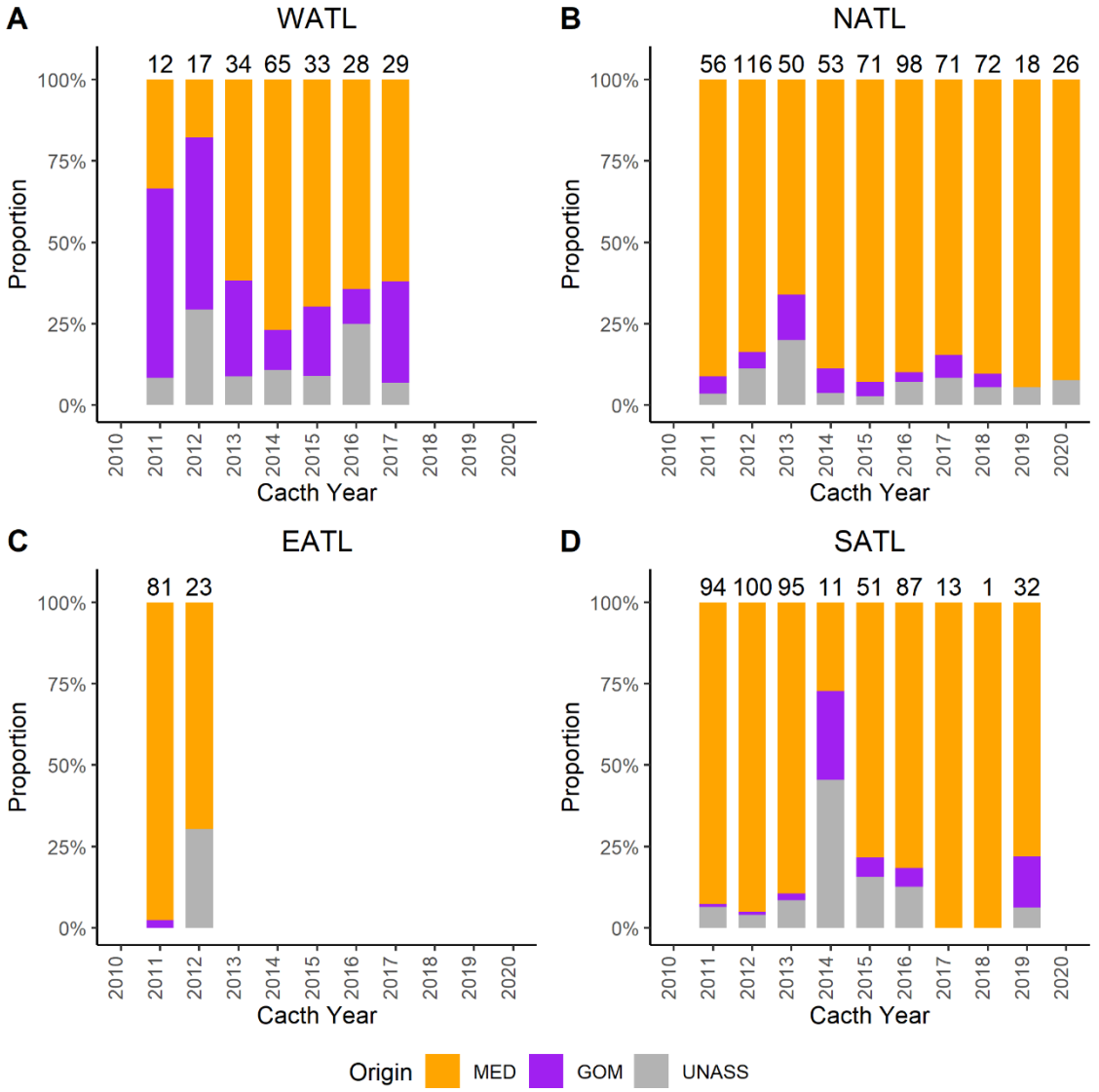

Figure 7.4. Estimated proportions of MED (orange), GOM (purple) and unassigned (grey) origin of Atlantic bluefin tuna samples collected from 2011 to 2020 in the West (WATL), North (NATL), East (EATL) and South (SATL) Atlantic Ocean.

For all areas analyzed there were significant differences among years in the proportion of fish assigned to MED/GOM origins (chi-squared test, $p<0.05$). However, we did not observe any consistent liner temporal trend (i.e., no increasing or decreasing of MED origin fish across years) in any area (Figure 7.5).

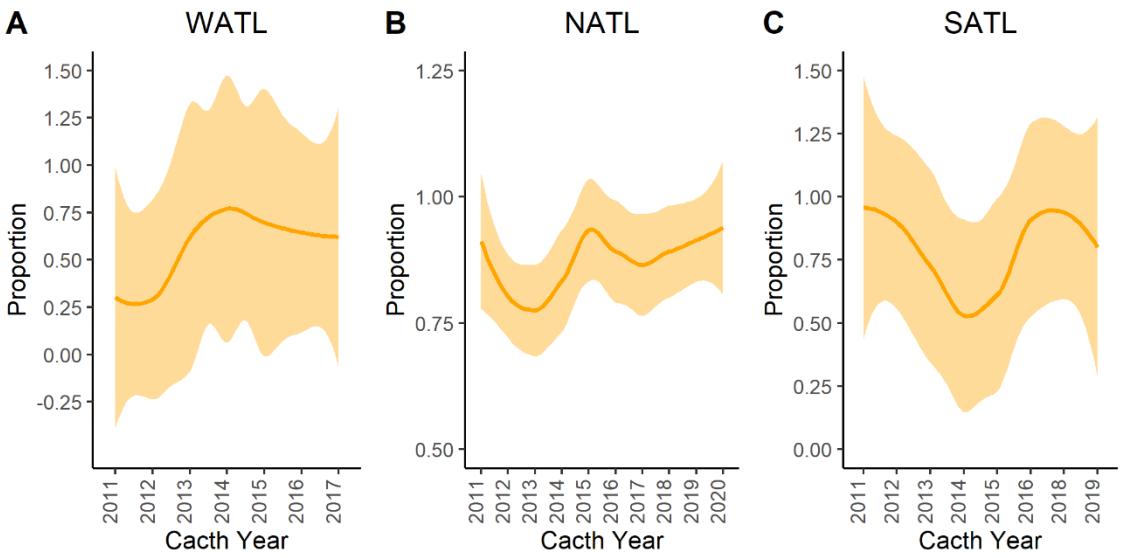

Figure 7.5. Temporal evolution of estimated proportions of MED origin of Atlantic bluefin tuna samples collected in the West (WATL), North (NATL) and South (SATL) Atlantic Ocean.

We also explored the variability in the sex ratio of GOM, MED and unassigned samples at each area based on individuals for which sex data was available (n=852, for EATL no fish with sex data was available). In the WATL, the proportion of males assigned to the MED origin was slightly higher than the proportion of males of GOM and UNASS origins (Figure 7.6A). In the NATL the Female:Male (F:M) proportion was similar among fish assigned to the different origins Figure 7.6B). In the SATL, higher proportion of females were unassigned, while the F:M proportion was similar among fish assigned to the MED origin (Figure 7.6C). Among GOM origin individuals only 2 specimens had sex data available, and this were females.

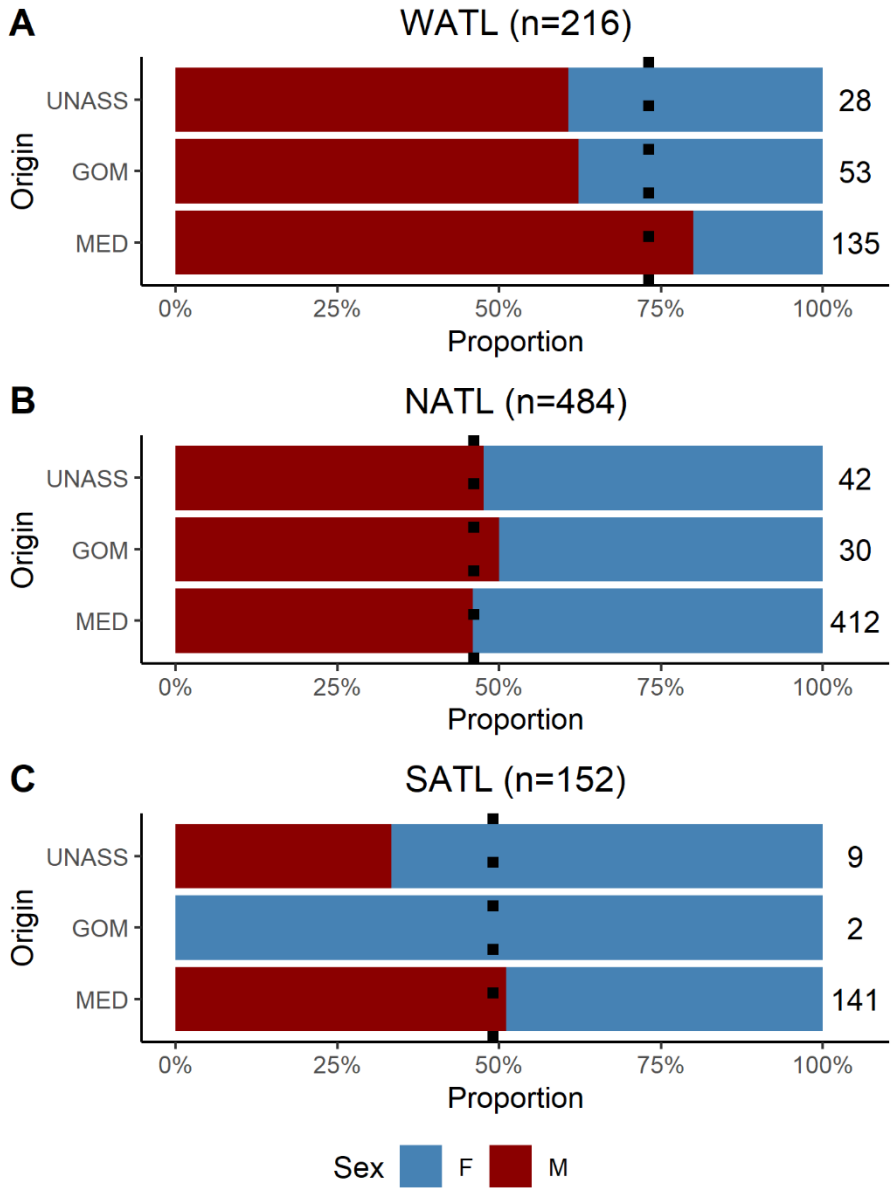

Figure 7.6. Female (blue) and male (red) ABFT proportions by assigned origin West (WATL), North (NATL) and South (SATL) Atlantic Ocean. Dotted line represents mean male proportion in the area.

7.3.2 Combined approach

Out of the 1809 individuals analyzed, 1135 were assigned to the same origin (i.e., MED, GOM or UNASS) with otolith stable isotopes and genetic markers (i.e., ~63% of the samples). Among them, most of the fish were assigned to the MED origin with both techniques, while the number of fish assigned as GOM or UNASS with both techniques was reduced (Figure 7.7). In the WATL a substantial proportion of GOM assigned fish was maintained (Figure 7.7A) but they were barely present in the NATL and SATL (Figure 7.7B and D), while no fish assigned to the GOM when combining both techniques was present in the EATL (Figure 7.7C). Therefore, when

both techniques are considered, it is more difficult to find “pure” GOM fish, where both otolith chemistry data (which reflects the natal geographical origin of an individual) and genetic data (which reflects genetic origin related to populations' evolutionary history) agree in assigned origin. Few individuals agreed to be considered as unassigned with both techniques, proportion of UNASS fish decreasing in all regions when compared to what was reported with stable isotope data only in Task 6.1 and genetic markers only in Task 4.2. Comparing with the rest of the areas, highest proportions of genetically and otolith microchemistry UNASS fish was found in the WATL (Figure 7.7A). When a fish is classified as UNASS with otolith microchemistry, it is mostly because otolith $\delta^{18}O$ values fall into the overlapping area of GOM and MED baseline signatures used for assignment. When a fish is classified as UNASS with genetic markers, it is because they are genetically intermediate between GOM and MED populations. The combined approach is thus useful for identifying individuals whose stable isotope signatures and genetic profiles, when taken together, are not characteristic of either the western or eastern spawning population. This could be fish derived from a spawning area not covered in this study (e.g., Slope Sea) as already suggest by Brophy et al., (2020).

The rest of the samples, 674 out of 1809, disagreed in the origin assigned with otolith stable isotopes and genetic markers. Among them, there were 253 fish with unassigned otolith origin that were assigned to MED or GOM populations with genetic markers, while 216 unassigned with genetics were assigned to MED or GOM with otolith microchemistry (i.e., ~26% of the total samples). Finally, 205 individuals (i.e., ~11% of the samples) show contradictory GOM/MED origins among otolith chemistry and genetic data.

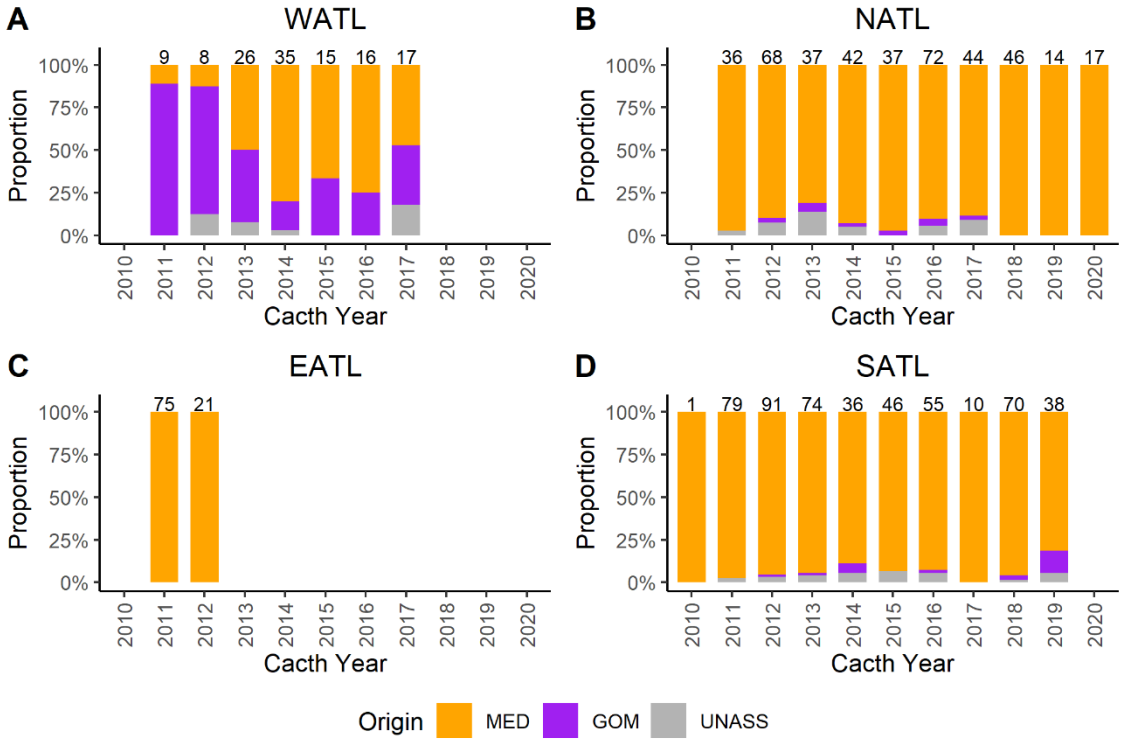

Figure 7.7. Estimated proportions of Atlantic bluefin tuna assigned as MED (orange), GOM (purple) and unassigned (grey) with both otolith stable isotopes and genetic markers collected from 2010 to 2020 in the West (WATL), North (NATL), East (EATL) and South (SATL) Atlantic Ocean.

By region, the WATL was the location with higher levels (~46%) of disagreement between otolith chemistry and genetic markers assigned origin (Figure 7.8). In the NATL the level of disagreement among techniques was of ~40% (Figure 7.9). The EATL showed the lower percentage of individuals with disputed otolith/genetic origin (~29%). Most of these, were individuals with MED-like otolith chemistry and UNASS or GOM genetic origin (Figure 7.10). Finally, in the SATL samples the disagreement between otolith chemistry and genetic assigned origin was of ~33% (Figure 7.11).

In all areas perhaps except in EATL, a common type of disagreement among UNASS individuals by otolith chemistry that fall on the overlapping area of MED and GOM baseline otolith stable isotopes values, but that had a MED-like genetic profile. This could be fish that leave the Mediterranean Sea quite early so that there is no time to fix the Mediterranean-like signal on the otolith (signal representing first year of life) or simply MED fish for which otolith chemistry did not allow to discriminate. There were also fish with GOM-like genetic profile and UNASS otolith microchemistry. Again, these could be indeed fish spawned in the Gulf of Mexico for

which otolith microchemistry signal did not allow to discriminate, or alternatively fish originated from some external source of origin, at it is known that some of the Slope Sea individuals can be confounded genetically with GOM origin individuals. There were also some fish with MED/GOM or GOM/MED origin assigned with otoliths/genetics that laid near this overlapping area. This are probably fish that have been mistaken by otolith microchemistry. However, in all areas there were also fish with GOM-like and MED-like genetic origin that have an otolith chemical signature that corresponds to the MED and GOM origin, respectively. As both techniques provide information over different ecological temporal scales (i.e., otolith microchemistry reflects individual life span, while genetic markers report on gene flow over evolutionary time scales and therefore act on a broader spatio-temporal resolution, Tanner et al., 2016), these results may highlight that mixing is currently occurring between fish spawned in the MED and GOM. Finally, there were some fish with UNASS genetic origin assigned to the MED with otolith chemistry in all regions. To lesser extent, there were also some UNASS genetic origin assigned to the GOM with otolith chemistry, especially in the WATL and NATL. While this could imply that otolith stable isotope data is resolving the uncertainty of some of the genetic markers assignments, it could also reflect that fish have been originated from alternative spawning grounds (e.g. Slope Sea or Bay of Biscay), with water physicochemical properties that can be confounded with the GOM or the MED. Although the Slope Sea has been described as an additional spawning area for ABFT, to date there has no been possible to characterize the otolith chemical signature that this fish may have to be represented in the baseline. However, isoscape predictions from Brophy et al., (2020) showed that the Slope Sea would be intermediate in terms of $\delta^{18}O$ values between the MED and GOM.

Of course, it must be considered that none of the techniques is perfect and there is a small percentage of failures in each one that can lead to these disagreements. On this regard, it is important to understand the direction of the potential biases of each technique in order to detect potential over/underestimation of one particular component. But all in all, the combined approach showed that can provide insights into ABFT population structure that can be masked when a single technique is used, or when both techniques are integrated, and can help to perform strongest inference population mixing and contingent structure as each technique covers different aspects of the biology of the species (Figure 7.12).

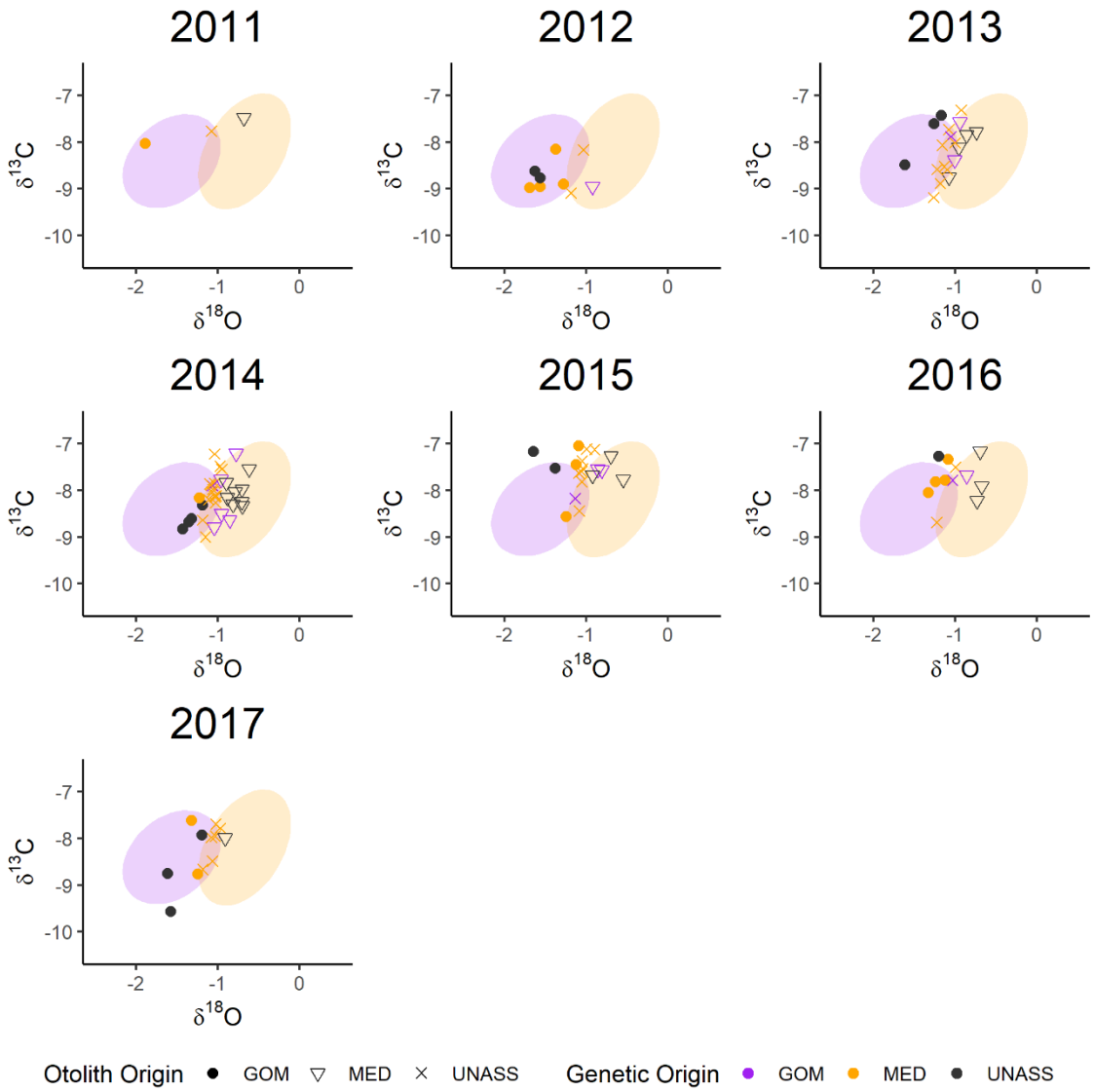

Figure 7.8. Atlantic bluefin tuna (Thunnus thynnus) individuals with disputed origin assigned by otolith stable isotopes and genetic markers and captured in the West Atlantic Ocean (WATL). Different symbols and colours represent different origins assigned with otolith stable isotopes and genetic markers, respectively. Dots are overlaid on the otolith stable isotope signatures ($\delta^{18}O$ and $\delta^{13}C$ values) of the reference baseline described in task 6.1.

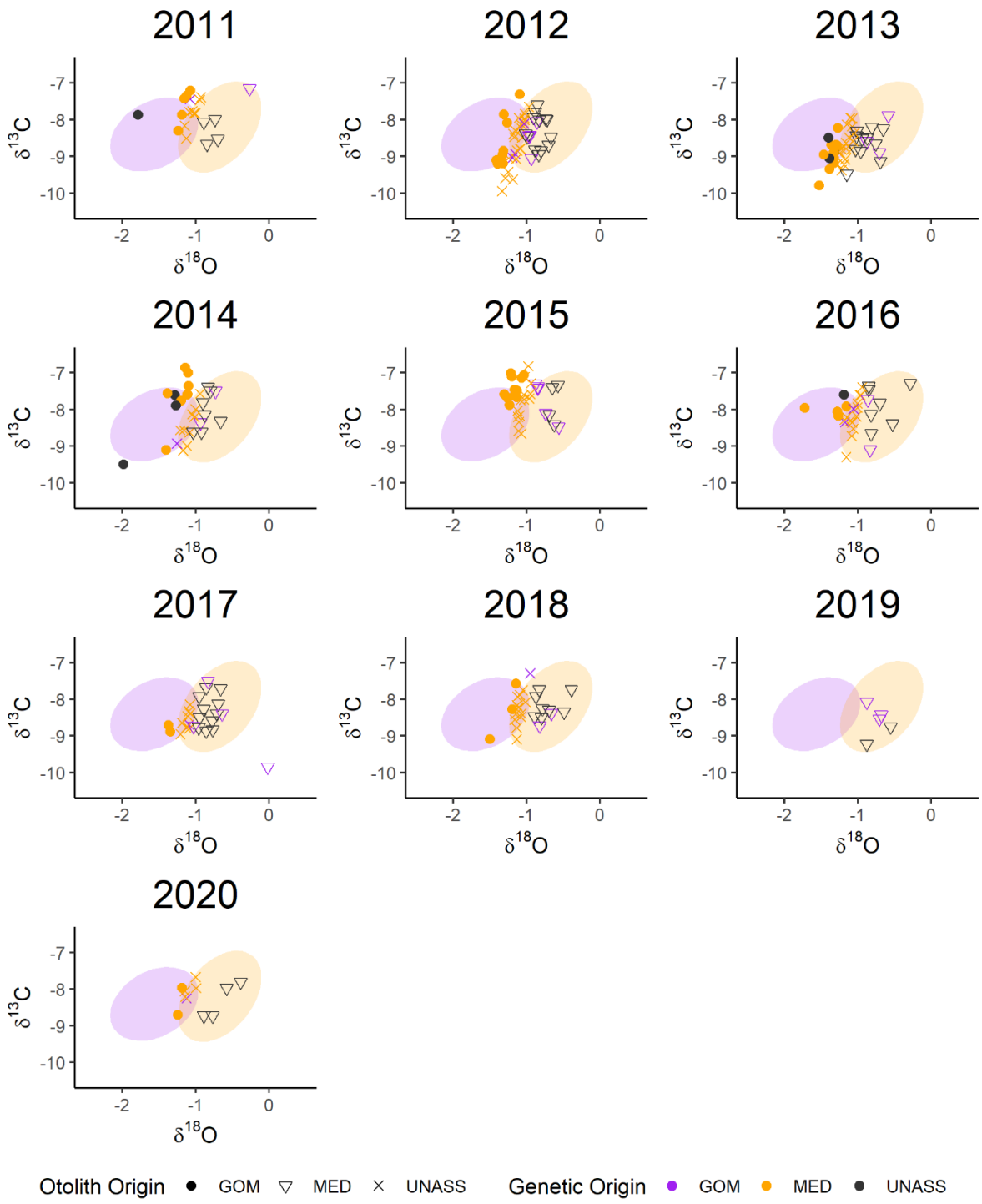

Figure 7.9. Atlantic bluefin tuna (Thunnus thynnus) individuals with disputed origin assigned by otolith stable isotopes and genetic markers and captured in the North Atlantic Ocean (NATL). Different symbols and colours represent different origins assigned with otolith stable isotopes and genetic markers, respectively. Dots are overlaid on the otolith stable isotope signatures ($\delta^{18}O$ and $\delta^{13}C$ values) of the reference baseline described in task 6.1.

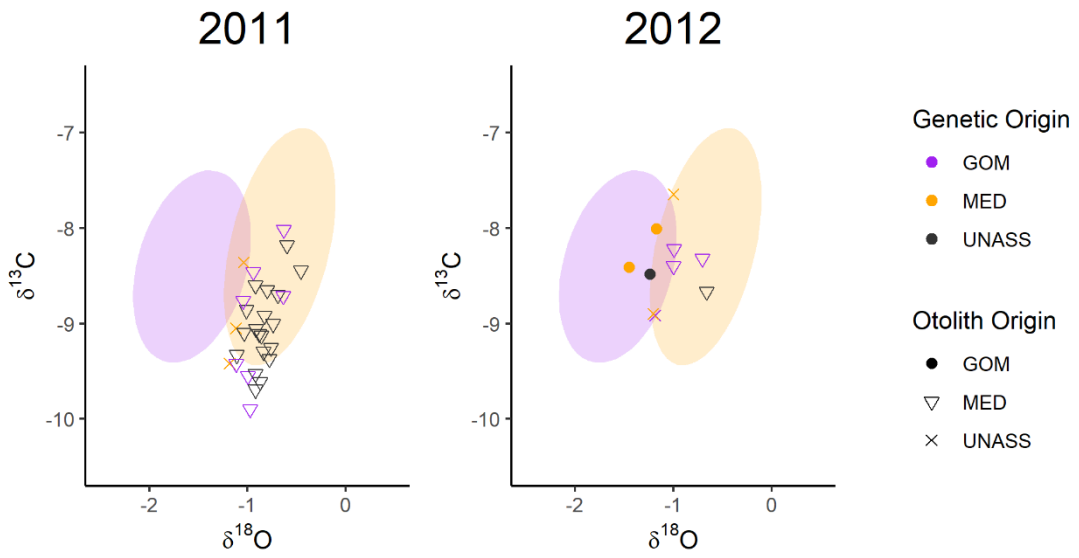

Figure 7.10. Atlantic bluefin tuna (Thunnus thynnus) individuals with disputed origin assigned by otolith stable isotopes and genetic markers and captured in the East Atlantic Ocean (EATL). Different symbols and colors represent different origins assigned with otolith stable isotopes and genetic markers, respectively. Dots are overlaid on the otolith stable isotope signatures ($\delta^{18}O$ and $\delta^{13}C$ values) of the reference baseline described in task 6.1.

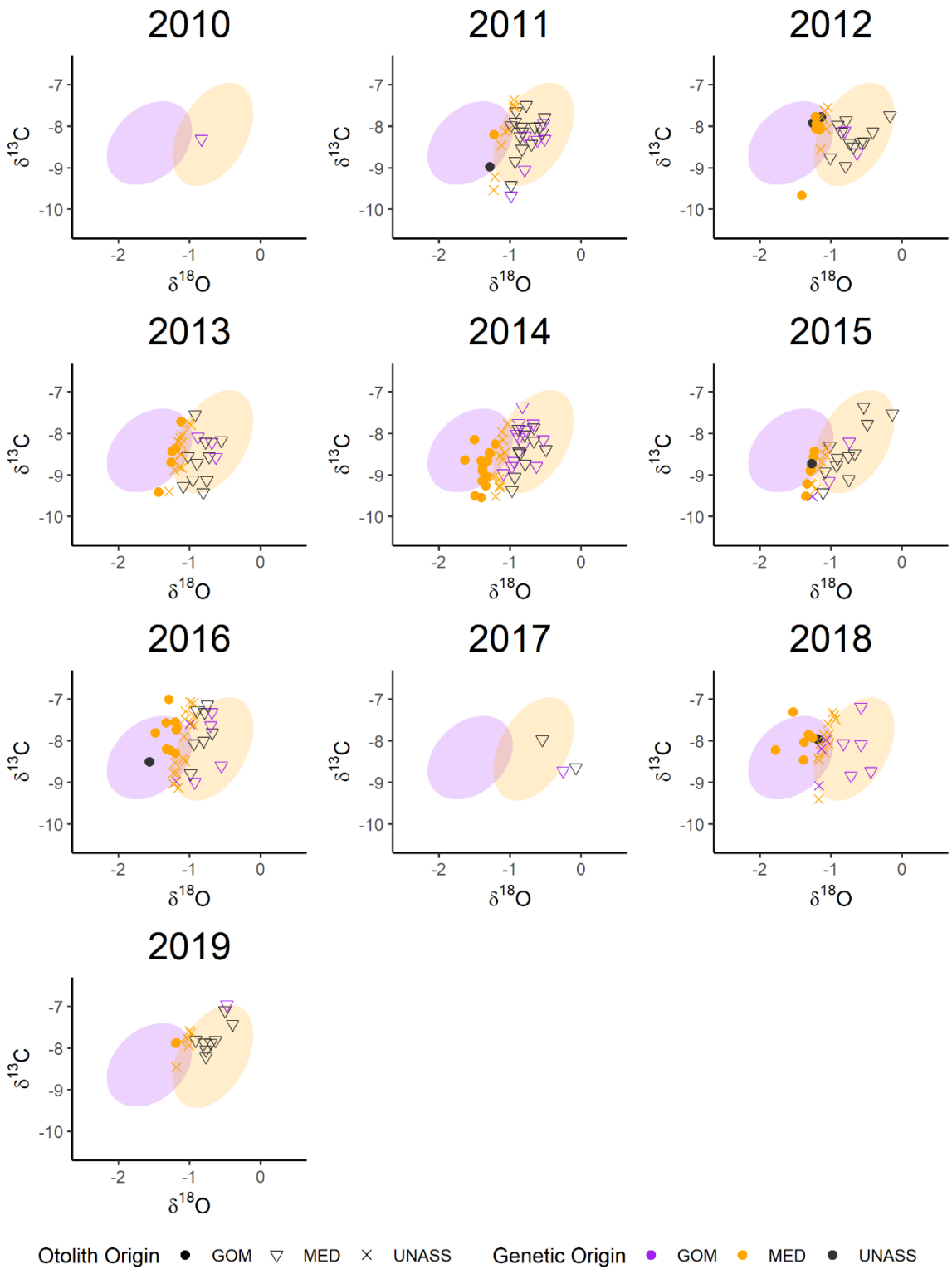

Figure 7.11. Atlantic bluefin tuna (Thunnus thynnus) individuals with disputed origin assigned by otolith stable isotopes and genetic markers and captured in the South Atlantic Ocean (SATL). Different symbols and colors represent different origins assigned with otolith stable isotopes and genetic markers, respectively. Dots are overlaid on the otolith stable isotope signatures ($\delta^{18}O$ and $\delta^{13}C$ values) of the reference baseline described in task 6.1.

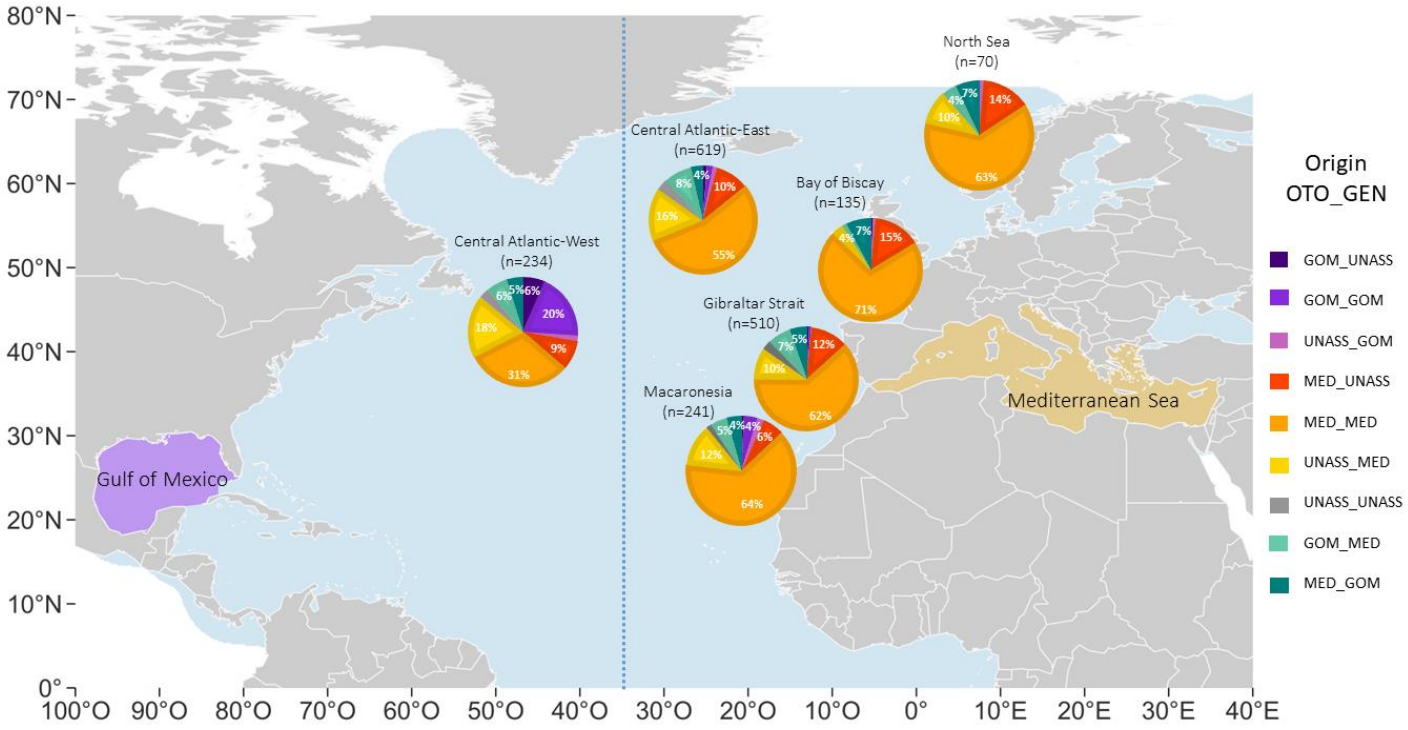

Figure 7.12. Atlantic bluefin tuna (Thunnus thynnus) individuals with combined origin assignment from otolith microchemistry and genetic markers (N=1809). Different colours are for different combinations (see legend). Blue dotted line represents the 45°W management boundary.

7.4 Conclusions

- Mixing of ABFT is more complicated than currently assumed in management, fish originated in both sides of the Atlantic cross the 45ªW line and mix with the other population in feeding aggregates of the Atlantic Ocean.

- The number of fish of each origin visiting different feeding areas changes over the years and no trend has been found.

- An holistic approach that considers both otolith stable isotopes and genetic markers data, can help to own a more complete view of the structure of ABFT in the Atlantic Oceans, and can reduce type I error in stock identification.

- The integrated method proved to increase the resolving power of stock discrimination in comparison to single approaches and resulted in lower numbers of unassigned individuals than otolith stable isotope only and genetic markers only models. Most important variables in distinguishing between the GOM and MED individuals was $\delta^{18}O$, followed by RAD 213, RAD 35 and RAD 26.

- The combined approach showed that can provide insights into ABFT population structure that can be masked when a single technique is used, or when both techniques are integrated, as it considers processes occurring at different temporal scales (i.e., individual life span vs evolutionary).

References

Brophy, D., Rodríguez-Ezpeleta, N., Fraile, I., & Arrizabalaga, H. (2020). Combining genetic markers with stable isotopes in otoliths reveals complexity in the stock structure of Atlantic bluefin tuna (Thunnus thynnus). *Nature Scientific Reports*, *10*(1), 1–17. https://doi.org/10.1038/s41598-020-71355-6

Cutler, D. R., Edwards, T. C., Beard, K. H., Cutler, A., Hess, T. K., Gibson, J., & Lawler, J. J. (2007). Random forests for classification in ecology. Ecology, 88(11), 2783–2792. https://doi.org/10.1890/07-0539.1

ICCAT. (2020). 2020 SCRS ADVICE TO THE COMMISSION. https://www.iccat.int/Documents/SCRS/SCRS_2020_Advice_ENG.pdf

Jones, C. M., Palmer, M., & Schaffler, J. J. (2017). Beyond Zar: the use and abuse of classification statistics for otolith chemistry. Journal of Fish Biology, 90(2), 492–504. https://doi.org/10.1111/jfb.13051

Kerr, L., Whitener, Z., Cadrin, S., Morse, M., Secor, D., & Golet, W. (2020). Mixed stock origin of Atlantic bluefin tuna in the US rod and reel fishery (Gulf of Maine) and implications for fisheries management. *Fisheries Research*, *224*, 10.1016/j.fishres.2019.105461. https://doi.org/10.1016/j.fishres.2019.105461

Rodríguez-Ezpeleta, N., Díaz-Arce, N., Walter, J. F., Richardson, D. E., Rooker, J. R., Nøttestad, L., Hanke, A. R., Franks, J. S., Deguara, S., Lauretta, M. V., Addis, P., Varela, J. L., Fraile, I., Goñi, N., Abid, N., Alemany, F., Oray, I. K., Quattro, J. M., Sow, F. N., … Arrizabalaga, H. (2019). Determining natal origin for improved management of Atlantic bluefin tuna. *Frontiers in Ecology and the Environment*, *17*(8), 439–444. https://doi.org/10.1002/fee.2090

Tanner, S., Reis-Santos, P., & Cabral, H. (2016). Otolith chemistry in stock delineation: A brief overview, current challenges and future prospects. *Fisheries Research*, *173*(3), 206–213. https://doi.org/10.1016/j.fishres.2015.07.019

8. SORTING, IDENTIFICATION AND COUNTING OF ATLANTIC BLUEFIN TUNA LARVAE PRESERVED IN ETHANOL 90% FOR GENETICS

Task Leader: Patricia Reglero (IEO-CSIC)

Participants:

IEO-CSIC: Asvin Perez-Torres, Melissa Martin, Mar Santandreu, Salsabil Bouaziz, Patricia Reglero.

8.1 Introduction

The collection of Atlantic bluefin tuna larvae in the main spawning area of the NW Mediterranean provides a novel opportunity to provide samples of the early life stages of this species to the biological sample bank. Adults and juveniles that can be potentially used for further studies including genetics, otolith microchemistry, basic biology has been long been sampled in the framework of GBYP. Less effort has been directed towards the early life stages of the species. National programs ensure collecting tuna larvae every summer in the main spawning ground for Bluefin tuna using Bongo nets. One collector is formalin preserved and these samples that are routinely used to identify bluefin tuna larvae since formalin is the best preservation method for the maintenance of pigments used for taxonomic identification and it is further used for the estimation of the larval index used in the assessments. However, preservation in formalin is not suitable for potential uses besides species identification which includes genetics, otoliths and many other applications. Only since 2019 one of the collectors used in the sampling is preserved in ethanol, the preservation method that ensures larvae can be used for other purposes rather than species identification. This activity is focused in providing larval samples preserved in ethanol to the GBYP so that a number of samples can guarantee in the future further analyses.

This is the main task, to select samples from the oceanographic survey conducted in 2022 in the main tuna spawning ground in the Western Mediterranean.

8.2 Field sampling and laboratory processing

We sorted and identified bluefin tuna fish larvae from 40 stations selected from a cruise that took place around the Balearic Islands, western Mediterranean Sea, during June 2022. One set of larvae were separated and identified from a Bongo net 90-cm diameter equipped with a 500-µm mesh size that was towed obliquely down to 30-m depth for 8-12 minutes at 2 knots cruising speed and preserved directly in 100% ethanol for further processing. The larvae were also separated and identified from a Bongo net 90-cm diameter equipped with a 1000-µm mesh size that was towed sampling that was towed obliquely down to 10-m depth and also preserved directly in 100% ethanol for further processing. We used a dissection microscope to identify bluefin tuna larvae and sorted them from the total plankton sample. The individuals sorted were preserved in 100% ethanol in different 4 ml jarks and kept in the freezer for the perfect conservation.

8.3 Results

We identified 7638 individuals from 40 samples collected during 2022. In 34 samples, bluefin tuna larvae were found and in 6 samples the absence of bluefin tuna larvae was confirmed (Table 8.1).

Table 8.1: Bluefin tuna larvae sampled at each station

Survey	Date	Sampler_Bongo	Mesh	Station	Order	Total sample or subsample	Number of Bluefin tuna larvae
TU0622	17/06/2022	B90	500	1402	14	Subsample	168
TU0622	19/06/2022	B90	500	1593	29	Total	384
TU0622	20/06/2022	B90	500	1131	39	Total	8
TU0622	20/06/2022	B90	500	1321	46	Total	0
TU0622	21/06/2022	B90	500	1323	51	Total	1
TU0622	22/06/2022	B90	500	1331	67	Total	18
TU0622	23/06/2022	B90	500	887	70	Total	0
TU0622	24/06/2022	B90	500	719	78	Total	68
TU0622	24/06/2022	B90	500	896	81	Total	0
TU0622	25/06/2022	B90	500	893	89	Total	145
TU0622	25/06/2022	B90	500	1245	94	Total	0
TU0622	26/06/2022	B90	500	1052	99	Total	0
TU0622	26/06/2022	B90	500	969	100	Total	0
TU0622	26/06/2022	B90	500	705	104	Total	1
TU0622	27/06/2022	B90	500	701	110	Total	7
TU0622	28/06/2022	B90	500	697	118	Total	1
TU0622	29/06/2022	B90	500	1152	85	Total	5
TU0622	17/06/2022	B90	500	1222	7	Total	27
TU0622	16/06/2022	B90	1000	1042	3	Total	3686
TU0622	16/06/2022	B90	1000	1044	2	Total	65
TU0622	17/06/2022	B90	1000	1127	5	Total	14
TU0622	21/06/2022	B90	1000	1137	58	Total	83
TU0622	17/06/2022	B90	1000	1222	7	Total	28
TU0622	20/06/2022	B90	1000	1230	47	Total	39
TU0622	21/06/2022	B90	1000	1232	50	Total	322
TU0622	25/06/2022	B90	1000	1241	96	Total	2
TU0622	21/06/2022	B90	1000	1323	51	Total	17
TU0622	22/06/2022	B90	1000	1420	63	Total	18
TU0622	18/06/2022	B90	1000	1492	19	Total	239
TU0622	20/06/2022	B90	1000	1499	43	Total	105
TU0622	21/06/2022	B90	1000	1503	53	Total	11
TU0622	21/06/2022	B90	1000	1505	54	Total	2
TU0622	18/06/2022	B90	1000	1589	21	Total	132
TU0622	19/06/2022	B90	1000	1593	29	Total	697
TU0622	19/06/2022	B90	1000	1694	30	Total	207
TU0622	19/06/2022	B90	1000	1696	33	Total	299
TU0622	18/06/2022	B90	1000	1793	25	Total	183
TU0622	27/06/2022	B90	1000	792	111	Total	89
TU0622	26/06/2022	B90	1000	884	106	Total	375
TU0622	25/06/2022	B90	1000	891	90	Total	192

9. ACKNOWLEDGEMENTS

This work was carried out under the provision of the ICCAT Atlantic Wide Research Programme for Bluefin Tuna (GBYP), funded by the European Union, by several ICCAT CPCs, the ICCAT Secretariat and by other entities (see: https://www.iccat.int/GBYP/en/Overview.asp). The contents of this report do not necessarily reflect the point of view of ICCAT or of the other funders, which have not responsibility about them, neither do them necessarily reflect the views of the funders and in no ways anticipate the Commission's future policy in this area.

10. APPENDICES

Appendix 1: Otolith reference collection

Appendix 2: Spine reference collection

Appendix 3: Database 2023 for ICCAT

Appendix 4: Individual origin estimates from otoliths analyzed in Phase-12